CHARACTERISATION OF THE NEW VPS35 p.D620N KI MOUSE MODEL OF PARKINSON'S DISEASE

by

Stefano Cataldi

B. Pharmacy, University of Ferrara, Italy 2014

A THESIS SUBMITTED IN PARTIAL FULFILLMENT OF

THE REQUIREMENTS FOR THE DEGREE OF

DOCTOR OF PHILOSOPHY

in

THE FACULTY OF GRADUATE AND POSTDOCTORAL STUDIES

(Neuroscience)

THE UNIVERSITY OF BRITISH COLUMBIA

(Vancouver)

April 2018

The following individuals certify that they have read, and recommend to the Faculty of Graduate and Postdoctoral Studies for acceptance, the dissertation entitled:

Characterisation of the new VPS35 p.D620N KI mouse model of Parkinson's disease

submitted by	The student	in partial fulfillment of the requirements for
the degree of	Doctor of Philosophy	
in	Neuroscience	

Examining Committee:

Matthew Farrer
Co-supervisor

Austen Milnerwood
Co-supervisor

Cheryl Wellington
Supervisory Committee Member

Stan Floresco
University Examiner

Thibault Mayor
University Examiner

Additional Supervisory Committee Members:

Anthony Phillips
Supervisory Committee Member

Abstract

Vacuolar protein sorting 35 (VPS35) is a core component of the retromer trimer required for endosomal membrane-associated protein trafficking. The discovery of a missense mutation, *Vps35* p.D620N, implicates retromer dysfunction in the pathogenesis of Parkinson's disease (PD). Our group have generated and characterized a knock-in mouse with a *Vps35* p.D620N substitution (herein referred to as VKI) from 3 to 18 months of age. Stereological counting of tyrosine hydroxylase (TH)-positive nigral neurons was comparable between mutant and wild-type animals. Quantification of extracellular dopamine by striatal microdialysis of freely moving animals, and high performance liquid chromatography, was comparable across genotypes at all ages. However, dopamine metabolites appear increased in young VKI mice, suggesting increase dopamine turnover. Assessment of nigrostriatal function by *ex-vivo* fast scan cyclic voltammetry (FSCV) revealed an increase in dopamine release in brain slices from 3-month-old VKI, and a reduction in older animals. Western blot analysis of VKI striata revealed increased in the vesicular monoamine transporter 2 (VMAT2), and decreased in dopamine transporter (DAT) levels, at 3 and 18 months of age. These results were supported by confocal imaging of the dorsolateral striatum, showing an increase in the size of VMAT2-positive synaptic structures, and a significant loss of DAT cluster density in VKI mice. Standardized behavioural testing failed to observe overt movement disorder. Cognitive evaluation showed altered exploratory behaviour and perseveration in both young and old VKI animals. These alterations in dopaminergic activity and behaviour are reminiscent of prodromal PD. Together these results implicate retromer in dopaminergic function and early PD stage symptoms and provide a molecular mechanism for dopamine dysregulation in VPS35 p.D620N parkinsonism.

Lay Summary

Parkinson's disease (PD) is a debilitating disorder that affect up to 2% of the population. Currently no treatment is able to halt or slow disease progression. The main reason we are missing a good therapy is unknown cause and mechanism of disease and the lack of a good model that replicates early alterations in the disease. Here in this study I evaluate a mouse model, carrying the vacuolar protein sorting (VPS35) p.D620N genetic substitution that affects rare families with PD. This model shows early alteration in the dopaminergic system, the main system affected in humans. The dysfunction in the dopamine system leads to cognitive alterations reminiscent of early stages of the disease, but curiously does not affect movement. This model replicates early alteration seen in people with PD, suggests mechanisms underlying disease, and may help develop new therapeutics.

Preface

This work was conducted in UBC's Djavad Mowafaghian Centre for Brain Health, in Prof. Farrer lab at the Centre for Applied Neurogenetics. I contributed to project design and methodology (under the guidance of Prof. Farrer and Dr. Milnerwood) and I was responsible for investigation, project data curation, and analysis. I was also responsible for animal colony management, from breeding, handling, and behavioural evaluation, to euthanasia and tissue collection.

The mouse was generated at Ozgene PLC (Australia) by Prof. Matthew Farrer and the team at the Centre for Applied Neurogenetics. The validation of the model described in chapter 2 and 3 was performed by Stephanie Bortnick and Emil Gustavsson.

I had the support of my team for western blotting and immunohistochemistry. While I was the person managing the animals, organizing the experiment and collecting the tissue, Jordan Follett [postdoctoral fellow], Chelsie Kadgien [PhD student] and Jesse Fox [technician] performed most of these assays, including analysis, and subsequent publication. A portion of chapter 3 was performed in Dr. Heather Melrose lab. I provided the tissue and directions, while the lab performed the immunohistochemical assay for pathology. Igor Tatarnikov [Master student] contributed to FSCV data collection and analysis.

Part of this work has been submitted for publication and it is currently under review. Stefano Cataldi, Jordan Follett, Jesse Fox, Igor Tatarnikov, Chelsie Kadgien, Emil K. Gustavsson, Jaskaran Khinda, Austen J. Milnerwood & Matthew J. Farrer. (2018) Altered dopamine release and monoamine transporters in *Vps35* p.D620N knock-in mice. I conducted the greatest portion of the experiments and with Prof. Farrer and Dr. Milnerwood authored the majority of the manuscript in equal contribution with Jordan Follett.

All breeding, housing and experimental procedures were performed according to Canadian Council on Animal Care regulations, with appropriate ethical approvals (protocol numbers A16-0088 for breeding procedures, and A15-0105 for experimental procedures and tissue collection).

Table of Contents

List of Tables

List of Figures

List of Abbreviations

6-OHDA	6-hydroxydopamine
Aβ	amyloid-β
AADC	amino acid decarboxylase
ACSF	artificial cerebrospinal fluid
AD	autosomal dominant
APP	amyloid precursor protein
AR	autosomal recessive
AR-JP	autosomal recessive juvenile Parkinson's disease
BAC	bacterial artificial chromosome
COMT	catechol-*O*-methyltransferase
D1R	D1-type receptor
D2R	D2-type receptor
DARPP-32	dopamine- and cAMP-regulated neuronal phosophoprotein 32
DAT	dopamine transporter
DBS	deep brain stimulation
DOPAC	3,4-dihydroxyphenylacetic acid
EOPD	early onset Parkinson's disease
EPM	elevated plus maze
FSCV	fast scan cyclic voltammetry
GPe	globus pallidus external
GPi	globus pallidus internal
Het	heterozygous

Homo	homozygous
HRP	horseradish peroxidase
HVA	homovanillic acid
IPI	inter-pulse-interval
L-DOPA	3,4-dihydroxy-L phenylalanine
LB	Lewy body
LC	locus coeruleus
LN	Lewy neurites
LRRK2	leucine-rich repeat kinase 2
MAO-B	monoamine oxidase B
MPR	mannose-6-phosphate receptors
MPTP	1-methyl-4-phenyl-1,2,5,6-tetrahydropyridine
MSNs	medium spiny neurons
PINK1	PTEN-induced kinase 1
PD	Parkinson’s disease
PFA	paraformaldehyde
RAM	radial arm maze
RBD	rapid eye movement sleep behaviour disorder
RME-8	receptor-mediated endocytosis 8
RPM	revolution per minute
RT	room temperature
SN	substantia nigra
SNpc	substantia nigra pars compacta

SNpr	substantia nigra pars reticulata
STN	subthalamic nucleus
s.q.	sub-cutaneous
SV	synaptic vesicle
TGN	*trans*-Golgi network
TH	tyrosine hydroxylase
TH+	tyrosine hydroxylase positive
VPS35	vacuolar protein sorting 35
VTA	ventral tegmental area
VKI	*Vps35* p.D620N knock-in mice
VMAT2	vesicular monoamine transporter 2
WT	wild-type

Acknowledgements

I gratefully acknowledge my supervisors, Prof. Matthew Farrer and Dr. Austen Milnerwood for their support throughout my PhD, and also for the final period of my undergrad. Thanks for teaching me hard work and confidence.

The lab and I are grateful for the funding from the Canadian Institutes of Health Research and in particular Parkinson Canada for the great support they gave me, both financially and emotionally. The work was also made possible through a Canada Excellence Research Chair and British Columbia Leadership Endowment funds.

I appreciate the efforts of staff at the Centre of Disease Modelling (CDM), University of British Columbia, for animal husbandry. Without their amazing job none of this work would have been possible. Thanks for taking good care of our animals.

I offer my enduring gratitude to the faculty, staff and my fellow students at UBC, who have inspired me to continue my work in this field. My class-mates who experienced the challenges of grad school with me, and provided help for technical procedures and experimental designs. Thanks for listening to me in difficult time and helping me in this project.

I owe particular thanks to Prof. Michele Morari, whose support was crucial on choosing my career path. I thank Prof. Anthony Phillips and Prof. Cheryl Wellington for enlarging my vision of science and providing coherent answers to my endless questions. I thank them for their support throughout the entirety of my PhD, almost as if I were their own student. Not only they helped intellectually, but provided equipment and resources to achieve some of the experiments described in this thesis. Particularly I thank Giada Vacca, Soyon Ahn, and Peter Axerio-Cilies from Phillips' group, and Sophie Stukas, Tom Cheng, and Asma Bashir from Wellington's team, always available to answer questions and help with experiments.

Dedication

It cannot be one person. It's a long list, and it would be hard to list them all. The merit goes to a combination of all the people I crossed path with, on my way to who I am today.

Thanks to the Parkinson Society of British Columbia. The path in science is never a straight road. There are many difficulties that someone can encounter. Sometime we lose track of the reason why we do what we do. PSBC gave me the wonderful opportunity to share this path with the people that are living Parkinson's disease. It made me remember the importance of what I do and gave me the strength to keep going with this hard and yet rewarding career. I had the honor to be part of the extraordinary work done by the society and become friend with the extraordinary people that are part of it. Last October I had a tattoo made, so I can always remember the beautiful time PSBC gave me. Keep up the good work.

Special thanks are owed to my parents, who supported me throughout all these years of education, both morally and financially. Having their kid moving to another country was not easy, yet they appreciated my choices. Thanks for always letting me follow my dreams.

Thank you to my friends in Vancouver, keeping me sane throughout this hard journey called PhD. Thanks for 4 wonderful years I will never forget. My friends in Ferrara, where I did my undergrad, for being still in touch and hosting me every time I go back to visit. Those were the best year of my life and it's good to know I can always find you there when I come back. My friends in Gallipoli, back home, were everything started. Thanks to the great support you gave me back in those fantastic years (and still do, no matter how far we are from each other).

One name I'm going to give. Thanks to Dr. Mattia Volta. The person who taught me everything when I joined the lab, who welcomed me in his life. Hopefully our path will cross again in this career we are pursuing.

Chapter 1: Introduction

1.1 Parkinson's disease

Parkinson's disease (PD) was first described in the ancient Indian medical system of Ayurveda, under the name "Kampavata" (Ovallath & Deepa, 2013). It was only in 1817 that the British physician Dr. James Parkinson gave the first medical description of the disease (Parkinson, 1817). The disease was later called after his name by Jean-Martin Chacot (Ovallath & Deepa, 2013), although it is now common to refer to a syndrome called parkinsonism that includes other diseases that present similar symptomatology to PD, but may or may not share similar causes and pathology (Dickson, 2012). To date very little is known about the etiology of the disease and no cure is available.

1.1.1 Clinical features

Clinically, PD is primarily characterized by motor alterations such as bradykinesia, rigidity, and resting tremor. Over the years the disease will inexorably progress in severity and manifestation. The course of this devastating disease was described in details by Dr.James Parkinson in his 'An Essay on the Shaking Palsy' in 1817, -: "The submission of the limbs to the direction of the will can hardly ever be obtained in the most ordinary offices of life"- such as feeding oneself, or grasping and lifting a glass of water. Even muscles that normally work automatically are affected: swallowing becomes difficult, drooling becomes common and, at the end of the line, moving the bowels requires, as Parkinson put it, "stimulating medicines of very considerable power".

Bradykinesia (slowness of movement with gradual loss of speed and amplitude during repetitive alternating movement) is the most recognizable clinical feature seen in PD patients

(Jankovic & Aguilar, 2008). Resting tremor usually occurs at the frequency of 4 to 6 Hz, differentiating it from other forms of tremors (Jankovic & Aguilar, 2008). It typically affects one side of the body before spreading to involve the other side. Rigidity is often present and is used to describe the increased resistance of muscle during passive movement. Due to the loss of postural reflexes, postural instability appears at the later stages of PD progression (Coelho & Ferreira, 2012). Motor dysfunction often spread and affects swallowing and speech, handwriting, and other basic motor functions, creating the need for constant care for people with the disease.

To this list of common symptoms noted by Parkinson, modern neurologists have added a long series of non-motor dysfunctions, including diminished sense of smell, sleep disorders, restless-leg syndrome, fatigue, impotence, visual problems, hallucinations, depression, anxiety, executive dysfunction, and, in late stages, cognitive impairment that can deteriorate to dementia (Goldman & Postuma, 2014). Indeed, these signs and symptoms often precede motor deficits by years and are underestimated in the clinic. Sleep disturbances, such as rapid eye movement sleep behaviour disorder (RBD), sleep apnea, sleep fragmentation, can appear as early as 20 years prior to obvious motor symptoms (Goldman & Postuma, 2014). RBD can often present with similar pathological burden found in PD, even without parkinsonism (Postuma et al., 2015). Depending on the study and population, it is now suggested that 60% of PD patients experience RBD, and about 80% of incidental RBD will eventually develop PD within 10-12 years (Todorova et al., 2014). If someone presents both sleep disturbances and loss of sense of smell, the risk of developing PD within 5 years increases significantly (Mahlknecht, Seppi, & Poewe, 2015).

As the whole body is affected, PD results in body weight changes; patients characteristically undergo diet-unassociated weight loss, starting early in the course of the

disease (Chen et al., 2003; Lorefalt et al., 2004). Despite a possible dopaminergic basis for these changes, alterations in food intake (Palmiter, 2007), olfactory dysfunction has also been implicated with an increased risk of weight loss in people with PD (J. C. Sharma & Turton, 2012; J. C. Sharma & Vassallo, 2014).

PD is considered now a multi-organ disorder, affecting not only the brain, but the gut, the heart, and the pancreas (among others), and asides dopamine, other neurotransmitters in the brain, including serotonin, acetylcholine and norepinephrine are implicated (reviewed in Titova et al., 2017). Alterations in different brain regions include several cortical pathways, suggesting contribution of these areas in at least some of the motor dysfunction and non-motor symptoms, if not even being a primary cause (Lefaucheur, 2005), proving quite challenging generating a valid treatment for PD.

1.1.2 Dopamine circuit dysregulation

At the time of diagnosis of PD it is estimated that 30-50% of nigrostriatal neurons are lost with only 30% of dopaminergic terminals in the striatum remaining (reviewed in Cheng et al., 2010). However, earlier loss of dopaminergic markers in the striatum suggests alterations and axonal denervation may precede nigral neuronal degeneration (Cheng et al., 2010).

Dopamine deficiency in PD was found in the 1960s, when significant dopaminergic neuronal loss was reported following examination of autopsy samples from patients with PD (Ehringer & Hornykiewicz, 1960). With the identification of the nigrostriatal pathway, dopaminergic defects were traced back to cell bodies in the substantia nigra pars compacta (SNpc) which innervates the striatum (reviewed in Hornykiewicz, 2006). Accompanying this neuronal loss is an increase in glial cells in the SN and a loss of neuromelanin, the pigment

normally contained in SN dopaminergic neurons (Hornykiewicz, 2006; Figure 1.1.B). Microglia are believed to facilitate the neurodegenerative process in PD. Accumulation and activation occurs in sites where neurons eventually die and are lost. Experimental studies from toxin-induced models would suggest that such inflammation is partially a cause of the neurodegenerative process, as it can be reversed with anti-inflammatory agents (reviewed in Orr et al., 2002). The role of neuromelanin in dopaminergic degeneration is controversial. Some studies would suggest that neuromelanin is protective as its levels increase with age and are correlated with catecholamines synthesis, although other models show a strong affinity towards toxic compounds that could increase dopamine oxidation and therefore cytotoxicity (Enochs et al., 1994; Swartz et al., 1992; and reviewed in Zecca et al., 2001).

The current model of basal ganglia function shows two main striatal output circuits, the direct and the indirect pathways, originating from distinct populations of striatal medium spiny neurons (MSNs) that project to specific target nuclei (described in the schematic in Figure 1.1 and more in details in section 1.5). This is an over-simplified view of the dopaminergic system, but for the purpose of this thesis I will only focus on these main two pathways. These circuits have opposite effects on movement and more generally behavioural action selection (reviewed in Kravitz, Tye, & Kreitzer, 2012). The direct pathway, characterized by the expression of D1-type dopamine receptors (D1R), promotes action selection (including movement). The indirect pathway, expressing D2-type dopamine receptors (D2R), inhibits action. Recent findings have revealed that this model might not fully account for the concurrent activation of both pathways during action selection (Calabresi et al., 2014).

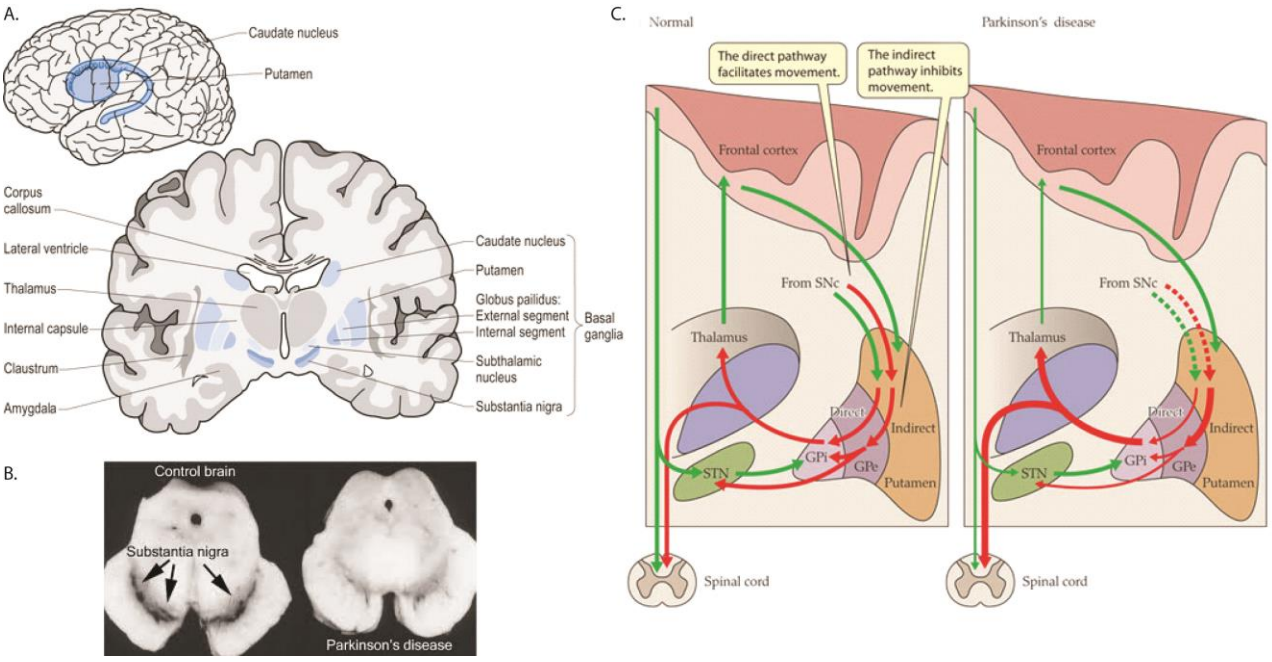

Figure 1.1 Dopaminergic loss and alterations in PD
A) Schematic of the basal ganglia (blue) structures and position in the human brain (image from Kandel et al., 2000). B) Comparison of a brain from a healthy individual (left) and a PD patient (right), showing clear loss of neuromelanin-positive neurons, the neurons containing dopamine in the substantia nigra. C) Schematic of the dopaminergic pathways in the basal ganglia and how they are affected by the loss of dopamine in PD (image from: animal physiology 3rd edition). The direct pathway reduces inhibition of the globus pallidus internal (GPi) causing increased inhibition of the thalamus. The indirect pathway reduces inhibition of the GPi and subthalamic nucleus (STN), with the final outcome of increasing inhibition of the thalamus. The overall result is inhibition of movements.

Apart from the decrease in striatal dopamine, L-aromatic amino acid decarboxylase (AADC) is also significantly reduced in people with PD in the same region (Lloyd, Davidson, & Hornykiewicz, 1975). Similarly, striatal levels of homovanillic acid (HVA, a major dopamine metabolite) and tyrosine-hydroxylase (TH, the rate-limiting enzyme in dopamine synthesis) are also decreased, albeit to a lesser extent (Lloyd et al., 1975). Furthermore, the dopamine transporter (DAT), which mediates dopamine reuptake from the extracellular space after release, was found to have a lower binding affinity to its agonist in PD cases, which has been confirmed in a PET imaging study (Frost et al., 1993). The lifecycle of dopamine is tightly regulated by the positioning of molecular chaperones that promote its synthesis and packaging through TH and

the vesicular monoamine transporter 2 (VMAT2), respectively. Specifically, when dopamine is produced through TH activity, the neurotransmitter is quickly packaged into vesicles by VMAT2. VMAT2 and DAT function are intrinsically linked to the activity of dopaminergic neurons and the maintenance of dopamine homeostasis. For example, BAC-transgenic VMAT2-overexpressing mice have increased dopamine vesicle volume, capacity to store dopamine, and evoked release (Lohr et al., 2014); thus, VMAT2 likely acts to counteract intracellular dopamine toxicity. Conversely, high expression of VMAT2 in mice ameliorates methamphetamine-induced dopaminergic neurodegeneration, by preventing loss of DAT and TH (Lohr et al., 2015). Despite this intrinsic regulation, how VMAT2 is actively recycled, and what influence this trafficking has on DAT localization, remains unknown.

Typically, in brain samples from PD patients, there is complete depletion of dopamine in the putamen of dorsal striatum, but not in the caudate nucleus of dorsal striatum. In the advanced stages of PD, striatal dopamine loss exceeds 80% of total dopamine, mostly from the putamen compared to caudate nucleus (reviewed in Hornykiewicz, 1998). This putamen-caudate difference is likely due to an uneven pattern of dopamine neurons loss in the SN. The SN is divided into two parts, the pars reticulata (SNpr) and the pars compacta (SNpc), with the latter being affected in PD. Another population of dopaminergic neurons constitute the ventral tegmental area (VTA). This specific area also shows loss of TH positive (TH+) neurons, but to a lesser extent. Nigral cell loss is pronounced in the ventral nigra (project to the putamen), compared to the dorsal nigra that innervates the caudate nucleus (Hornykiewicz, 1998). Several differences between these nigral and VTA populations of dopaminergic neurons could account for the selective sensibility of the SNpc. For instance the number of neurons is different with fewer dopaminergic neurons in the SNpc compared to the VTA (reviewed in Brichta &

Greengard, 2014), with GABAergic neurons present in both and a small population of glutamatergic neurons present in the VTA but not in the SNpc (Brichta & Greengard, 2014). This difference between SNpc and VTA is not obvious in mice and rats, although technical procedures used for neuronal counting have to be taken in consideration and could explain these differences (Brichta & Greengard, 2014). The complexity of the connections could also explain this selectivity, with SNpc dopaminergic neurons having greater arborization (reviewed in Bolam & Pissadaki, 2012)

A combination of retrograde tracing, electrophysiological and basic molecular studies in mice demonstrated that distinct subgroups of VTA and SNpc dopaminergic neurons project to specific striatal, cortical and limbic target regions, and these neurons can be distinguished by their expression levels of DAT, their electrophysiological properties, and their capacities for D2R signaling (reviewd by Lammel et al., 2008). A functional analysis of the gene expression patterns of SNpc and VTA dopaminergic neurons suggested that many transcripts related to metabolism, mitochondrial proteins, lipid-protein vesicle-mediated transport, and kinase/phosphatase signaling are highly expressed in SNpc neurons, whereas transcripts implicated in axon guidance or neuropeptide signaling are mainly enriched in VTA neurons (Chung et al., 2005; Greene, Dingledine, & Greenamyre, 2005).

In PD the striatal dopamine changes remain clinically silent until the threshold value of 60-80% SNpc cell loss is reached. The degree of loss of dopamine correlates (in later stages) with the severity of the motor symptoms (reviewed in Hornykiewicz, 1998), although other studies would suggest that dopaminergic neurons degenerate during the early course of the disease and the clinical symptoms are manifestation of the loss of compensatory mechanism or degeneration of non-dopaminergic neurons (Vogt Weisenhorn, Giesert, & Wurst, 2016).

Compensatory biochemical changes in PD striatum maintain proper motor function until the threshold is reached. First, the remaining dopamine neurons increase their dopamine metabolism (release and synthesis shown by increased HVA over dopamine; Hornykiewicz, 1993). Second, in later stages where loss is greater than 80-90%, the number of postsynaptic D2R sites increases in the striatum, to potentially rescue signaling in the presence of lower dopamine (Hornykiewicz, 1998). This proposition is controversial, with other studies showing different results. A study looking at postmortem brain samples from patients with PD revealed a decrease in D2R density with no changes in D1R density (Pierot et al., 1988); however, a separate study did not detect any change in D2 receptor density (Guttman et al., 1986). Whether these divergent findings can be reconciled remains to be seen, and remains a challenge for current therapies. Additionally, surviving dopaminergic neurons appear to be compensating for the neuronal loss via axonal sprouting, although the pattern of these new connections may not be functionally the same as prior to cell loss (Arkadir, Bergman, & Fahn, 2014).

Understanding the selective degeneration and the early changes in such complex population of neurons will surely be of great help to develop more effective drugs and protective therapies.

1.1.3 Pathological features

Together with the loss of dopamine neurons in the SNpc, PD is typically associated with the formation of intracellular proteinaceous inclusions, termed Lewy bodies (LB), in the surviving neurons (reviewed in Goedert et al., 2013).

LBs, mostly found in the brain stem, appears as spherical inclusions with a hyaline eosinophilic core and a pale peripheral halo in the cell body (Forno, 1996). Another type of LB -

'cortical Lewy bodies'- was first found in the cerebral cortex, and has pale staining and less compact than classic LBs (Ikeda et al, 1978). As a milestone in PD, LBs were found to contain α-synuclein in its aggregated form (Spillantini et al., 1997). Additionally, antibodies to neurofilament (Galvin et al., 1997), ubiquitin (Kuzuhara at al., 1988), and the ubiquitin binding protein p62 (Kuusisto at al., 2003), are consistently associated with LBs. α-synuclein immunoreactivity is also found in the degenerating neuronal processes, termed Lewy neurites (LNs; Braak et al., 1999). To evaluate the association between LBs and PD, Braak and colleagues have developed a staging criterion based on the distribution of α-synuclein-related pathology. It usually starts from the olfactory bulb and dorsal motor vagal nucleus, then evolves to the brainstem, and finally reaches the cortical motor and sensory areas (Braak et al., 2003).

Despite PD being mostly characterized by α-synuclein aggregation, other protein aggregates are often found in brains from people with PD. These include the proteins tau and amyloid- β (Aβ; Kurosinski, Guggisberg, & Götz, 2002; Compta et al., 2014).

Although LBs are essential for diagnosing PD from a pathological perspective, they are not exclusive to, nor required for, all PD cases. They are also present in multiple system atrophy and dementia with Lewy bodies (Dickson, 2012), absent in Parkin familial PD and in nearly half of PD due to leucine-rich repeat kinase 2 (LRRK2) mutations (Farrer et al., 2001; Zimprich et al., 2004). The genetic link between tau and LRRK2 is intriguing. LRRK2 is often associated to tau tangles rather than LB pathology (Zimprich et al., 2004). Evidence for a functional link between LRRK2 and tau has been observed in several *in vitro* models and the presence of tau pathology is shown in many mouse models carrying the LRRK2 mutation (MacLeod et al., 2006; Yue et al., 2015).

The microtubule-associated protein tau is a predominantly neuronal protein whose major function is to bind to and stabilize microtubules. In neurodegenerative disease, hyperphosphorylated, insoluble aggregates of tau are observed in neurons and glia of affected brain regions. Such disorders are collectively named the tauopathies, the most well-known of which is Alzheimer's disease, where neurofibrillary tangles comprised of hyperphosphorylated, insoluble tau are one of the defining pathological features of the disease, alongside extracellular plaques composed of Aβ peptide (Grundke-Iqbal et al., 1986). Tau is subject to heavy post-translational modification, and hyperphosphorylation, truncation, and glycosylation have all been linked to disrupting tau function and promoting tau aggregation. Acetylation is also a factor, and has been shown to alter tau degradation, possibly leading to tauopathies and consequent cognitive deficits (Min et al., 2010, 2015). There are a number of examples of disorders where tau deposition is linked to a movement disorder phenotype and several reports describing the presence of tau tangles in PD brain at post-mortem at a higher frequency than in controls (Wray & Lewis, 2010). Additionally, the gene MAPT is associated with risk of developing PD, suggesting importance in this gene and protein in the mechanism of disease (Wider et al., 2010).

In vitro work has shown that α-synuclein and tau are able to influence each other's polymerization, and diffuse tau pathology is observed in transgenic mice expressing the α-synuclein A53T mutation (Giasson et al., 2003). Moreover α-synuclein has been shown to indirectly mediate tau phosphorylation at the pathological epitope S396, same site observed in samples from PD patients (Duka et al., 2009; Muntané et al., 2008). Whether these proteins are directly linked or are parallel mechanism of pathology is yet to be understood.

1.1.4 Therapeutic treatments

Currently, no treatment has proved effective in halting or slowing the progression of the neurodegenerative process in PD (Meissner et al., 2011). Most treatments are able to help symptoms, but often lose effects after a few years, or present with side effects as the disease progresses.

To date, the best pharmacological treatment strategy is based on the restoration of striatal dopamine levels. Unfortunately it is impossible to have a therapeutic effect by the simple administration of dopamine itself, as this neurotransmitter does not cross the blood brain barrier. An intermediate in the synthesis of dopamine, L-DOPA (3,4-dihydroxy-L phenylalanine), has been used instead. After oral ingestion, L-DOPA is absorbed through the aromatic aminoacid transporter. Because of the hepatic metabolism and distribution of L-DOPA in other parts of the body, only a small percentage of the molecule is able to reach the brain (Nutt et al, 1984). Once in the brain, L-DOPA is rapidly converted into dopamine by AADC.

Co-administration of other drugs can affect bioavailability and increase the effectiveness of L- DOPA. The inhibition of the conversion of L-DOPA into dopamine in the periphery can be useful for two reasons: to increase the concentration of L-DOPA available for the passage across the brain barrier and to decrease the possible side effects due to the peripheral actions of dopamine. For example, D1Rs mediate the response to direct vasodilation of renal, mesenteric, and coronary artery while D2Rs inhibit the release of norepinephrine at the sympathetic nerve endings and then inhibits the release of prolactin from the pituitary.

In order to inhibit peripheral conversion of L-DOPA in dopamine, AADC inhibitors are administered, such as benserazide or carbidopa. The half-life of L-DOPA can also be increased with the inhibition of catechol-*O*-methyltransferase (COMT) by administration of entacapone, a

peripheral inhibitor, and tolcapone, a peripheral and central inhibitor (Nutt & Carter, 2000). At the central level, inhibition of monoamine oxidase B (MAO-B) using selegiline and rasagiline, increases the half-life of dopamine (reviewed in Jankovic & Aguilar, 2008). MAO-B and COMT are the main regulators of dopamine metabolism, mostly present in the extracellular space and other brain cells (including glia), with MAO also being present in the neuron itself (reviewed in Meiser, Weindl, & Hiller, 2013). Dopamine homeostasis is tightly regulated to reduce oxidative species that can derive from dopamine metabolism. Diffusion from the extracellular space, as well as re-uptake of dopamine are important to minimize dopamine content in the synaptic cleft. Re-uptake is also crucial to reduce synthetic demand/energy consumption, by re-using dopamine for further release (Meiser et al., 2013). The complexity of this system makes dopamine therapy hard to control and creates several problems with long-lasting treatments, especially as the progression of the disease and neuronal degeneration contines.

After 5 years of treatment with L-DOPA more than half of the patients develop motor disorders of a different nature: i) wearing-off, which consists of a loss of effect of L-DOPA after a period of treatment; ii) "on-off " phenomena, which consist of an abrupt transition, sometimes in a few seconds, from complete autonomy (being "on"), to the total block (phase "off") at any time, place or circumstance; iii) dyskinesia, a series of rapid involuntary chorea-like movements, mainly dependent on the segmental distal muscles, the appearance of which can be delayed by treatments that tend to increase the plasma half-life of L- DOPA (Cotzias et al., 1969; Bezard et al., 2013).

Novel strategies to deliver L-DOPA, as well as novel and more selective COMT and MAO-B inhibitors, have been developed, markedly improving the quality of life for people with

PD (Poewe & Antonini, 2015). This includes non-oral routes of administration of the drug, gel formations, slow release apparatus, and even subcutaneous and intrapulmonal delivery routes, keeping L-DOPA the "gold standard" for treatment and a drug still in active development (Poewe & Antonini, 2015).

Modern therapies in developing better delivery of dopaminergic drugs, including L-DOPA, are of great importance given the normal fluctuations of dopamine in the body and also the difficulty of administration for a lot of patients who often are in their old age and can have problems with drug compliance (Schapira, 2007). Alternative delivery strategies become more important considering the grastro-intestinal dysfunction among the classic PD symptoms (Ray Chaudhuri et al., 2016). DUODOPA®, a combination of L-DOPA and carbidopa is just one of the many examples of innovative therapies. In the form of a gel delivered through an intestinal pump, DUODOPA® only recently became available in many provinces across Canada (from www.parkinson.bc.ca on April 4th, 2018).

As PD progresses over time, symptoms that do not respond to L-DOPA develop, such as flexed posture, the freezing phenomenon, and loss of postural reflexes. Moreover, bradykinesia (that responded to levodopa in the early stage of PD) increases as the diseases worsens and no longer fully responds to L-DOPA, increasing immobility and balance difficulties (reviewed in Jankovic & Aguilar, 2008).

Ideally, the use of dopaminergic agonist would avoid certain side effects and the appearance of dyskinesia. While this is true for long-term dopaminergic agonist treatments currently available, the effect is less than that of L-DOPA, and increasing the dose only leads to other serious side effects such as psychotic reactions (Jankovic & Aguilar, 2008).

Co-administration of L-DOPA with other dopamine agonists reduces the risk of occurrence of side effects. It is recommended, especially at the beginning of therapy, the use of L-DOPA in combination with other drugs such as dopamine-mimetics, amantadine or anticholinergic substances (reviewed in Schapira, 2007). This therapeutic approach is especially recommended in young patients, who are predisposed to developing dyskinesia (Jankovic & Aguilar, 2008).

At the beginning of therapy, L-DOPA can cause vomiting, postural hypotension, and more rarely cardiac disorders. Neuropsychiatric hallucinations can be observed, vivid dreams, nightmares, confusion, paranoia, and manic states, depending on the dose. The co-administration of other dopamine agonists such as quetiapine or clozapine can cause the appearance of compulsive behaviors, nymphomania, and propensity to develop drug addiction (Jankovic & Aguilar, 2008).

Surgery for PD has evolved rapidly and now includes destructive lesions and deep brain stimulation (DBS). Surgery often does not benefit those with atypical parkinsonism or with prominent non-motor complications (Schapira, 2007). Pallidotomy can provide long-term improvement in contralateral dyskinesia and some improvement in bradykinesia and rigidity in patients (Lang et al., 1997). DBS avoids the need to make a destructive brain lesion and can be used for bilateral procedures with relative safety. Also the stimulator can be adjusted to maximize benefits and reduce adverse effects. DBS consists of pacemaker assisted stimulation of stereotactically placed electrodes, either in the STN or in the GP, so reducing imbalance in the basal ganglia motor circuitry (reviewed in Oertel, 2017). This procedure has been shown to be effective in very advanced PD patients and in those with early motor complications. Despite providing great benefits, similar to drug replacement therapies, this procedure does not stop

disease progression (reviewed in Schapira, 2007), albeit significantly reducing the use of additional therapies that can generate adverse effects (Oertel, 2017). Nevertheless, adverse events can be related with DBS, often depending to the intracranial procedure (Schapira, 2007).

Modern therapies include stem cell and gene therapies, although it is not clear whether people benefit from such procedures (Schapira, 2007). The use of fetal tissue is problematic in terms of low availability and high variability, and it is also associated with ethical concerns that vary between countries (reviewed in Parmar, 2018). The field has been investigating new sources of therapeutic stem cell and now generation of midbrain dopaminergic neurons from pluripotent stem cells appear feasible and new trials are approaching (Parmar, 2018). Nevertheless, this therapeutic approach remains controversial, and may not be beneficial given the progressive loss of dopamine cells, the difficulty of rewiring newly added cells in similar ways to lost neurons, and the possibility of spreading of misfolded priogenic proteins into the newly transplanted cells (Schapira, 2007; Torrent et al., 2015).

With growing research in genetic forms of PD, particularly mutations and multiplications of α-synuclein, and the hypothesis of propagating misfolded forms of α-synuclein, therapies targeting either aggregation of α-synuclein, or total levels of the protein are becoming a hot topic with some compounds currently in early phase clinical trials (Oertel, 2017). Additionally, compounds able to reduce or modify LRRK2 levels or activity, are promising for PD therapy, given the interaction of LRRK2 with other PD-linked proteins, and their suggested role in sporadic PD (West, 2015).

More limited is the management of non-motor symptoms or alterations not dependent on dopaminergic neuronal loss. The variety of additional drugs is high and dependent on the

individual phenotype, including modulator of the serotoninergic and noradrenergic systems. Because of the extent and complexity of such topic, this is not discussed in this work.

Briefly, is important to mention, the increase in complimentary therapy in the treatment of PD. Particularly certain activity, such as exercise and dancing, are proving quite beneficial in the management of both motor and non-motor symptoms. A variety of non-medical supportive therapies can be helpful, including speech therapy, physiotherapy, physical exercise, logopedic training, and more (Oertel, 2017). Patricia Needle, participant of the 'Dance for PD' project comments: "I am awed by the power of dance to transform and alleviate pain. Despite the steady advance of Parkinson's, we show up. We move. We laugh. We share our best selves". Possibly in future therapies we will be able to reduce the use of drugs to cure PD and similar diseases. For now, in this work, we aim to understand the cause and pathophysiology of PD at early stages, in order to prevent disease onset in the first place.

1.1.5 Epidemiology and etiology

The majority of PD cases are sporadic and idiopathic, meaning that the cause is unknown. The prevalence of PD is age-dependent, with ~1% of the population at the age over 65 years old and increasing to 4-5% in the individuals older than 85 years. The age of onset is typically 60-65 years old, with fewer cases of early-onset PD (EOPD; de Lau & Breteler, 2006). According to the reports from Parkinson Canada, nearly 100,000 Canadians have PD. The estimated prevalence rate is 100 to 200 every 100,000, with an incidence rate of 10 to 20/100,000 every year (from Parkinson Canada www.parkinson.ca Dec 27, 2017). These numbers are predicted to rise dramatically over the next 30 years. Additionally, PD causes enormous social and economic burden with the estimated annual cost of over $120 million nationwide, ranking as third among

the most expensive diseases for the healthcare (from Parkinson Canada www.parkinson.ca Dec 27, 2017).

Although correlated with aging, there are identifiable causes for many forms of parkinsonism. The event that for the first time suggested environmental factors may contribute to the etiology of PD was the recognition of an induced state of acute parkinsonism by accidental poisoning from 1-methyl-4-phenyl-1,2,5,6-tetrahydropyridine (MPTP, Langston et al., 1983). This compound was discovered accidentally in 1982, when a group of young drug addicts in California developed subacute onset of severe parkinsonism, caused by contamination of illicitly produced synthetic heroin with MPTP (Langston, 1983). The administration of MPTP was subsequently shown to model parkinsonism in both rodents and non-human primates. Not much later after the discovery of MPTP, several cases of PD were associated to pesticides, such as paraquat and rotenone (reviewed in Langston, 2017). More factors seems to favor the environmental nature of PD, including the fact that smoking and drinking coffee appears to be protective against development of the disease (Langston, 2006).

Genetics can also play an important role in PD development, if not being responsible for most cases, whether via direct gene mutations of gene variants increasing susceptibility to disease (Lesage & Brice, 2009). Nevertheless, a genetic basis for PD had long been controversial. Twin studies measuring concordance rates in monozygotic and dizygotic twins indicate that genetics plays a greater role in younger onset patients than in patients with onset greater than age 50 years (de Lau & Breteler, 2006). That said, in the last years several gene mutations have been discovered to cause PD in a number of families (reviewed in Trinh & Farrer, 2013). Genetic causes may contribute to 10% of all cases of PD (reviewed in Klein & Westenberger, 2012). They may present either as autosomal dominant or recessive disorders.

The former are generally more similar to idiopathic PD, while the autosomal recessive forms present mostly as EOPD (Klein & Westenberger, 2012). A long list of genes have been identified so far, as listed in Table 1.1 and described in better detail in the following paragraphs.

1.2 Genetics of PD

The term PD encompasses a variety of clinical presentations, due to a multitude of factors, for which genetic causes are arguably some of the best defined. Although familial aggregation of the disease has been consistently noted, heritability estimates that are based on twin studies do not favor a genetic basis for the condition, and most epidemiological studies have focused on potential environmental risk factors. However, despite this unpromising background, in the past decade multiple mutations in genes have been described in families with a Mendelian pattern of PD inheritance (reviewed in Trinh & Farrer, 2013). Linkage mapping efforts have identified many causal mutations, and candidate gene and genome-wide association studies have nominated multiple susceptibility variants.

The notion of genetic factors contributing to the etiology of PD started in 1997, when the mutation in the α-synuclein (*SNCA*) gene was identified in familial PD (Polymeropoulos, 1997). Since then, studies of PD-linked mutations and PD-associated risk loci have flourished. PD is categorized into sporadic and familial PD, with the latter accounting for 10%-15% of PD cases (Gasser, 2009; Klein & Westenberger, 2012). Linkage analyses have discovered mutations in the *SNCA* gene related to PD including both missense point mutations (Appel-Cresswell et al., 2013; Krüger et al., 2001; Lesage et al., 2013; Polymeropoulos, 1997; Proukakis et al., 2013; Zarranz et al., 2004) and gene multiplication (Chartier-Harlin et al., 2004; Singleton et al., 2003).

There are several other genes linked to familial PD, among others LRRK2 (Zimprich et al., 2004), Parkin (Kitada et al., 1998), DJ-1 (Bonifati et al., 2002; Djarmati et al., 2004), PINK1 (Valente et al., 2001), ATP13A2 (Ramirez, Tonegawa, & Liu, 2013), PLA2G6 (Paisàn-Ruìz et al., 2005), and more recently VSP35 (Vilariño-Güell et al., 2011b; Zimprich et al., 2011) and DNAJC13 (also known as RME8; Vilariño-Güell et al., 2014).

Of particular interest is the role of several of these proteins in similar pathways, suggesting a common mechanism for PD, at least for the genetic forms. For instance, LRRK2, VPS35, and RME8 share some functions in endosomal trafficking, synaptic vesicle formations, and neurotransmitter release (Vilariño-Güell et al., 2014). All of them have an important role in mitochondrial function and autophagy linking them to other important proteins such as PINK1 and parkin. Some of these interactions of relevance for the work described here are shown in Figure 1.2, suggesting interaction between LRRK2, VPS35, RME8, and SNCA in the release and recycling of synaptic vesicle, either by direct trafficking of proteins and/or vesicle formation, or by phosphorylating proteins that are necessary for this machinery. This includes the big family of Rab proteins. Rab GTPases comprise ~70 family members in humans, and they are key players in all forms of intracellular vesicular trafficking events (Rivero-Ríos et al., 2016; Stenmark, 2009). Apart from Rab7L1, several other Rab family members have been associated with PD pathogenesis. For example mutations in Rab39b (PARK21 locus) predispose to PD in humans (Giannandrea et al., 2010; Wilson et al., 2014; Mata et al., 2015).

In the following section and briefly in Table 1.1, I describe the most common mutations and the importance in PD pathophysiology, with a separate section dedicated to VPS35, being the main focus of this work.

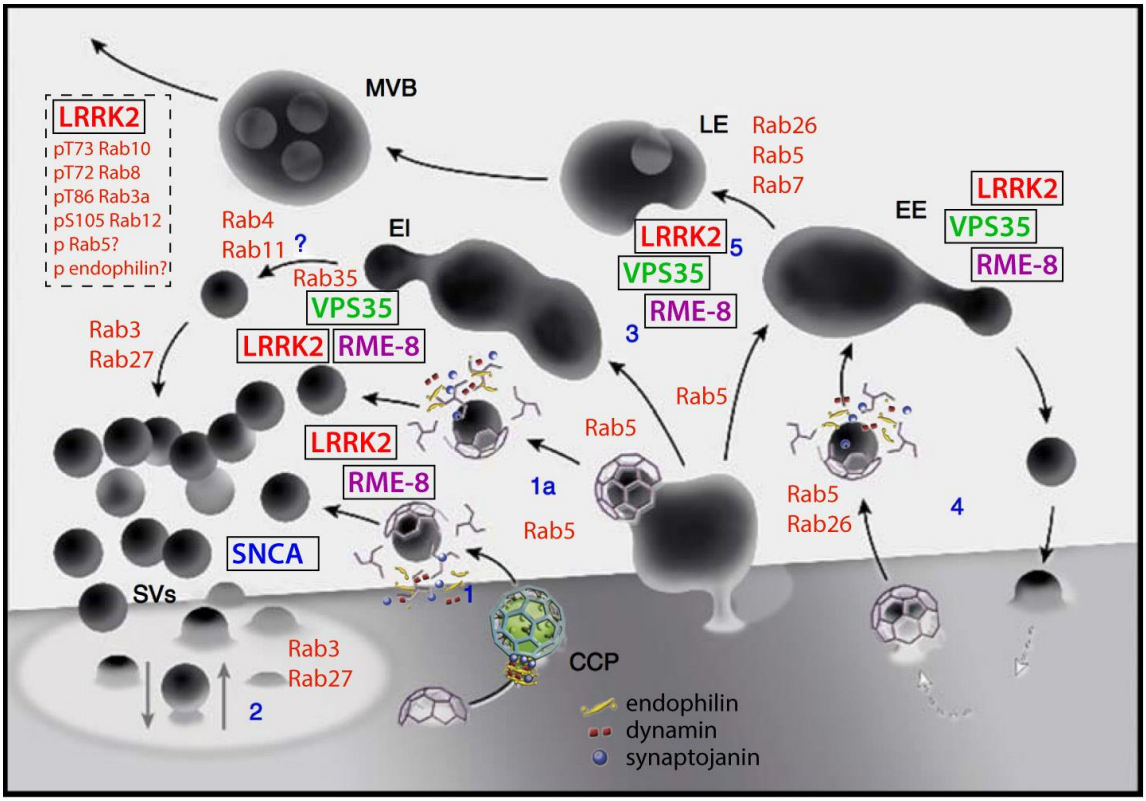

Figure 1.2 Schematic of interaction of proteins genetically associated with PD.
Membrane traffic in axon terminals illustrating endocytosis of synaptic vesicle (SV) membranes via clathrin-coated pits (CCP) from the plasma membrane deep infoldings (1 and 1a), "kiss and run" (2), and bulk endocytosis (3) followed by vesicle formation via unknown mechanisms (?) from endocytic intermediates (EI). This recycling is interconnected with housekeeping membrane recycling (4) involving endocytosis, canonical early endosomes (EE) and traffic to the cell body (5) via late endosomes (LE) and multivesicular bodies (MVBs). Rab GTPases implicated in the steps are show in red. Proteins known to carry familial PD mutations (VPS35, RME8, LRRK2 & SNCA) are boxed. Membrane fission and clathrin uncoating is performed by endophiln, dynamin and synaptojanin. Clathrin removal is regulated by RME-8, which facilitates Hsc70 binding. LRRK2 binds clathrin. VPS35 and RME8 are likely involved in the endosomal sorting steps regulating the retrieval of synaptic vesicle membranes and proteins from EE (5), IE to the cycle (?) and LE and MVB housekeeping pathways. LRRK2 and RME-8 co-immunoprecipitate with VPS35. LRRK2 contains GTPase and kinase activities, with an increase in kinase activity produced by PD mutations. A partial list of LRRK2 substrates and putative substrates, with the specific residues where known, is shown (dashed box). LRRK2 potently phosphorylates a subset of Rabs. Endophiln is a putative LRRK2 substrate, and dynamin is a potential LRRK2 disease modifier. A working hypothesis is that LRRK2 hyperphosphorylation impairs Rab5 to Rab7 conversion of EE-LE (5), increasing availability of vesicles in (3) and altering release. VPS35 (and potentially RME8) mutations produce similar increases in vesicle release/availability. Increased vesicle availability, but decreased LE clearance may result in a lack of efficient degradation and protein quality control (in line with other roles of VPS35/LRRK2 in lysosomal degradation & autophagy) and reduced quality control of active cycling proteins/membranes including α-synuclein (SNCA). Alterations to release may be intrinsically toxic through aberrant transmission or accelerate α-synuclein secretion/re-uptake/pathogenic seeding and spread. Image provided by Austen Milnerwood (adapted from: Binotti 2016, Inoshita 2015, Saheki & De Camilli 2012).

Table 1.1. List of mutations and variants associated with PD

Gene	Disorder	General features	Pathological features	References
SNCA	EOPD and classical PD	AD. Several mutations. Duplication, triplication.	Neuronal degeneration in SN and LC, widespread LB in cortex and brainstem	Polymeropoulos, 1997; Krüger et al., 2001; Zarranz et al., 2004; Lesage et al., 2013; Proukakis et al., 2013
Parkin	EOPD	AR. Several mutations, including sporadic cases	No LB, loss of neurons from SN, neurofibrillary tangles in cortex and brainstem	Kitada et al., 1998
DJ-1	EOPD	AR	LB with SN and LC neuronal loss	Bonifati et al., 2003; Djarmati et al., 2004
PINK1	EOPD	AR. Several mutations. Most common cause of EOPD	Neuronal loss in SNpc and LB in brainstem, SNpc and nucleus basalis of Meynert	Valente et al., 2001
LRRK2	Classical PD	AD. Several risk-conferring variants and disease causing mutations	Heterogeneous: LB in brainstem & loss of neurons in SN. Some cases: neurofibrillary tangle and nigral loss without LB	Zimprich et al., 2004; Paisàn-Ruìz et al., 2005
VPS35	Classical PD	AD. Most common mutation: D620N	No pathology information to date	Vilariño-Güell et al., 2011; Zimprich et al., 2011
DNAJC13	Classical PD	AD. Controversial linkage	LB and nigral loss	Vilariño-Güell et al., 2014
RAB39B	EOPD and X-linked intellectual disability	Loss of gene and missense mutation	Extensive dopaminergic loss in SN and classic LB disease	Giannandrea et al., 2010; Wilson et al., 2014; Mata et al., 2015
GBA	Gaucher's disease and parkinsonism	Risk factor	If parkinsonism present, mild Gaucher's symptoms. Classic PD presentation.	Neudorfer et al., 1996; Tayebi et al., 2003
MAPT	Parkinsonism and PSP	Risk factor		Fung et al., 2006; Kalinderi et al., 2009

EOPD = early onset PD, AD = autosomal dominant; AR = autosomal recessive; LB = Lewy Bodies; SN = substantia nigra; LC = locus coeruleus. Adjusted from Ferreira & Massano, 2017)

1.2.1 Recessively inherited disease

Parkin

The protein Parkin is encoded by the PARK2 gene in humans. The precise function of this protein is unknown; however, it is a component of a multiprotein E3 ubiquitin ligase complex which is part of the ubiquitin-proteasome system that mediates the targeting of proteins for degradation. It has been shown to interact with PD-linked proteins, such as PINK1, and to be involved in mitochondrial dysfunction (Narendra & Youle, 2011). Mutations in the gene are known to cause a familial form of PD known as autosomal recessive juvenile Parkinson's disease (AR-JP). Its defect may interfere with the ubiquitin-mediated proteolytic pathway leading to death of nigral neurons (Kitada et al., 1998).

Point mutations are the most common genetic lesions in parkin, although exonic rearrangements, deletions and duplications are also common (Mata, Lockhart, & Farrer, 2004). Patients with homozygous exonic deletions leading to complete loss of parkin expression show selective loss of dopamine neurons in SN without LB or neurofibrillary tangle (tau) pathology, in contrast to that described in patients with heterozygous mutations (Pramstaller et al., 2005). These different outcomes might be mutation-specific, but, as shown also for LRRK2 mutations, different end-stage pathologies might share the same primary cause.

DJ-1

DJ-1 is a protein which in humans is encoded by the PARK7 gene. PARK7 belongs to the peptidase C56 family of proteins. DJ-1 is a member of the ThiJ/PfpI family of molecular chaperones (Gasser et al., 2009; Moore et al., 2006). It acts as a redox-sensitive chaperone, apparently protecting neurons against oxidative stress and cell death. PD-associated mutations

cause DJ-1 loss of function upon defective dimer formation or lack of expression (Moore et al., 2003). Defects in this gene are the cause of autosomal recessive early-onset PD. Two genetic alterations have been found: deletion of several exons, which prevents the synthesis of the protein, and a point mutation that makes the protein less stable and promotes degradation through the ubiquitin-proteasome pathway, thereby reducing the amount of DJ-1 to low or absent levels (Bonifati et al., 2002).

PINK1

Homozygous mutations in PTEN-induced kinase 1 (PINK1) were originally found to co-segregate with early-onset parkinsonism in a family-based linkage study (Valente et al., 2001). Mutations were then identified in 1-2% of cases of early-onset disease (Hatano et al., 2004). The function of PINK1 is not fully understood. It appears to help protect mitochondria from malfunctioning during periods of cellular stress. Two specialized regions of PINK1 are essential for the protein to function properly. One region, the mitochondrial-targeting motif, serves as a delivery address. Another region, called the kinase domain, probably carries out the protein's protective function. The kinase domain sequence is shared with the Ca2+/calmodulin family of serine-threonine kinases (Valente et al., 2001).

There are accepted hypotheses that parkin and PINK1 are engaged in a common signaling pathway, with PINK1 working upstream of parkin.

1.2.2 Dominantly inherited disease

α–synuclein

The first gene discovered to be mutated in a family with PD is SNCA (mutation p.A53T), coding for the protein α–synuclein (Polymeropoulos, 1997). Interestingly, α–synuclein has been found as the main protein component of Lewy pathology (Spillantini et al., 1997).

Individuals with PD who have a mutation in *SNCA* have similar clinical course and pathologic presentation to those with idiopathic PD, including responsiveness to levodopa and the presence of Lewy bodies (Farrer et al., 2004).

Mutations in *SNCA* are not a common cause of familial PD (Farrer et al., 1999). *SNCA* genomic multiplications, including triplications and duplication, have also been described (Singleton et al., 2003; Chartier-Harlin et al., 2004; Ibáñez et al., 2004). SNCA dosage is correlated with mRNA and protein expression in the brain, and associated with age of onset and disease duration (Farrer et al., 2004). These data suggests mutant α–synuclein behaves differently from wild-type protein in a quantitative rather than a qualitative manner.

α–synuclein is specifically regulated in a discrete population of presynaptic terminals of the brain during a period of acquisition-related synaptic rearrangement and has potential roles in learning, synaptic plasticity, and dopamine synthesis (reviewed in Stefanis, 2012). It has been shown that it significantly interacts with tubulin, and may have activity as a potential microtubule-associated protein, like tau (Alim et al., 2004).

Recent evidence suggests that it functions as a molecular chaperone. Indeed, there is growing evidence that α-synuclein is involved in the functioning of the neuronal Golgi apparatus and vesicle trafficking (Lotharius et al., 2002; Sidhu et al., 2004), via interaction with Rab proteins (Gitler et al., 2008).

LRRK2

Mutations in LRRK2 gene have emerged as the most common genetic determinant of PD (Healy et al., 2005; Zimprich et al., 2004) accounting for 2-6% of hereditary PD and 1-2% of sporadic (Brice, 2005; Healy et al., 2008; Lesage et al., 2006). Seven pathogenic LRRK2 mutations have been confirmed across different studies, including p.G2019S, p.I2020T, p.N1437H, p.R1441G/C/H, and p.Y1699C (Trinh & Farrer, 2013).

The vast majority of LRRK2-linked cases display neuropathology typical of sporadic PD, characterized mainly by a dramatic loss of dopaminergic neurons in the SNpc (Giasson et al., 2006) and LB disease (Ross et al., 2006). Patients harboring the G2019S mutation are clinically indistinguishable from sporadic PD cases (Aasly et al., 2005). Interestingly, tau pathology appears to be more common in LRRK2-PD, either accompanying α-synuclein aggregation or in some case instead of typical LB (Rajput et al., 2006).

LRRK2 contains several domains, including a Ras/GTPase-like, a C-terminal of Roc, a kinase, and a WD40 domain, often flanked by N-terminal and C-terminal cysteine-rich domains (Gilsbach & Kortholt, 2014).

LRRK2 is present largely in the cytoplasm and is widely expressed in the brain and peripheral tissues, with the highest mRNA abundance in kidneys, lungs and lymph nodes.

LRRK2 is part of a functional protein network that controls synaptic vesicle trafficking within the recycling pool by interacting with a subset of presynaptic proteins. Its function is linked to the regulation of synaptic vesicle protein localization or synaptic vesicle trafficking (Shin et al., 2008; Matta et al., 2012; Beccano-Kelly et al., 2014). Moreover, electrophysiological properties as well as vesicular trafficking in the presynaptic pool depend on the presence of LRRK2 as an integral part of presynaptic protein complex (Piccoli et al., 2011).

At present, the prevailing hypothesis concerning the role of LRRK2 in PD is that an increase of its kinase activity (e.g. achieved by introducing the G2019S mutation and others) represents a significant pathogenic mechanism (West, 2015). While numerous are the proteins shown to be phosphorylated by LRRK2, many others substrates remain unidentified, thus leaving uncertainties on the actual weight of the activity of phosphorylation. Among these, recently a broad number of Rab proteins have been found to be directly phosphorylated by LRRK2 and may also interact with other PD-linked proteins, such as VPS35 and PINK1 (Ferreira & Massano, 2017; MacLeod et al., 2014; Steger et al., 2016). It has also been shown how LRRK2 can autophosphorylate itself, possibly influencing protein stability (Greggio et al., 2006; Sheng et al., 2012; West et al., 2005).

Several studies have reported possible interactions of LRRK2 with macroautophagy, a process that involves sequestration of portions of cytosol in double-membrane vesicles or autophagic vacuoles that then fuse with lysosomes (Mizushima, Levine, Cuervo, & Klionsky, 2008). Thus, LRRK2, frequently involved in the formation of protein-protein interactions, can undergo degradation in lysosomes via chaperone-mediated autophagy (Orenstein et al., 2013).

DNAJC13

Recently, an asparagine to serine (p.N855S) substitution on the DNAJC13 protein, also known as receptor-mediated endocytosis 8 (RME8) has been found (Vilariño-Güell et al., 2014). Most about RME8 role is unknown, although it is clear the importance of this protein in endosomal trafficking, possibly in similar and overlapping mechanism as VPS35. The role of RME8 in PD remains still controversial (Farrer, Milnerwood, Follett, & Guella, 2017), but this discovery highlights once again a temporal and functional interaction that connects synaptic exo- and

endocytosis, vesicular trafficking, endosomal recycling and the endo-lysosomal degradative pathway (Freeman et al., 2014; Piccoli et al., 2011; Schreij et al., 2015; Seaman & Freeman, 2014; Vilariño-Güell et al., 2014). Alterations to either of the proteins involved in these processes, whether LRRK2, VPS35 or DNAJC13, among others, lead to a similar parkinsonism to idiopathic PD (Aasly et al., 2005; Ferreira & Massano, 2017; Vilariño-Güell et al., 2011, 2014), suggesting a possible common mechanism across all forms of PD.

1.3 Vacuolar protein sorting 35

Our group and others, previously linked a pathogenic aspartic acid to asparagine (p.D620N) substitution in VPS35 to dominantly-inherited late-onset parkinsonism, a form of PD that is clinically indistinguishable from idiopathic PD (Struhal et al., 2014; Vilariño-Güell et al., 2011b; Zimprich et al., 2011). To date, more than 61 patients with PD have been described carrying *Vps35* p.D620N, with a frequency estimated to be 1.3% and 0.3% in familial and sporadic PD, respectively (Deutschländer, Ross, & Wszolek, 2017). Other mutations on VPS35 have been identified since, however proof that these are truly pathogenic remains equivocal (Deng, Gao, & Jankovic, 2013; M. Sharma et al., 2012).

VPS35 is a core structural component of the retromer trimer that, together with VPS26 and VPS29, forms a functional pentamer with pairs of sorting nexin proteins, typically SNX1 or 2 with SNX5 or 6. A well characterized role of retromer is to recycle transmembrane cargoes from recycling endosomes back to the plasma membrane or to *trans*-Golgi network (TGN; Spang, 2011), as well as trafficking to lysosome for degradation (Figure 1.3).

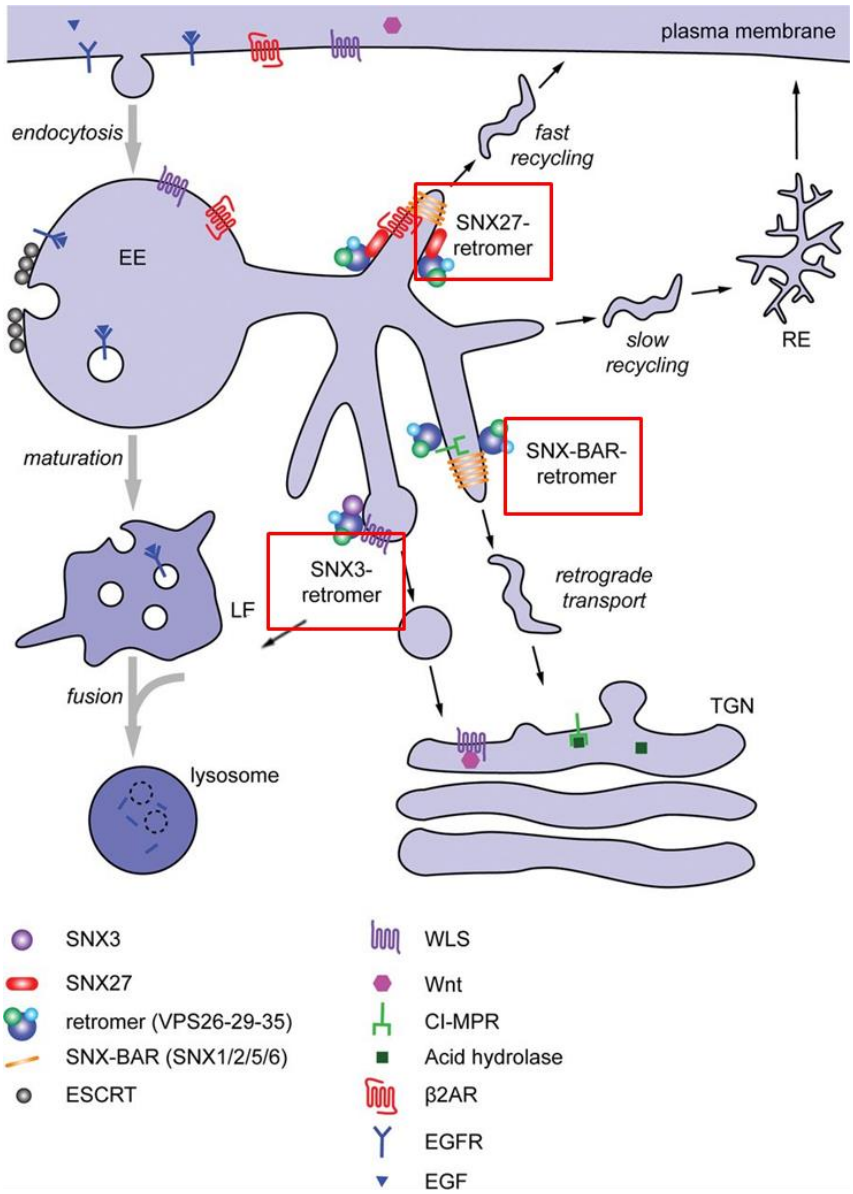

Figure 1.3 Retromer function in endosomes
Schematic representing the retromer role in endosomal trafficking. Squared are the main directions of trafficking from endosomes to surface (top), to TGN (middle), and to lysosome for dregadation (bottom). Image adapted from Gallon & Cullen, 2015.

The TGN is the last sorting station of the secretory pathway from which soluble or membrane proteins and lipids are sorted for subsequent transport to different destinations: the cell surface, the endosomal system and synaptic domains in neurons (Anitei et al., 2010). This

includes transmembrane proteins cycling between the TGN and endosomes, such as mannose-6-phosphate receptors (MPR; Bonifacino & Hurley, 2008; Anitei et al., 2010).

The retromer complex is implicated in the recycling of receptors needed for neurotransmission, to name a few, β-adrenergic receptors, GluA1-subunit-containing AMPA-type glutamate receptors, and D1R (Temkin et al., 2011; Zhang et al., 2012; Choy et al., 2014; Munsie et al., 2015; Tian et al., 2015; Wang et al., 2016). However, how dysfunction of retromer-mediated trafficking may alter nigrostriatal function and dopaminergic transmission is unknown. In addition to MPR recycling, retromer function is necessary for normal endocytosis, as in the case of progranulin (Anitei et al., 2010; Hu et al., 2010), associated with fronto-temporal dementia, and for processing of the amyloid precursor protein (APP; Vieira et al., 2010), associated with Alzheimer's Disease. Moreover, the retromer complex has important roles in actin cytoskeletal organization, synapse formation, Wnt signaling, mitochondrial peroxisome trafficking, and nuclear export (Attar & Cullen, 2010).

The D620N mutation lies within the binding site of VPS35 with other proteins, such as VPS29 and even CIMPR, although not affecting binding with these proteins (reviewed in Mohan & Mellick, 2016). Trafficking alterations with mutant VPS35 may be dependent on interaction with other complexes, such as the WASH complex, particularly with the protein FAM21. The affinity with which VPS35 binds to the FAM21 tail is reduced in cells expressing the D620N mutation (Zavodszky et al., 2014).

The discovery of VPS35 mutations in PD provides a compelling genetic link for the retromer in neurodegeneration. Endosomal trafficking appears to be a common pathway disrupted in neurodegenerative diseases. Indeed, protein trafficking, recycling and degradation

are essential for the creation and maintenance of neuronal architecture, synaptic plasticity and connectivity (Lasiecka & Winckler, 2011; Sann, Wang, Brown, & Jin, 2009).

1.4 Models of parkinsonism

The discovery of genetic and environmental components in PD etiology has made possible the generation of numerous animal models. Each model has its own specific features and limitations, and the choice of the most appropriate depends on the specific question that has to be answered.

The choice of species is dependent on the specific question. Mice are common because as mammals they are closely related to humans, can have up to 8-10 offsprings per litter, and a litter every one-two months, well-developed genetic manipulation technologies, and low costs due to small size, fast generation time and short lifespan. *Drosophila* and *C. elegans* are also quite common because they are easy to genetically manipulate, have a high reproductive rate and short life-span. Experiments can be performed within weeks in several generations of animals with identical genetic backgrounds, reducing variability between subjects, to detect disease alterations in a statistically significant manner (reviewed in Hirth, 2010). Non-human primates are the closest to humans in terms of life-span and brain organization, but their use is not as common given the costs of housing and difficulty of experimentation. Nevertheless, primates are a necessary step for drug screening before translation to clinical trials (Didier et al., 2016).

In order to be both a good model of human PD and a good test subject for new therapies, the ideal animal model should have a number of characteristic features. Phenotypes should be age-dependent and progressive, since degeneration usually begins in late adulthood in PD. In addition to the eventual loss of dopamine neurons, there should be motor dysfunction including slowness of movement, rigidity, resting tremor, and postural instability that is responsive to

dopamine replacement therapy. Another key determinant of this disorder is the presence of LB and LN that contain a-synuclein and ubiquitin-proteasomal proteins amongst others. However, some genetic forms of PD do not have LB, including some patients with parkin and LRRK2 mutations. Despite this idealistic view of the perfect animal model, is important to note that is difficult to obtain in animals, given differences among species, especially when compared to humans. Mainly, most animals used for models do not live a life long enough to create the background for neurodegeneration such as what we see in PD and similar disorders. This may not be the correct approach. Indeed, the choice of the most appropriate model depends on which hypothesis has to be tested.

Most recently, growing evidence supports the notion that a disruption of synaptic activity, occurring at nerve terminals, represents the primary event in disease pathogenesis, with subsequently retrograde cell body degeneration (Volta et al., 2017; Yue et al., 2015). With this idea in mind more recent models focus on mild modifications. This can be achieved with a monogenic mutation, allowing us to study early alterations in the disease, rather than classic neuronal loss seen in later stages of PD.

In the next few sections I give an overview of the most common animal models of parkinsonism, for a better understanding of the reasoning behind the generation of the animal model focus of this study.

1.4.1 Toxin-treated rodent models

Toxin models have been widely used over the years, since they provide means to replicate pathological and phenotypic features of late-stage disease. These models usually target the dopaminergic nigrostriatal neurons, causing cellular dysfunction and death.

The false neurotransmitter 6-hydroxydopamine (6-OHDA) has been used to produce nigral degeneration in mice, rats, cats and primates. Since it does not cross the BBB the standard approach is to inject 6-OHDA in one side of the brain to create a unilateral lesion. This is then evaluated by administration of amphetamine, which induces ipsilateral rotations, i.e. the animal starts rotating 'away from' the lesion. This rotational behavior can be reversed, for example by treatment with dopaminergic stem cells that restore normal circuitry (Bové et al., 2005). 6-OHDA models have been extensively used to understand changes in circuitry during dopaminergic neurons loss, and are still widely used to explore treatment-induced dyskinesia (Cenci & Lundblad, 2007; Aristieta et al., 2012; Sgroi, Kaelin-Lang, & Capper-Loup, 2014). Advantages of such models include high replicability, precision of administration and localized lesions (Tieu, 2011).

The pesticide rotenone can also be used to create an animal model, as it inhibits complex I of the mitochondrial electron-transport chain. Greenamyre and his group produced a model of PD by infusing rats intravenously with rotenone (Betarbet et al., 2000). The rats developed progressive degeneration of nigrostriatal neurons as well as cytoplasmic inclusions reminiscent of LBs. They also exhibited bradykinesia, postural instability and an unsteady gait, all of which improved after treatment with the dopamine agonist apomorphine (Betarbet et al., 2000). Other compounds that have been shown to produce selective degeneration of dopaminergic neurons include paraquat and trichloroethylene, both of which have been implicated in the etiology of human PD (Bové et al., 2005). However, there is substantial variability in all these models, which limits their usefulness for therapeutic development.

The best characterized toxin-based model of PD is based on the administration of MPTP, inhibiting part of the electron-transport chain in dopaminergic neurons of the SN (Nicklas et al.,

1985; Przedborski & Jackson-Lewis, 1998). This leads to a reduction in ATP generation, but a more important effect might be an increase in free-radical production. It has therefore proved useful, although limited, to study the striatal circuitry involved in the pathophysiology of the disease. MPTP also causes loss of locus coeruleus neurons, which are particularly vulnerable to the pathologic process, whereas other neurons — such as those of the dorsal motor nucleus of the vagus and nucleus basalis of Meynert — are spared. Acute administration of MPTP does not cause LB formation, although chronic administration produces synuclein inclusions. Overall, although a large number of therapeutic approaches have been tried in the MPTP model, its predictive value for humans has been inconsistent (Beal, 2010).

Even though toxin-based models are convenient ways to quickly replicate much of the cellular loss seen in PD, the extent to which they effectively and reproducibly mimic the human condition is controversial. Particularly, the induced neurodegeneration induces a massive loss of nearly 70-80% of dopaminergic neurons, making it difficult to explore early dysfunction and progression (reviewed in Beal, 2010), and of little or no relevance to disease etiology.

1.4.2 Genetic rodent models

As an alternative to toxins, newer animal models have been used by genetic technologies, facilitated by a greater understanding of the genetic basis of PD. One of the major drawbacks of the traditional models is the lack of LB pathology. Thus, different rodent models have been developed with the aim of reproducing neurotoxicity and recapitulating the main features of PD. The outcomes and phenotypes from these models have been inconsistent.

α-synuclein is a major structural moiety of LBs. Mice overexpressing wild-type α-synuclein develop progressive accumulation of α-synuclein and ubiquitin-immunoreactive

inclusions in the neocortex, hippocampus and SNpc (Masliah et al., 2000). The inclusions are composed of fine granular material, but lack the fibrillar aggregates that are characteristic of actual LB. Dopaminergic neurons within the SNpc are spared, although there is a loss of dopaminergic terminals in the striatum. A53T transgenic mice exhibit a full range of pathology including α-synuclein aggregation (oligomers and fibrils), phosphorylation and progressive age-dependent neurodegeneration (Lee et al., 2002). These mice, however, do not show a loss of substantia nigra dopaminergic neurons, and motor deficits are caused by a loss of brain stem neurons and anterior horn motor neurons of the spinal cord, dependent on the use of the murine prion protein promoter, making these mice a closer model of spinal cord disease than PD (Lee et al., 2002). Amongst the many α-synuclein mouse models, the Thy-1 α-synuclein overexpressing mice are the best characterized. Thy-1 mice present with early increase in extracellular dopamine, correlating with hyperactive behaviour, and later decline in dopamine levels and hypoactivity, including progressive formation of insoluble proteinase K resistant α-synuclein aggregates (Lam et al., 2011; Rockenstein et al., 2002). Alongside described alterations, the Thy-1 mouse presents with cognitive deficits and anxiety-related alterations at a young age, including sleep disturbances and social recognition deficits. They also have gastrointestinal alterations, olfactory dysfunction, and immuno-related changes (reviewed in Chesselet et al., 2012).

Parkin knock-out mice show subtle abnormalities in both the dopaminergic nigrostriatal and the locus coeruleus noradrenergic systems. Some mutations of parkin appear to be autosomal dominant and, when produced by overexpression of mutant human parkin using a bacterial artificial chromosome (BAC) transgenic model, lead to progressive degeneration of dopaminergic neurons, supporting the idea that some parkin mutants might act in a dominant-negative fashion (Lu et al., 2009).

As with parkin, PINK1 knock-out and DJ-1 knock-out mice do not exhibit any major abnormality, and the number of dopaminergic neurons and level of striatal dopamine are unchanged (Beal, 2010). *DJ-1*-knock-out mice do, however, show increased vulnerability to MPTP toxicity (Beal, 2010).

To date, mouse models of LRRK2 mutations have so far failed to produce neurodegeneration of dopaminergic neurons (Beal, 2010). A mouse overexpressing the LRRK2 R1441G mutation by the use of BAC (Li et al., 2009) developed age-dependent motor deficits leading to immobility and impaired rearing, that was responsive to L-DOPA and apomorphine. In addition, there was impaired dopamine release in the striatum at ten weeks of age. Surprisingly, however, there was no loss of striatal dopamine or dopaminergic neurons within the SNpc. In contrast to the typical LBs, the major pathology observed in these mice was axonal spheroids, composed of phosphorylated tau, which were seen in both the striatal and the cortical regions. These authors showed improved motor performance in hLRRK2-WT mice, which was associated with increased dopamine release in the striatum. In hLRRK2-G2019S animals, an age-dependent decrease in the content of the release and uptake of dopamine in the striatum occurs. These neurochemical changes, however, were not associated with neuronal degeneration or death. Finally, no motor deficit was observed up to the age of 12 months (Li et al., 2009). In LRRK2 animals carrying the G2019S mutation an abnormal exploratory behavior was observed, suggesting anxiety and/or fear (Winner et al., 2011), indicating non-motor behaviours can also be observed in certain models.

In another study, BAC hLRRK2 and G2019S-hLRRK2 mice showed lower levels of extracellular DA in the striatum, compared to non-transgenic controls (Melrose et al., 2010).

LRRK2 knock-out mice do not have a PD-like phenotype or impaired dopaminergic system, but do display alterations in exploratory and motor co-ordination behaviors (Hinkle et al., 2012). Loss of LRRK2 appears to have a positive impact on rotarod performance, although the mechanisms are unclear. LRRK2 knock-out mice show alterations in other organs, such as lungs and kidneys (Herzig et al., 2011), therefore negating a loss-of function effect of PD mutations, and questioning the safety of LRRK2 silencing therapies as a treatment for PD.

Acute G2019S-LRRK2 overexpression in a tetracycline transactivator (tTA) model in aged rats results in hyperactivity, hyperdopaminergia and impaired dopamine reuptake, phenotypes that are not observed in transgenic rats constitutively expressing the gene (Zhou et al., 2011). An additional BAC G2019S LRRK2 over-expressing rat model shows behavioural deficits without overt dopaminergic dysfunction up to 12 months of age (Walker et al., 2014). Transgenic rodent models developed to date, however, fail to achieve significant levels of LRRK2 overexpression in the SNpc and do not display dopaminergic neuronal loss.

More recent models focus on knock-in genetic strategy to avoid the confounds of random transgene insertion, overexpression artefacts or background endogenous proteins.

Knock-in models show a physiological expression of the proteins due to the mutation being in the endogenous mouse gene. With this strategy ‘genetically faithful’ models have recently been published. LRRK2 knock-in mice show age dependent dopamine alterations with early hyperdopaminergic function correlated with hyperactive behaviour, that later decreases to WT levels (Volta et al., 2017). This model does not show typical pathological signs of PD, including absence of neuronal degeneration or α-synuclein aggregation; however, LRRK2 G2019S knock-in mice show neurotransmission deficits in both dopamine and glutamate transmitter systems and latent tau phosphorylation (Yue et al., 2015; Beccano-Kelly et al., 2015;

Volta et al., 2017). Thus, G2019S knock-in mice provide a tool to study the etiology and early alterations in disease processes. Similarly, another G2019S LRRK2 KI model shows early hyperactivity, dependent on LRRK2 kinase function (Longo et al., 2014), accompanied by alterations in DAT and other components of the dopaminergic machinery (Longo et al., 2017). Although these models develop a robust behavioral phenotype, the lack of degeneration of dopaminergic neurons might limit their use in the development of therapeutic agents. The kinase domain of LRRK2, however, might prove to be a useful target for drug development, and could potentially be of benefit for patients with mutations in LRRK2, other familial forms, and sporadic PD (reviewed by West, 2015).

A line of *Vps35* p.D620N knock-in mice was recently reported without a behavioural phenotype, although striatal microdialysis revealed a reduction in evoked striatal dopamine in homozygous animals (Ishizu et al., 2016). Here I report an independent *Vps35* p.D620N knock-in mouse model (VKI) developed to preserve a physiological 1:1:1 stoichiometry of the retromer complex.

1.4.3 Non-rodent models

Other animals have been crucial in understanding of pathophysiology of PD, mostly providing information of the role of the many pathogenic mutations now associated with the disease. For instance, fly models have shown strong PD-related phenotypes, including reduced locomotion, loss of dopaminergic neurons, problems with reactive oxygen species, mitochondrial dysfunction, and protein aggregation (Feany & Bender, 2000; more rewieved in Whitworth, 2011). Fly models have also been successful because of a uniquely powerful genetic toolbox has allowed tissue or neuron specific mutant expression (Venken, Simpson, & Bellen, 2011).

LRRK2, VPS35, DJ-1 and others have been extensively studied in *Drosophila* models, leading to a greater understanding of the function of these proteins (Arranz et al., 2015; Korolchuk et al., 2007; Miura et al., 2014; Moore et al., 2006). Indeed, it was in a fly model that α-synuclein was associated with tau dysfunction, linking two pathological markers of the disease in a common pathway (Roy & Jackson, 2014). PINK1 was also shown to be upstream of Parkin, in the same pathway.

The importance of non-human primate models comes from their similarities with humans, in behaviour but particularly in brain specialization, including complex motor skills, visual development and cognitive abilities (reviewed in Izpisua Belmonte et al., 2015). With advances in genetic manipulation in non-human primates only recently within reach (Izpisua Belmonte et al., 2015), the majority of primates models of PD are surgical or toxin-based, with MPTP injected primates being the most commonly used. This model has been particularly valuable in the study and development of deep brain stimulation in the treatment of PD (Tass et al., 2011). Since the brains of non-human primates are anatomically very close to those of humans, disease states and the effects of medical and surgical approaches can be more faithfully modeled in non-human primates than in other species (Wichmann, Bergman, & DeLong, 2018).

While *in-vivo* studies are important to understand progression of the disease and develop treatments, mechanistic aspects of a disease often emerge from studies at the cellular and subcellular level. To this end, mammalian cell lines are often used, but recently the budding yeast *Saccharomyces cerevisiae* has shown itself as a valuable model providing insight into molecular mechanisms underlying PD (Gitler et al., 2008; Shin et al., 2008; Franssens et al., 2013; Dhungel et al., 2015). Similarly, cellular reprogramming of somatic cells to human pluripotent stem cells (iPSC) represents an efficient tool for *in vitro* modeling of human brain

diseases and provides an innovative opportunity to develop new therapeutic drugs. Patient-specific iPSC can be differentiated into disease-relevant cell types, including neurons, carrying the genetic background of the donor and enabling generation of a humanized cellular model of PD (reviewed in Torrent et al., 2015).

1.4.4 Limitations of current models

Yeast, worms, and fruit flies are useful for studying fundamental cellular processes involved in PD, and determining the function of proteins involved in the disease. Indeed, some of these factors are present across species, albeit important protein-protein interactions may not be evolutionarily conserved. In addition these small animal models cannot be used to study many of the clinical manifestations of the disease (reviewed in Potashkin, Blume, & Runkle, 2011). There are several excellent studies that have used dogs, cats and non-human primates for PD studies, but the ethical concerns and costs of such studies have limited their utility (Potashkin et al., 2011).

Rodents have been used more extensively but also have limitations. It remains unclear why there is no meaningful degeneration of dopaminergic neurons in any of the major genetic rodent models of PD. Most transgenic mouse models have failed in replicating a robust parkinsonian phenotype, degeneration of nigrostriatal dopaminergic neurons and LB, despite achieving aspects of these traits. Part of the problem with studying PD in animals is not simply the model that is chosen, but also the assays used to assess changes between the healthy and diseased state. When assessing behavioural changes in rodent models, it is important to keep in mind that although the neuroanatomical components underlying motor control may be similar for

humans and rodents, the manifestation of these motor deficits may be expressed differently between species (Potashkin et al., 2011).

Parkinsonian non-motor symptoms such as olfactory dysfunction, constipation, depression and cognitive impairments are seldom described in these these models. Nevertheless, non-motor symptoms have seldom been investigated, and their presence should not to be excluded. Many authors are put increasing emphasis on non-motor symptoms of PD, as they are particularly difficult to treat yet contribute greatly to the disability of patients with the disease.

Each model has different advantages and disadvantages. Despite the prevalent belief being that none of these models has reproduced key PD features, there is a strong need to discover and define the underlying mechanism of disease, and this can only be achieved by the generation and extensive evaluation of animal models.

1.5 Dopamine, locomotion and cognition in PD

In this section I describe the role of dopamine in locomotion as well as cognition, in healthy people and people affected by PD.

When the pre-frontal region of the cerebral cortex, which is generally involved in decision making and planning, determines that motor activity must be executed, it sends activating signals to the motor cortices. The motor cortices send activating signals to the direct pathway through the basal ganglia, which stops inhibitory outflow from parts of the GPi and the SNpr. The net effect is to allow the activation of the ventrolateral nucleus of the thalamus which, in turn, sends activating signals to the motor cortices. These events amplify motor cortical activity that will eventually drive muscle contractions. Simultaneously, in the indirect pathway, the motor cortices send activating signals to the caudate and putamen. The cells in these regions

once activated send inhibitory signals to the globus pallidus external (GPe), reducing its activity. The GPe normally sends inhibitory signals to the STN. On activation of the indirect pathway, these inhibitory signals are reduced, which allows more activation of the STN. STN cells can then send more activating signals to some parts of the GPi and SNpr. Thus, parts of these two nuclei are driven to send more inhibitory signals to the ventrolateral nucleus of the thalamus, which prevents the development of significant activity in the motor cerebral cortices. This behaviour prevents the activation of motor cortical areas that would compete with voluntary movement (reviewed in Pollack, 2001; schematic in Figure 1.1).

With the reduction in dopamine signal in the striatum, both pathways are affected and the final outcome is to increase the inhibition of thalamic activity hence reducing motor activity.

The lack of neuronal loss and the classic PD motor phenotype present a challenge for many animal models. Current understanding of dopamine function and its role in behaviour, in the presence of the disease or in healthy subjects, shows the importance of proper dopamine homoeostasis for several cognitive abilities. With the increasing importance of non-motor dysfunction in PD, animal models are now becoming an important instrument in understanding early stages of the disease. Despite genetic models lacking degeneration and pathology, they often present early dysfunction in neurotransmission that correlates with cognitive deficits (reviewed in Beal, 2010 & Blesa et al., 2012).

Anxiety is a common feature of PD that often appears years prior to motor symptoms. Several studies show dopamine regulation of cognitive function, and not just its involvement in motor activity. For instance, cocaine, which blocks DAT and increases extracellular time of dopamine (Kuhar, Ritz, & Boja, 1991), has an anxiogenic effect in rats (Rogerio & Takahashi, 1992). Further evidence has shown the involvement of the striatum in anxiety, i.e. the co-

occurrence of adolescent striatal development with the peak vulnerability of adolescents to anxiety disorders (reviewed in Lago et al., 2017). Moreover, the role of the striatum in behavioural processes that affect anxiety, such as attention, conditioning, predictive error and motivation, has extensively being studied (reviewed in Lago et al., 2017).

Similarly, RBD is a common non-motor symptoms that often appears a decade prior to motor symptoms and correlated neuronal loss (Goldman & Postuma, 2014). Of note, reduced DAT uptake has been shown in the putamen of incidental RBD patients (Iranzo et al., 2010, 2011).

Attention deficits are also associated with PD, and visuospatial deficits and impaired performance in behavioural switching tasks, have been associated with dopaminergic dysfunction (Rinne et al., 2000). Work from Rinne and colleagues found a correlation between reduced ^{18}F-DOPA uptake in the caudate and frontal cortex with attentional and working memory deficit in PD patients (Rinne et al., 2000). Further evidence supports dopaminergic deficit within the frontal cortex, alongside cingulate and the dorsolateral prefrontal cortex in brains from people with PD (Brück et al., 2005).

The role of dopamine in non-motor symptoms is in its infancy. Most available animal models have not been evaluated for non-motor dysfunction. Given the selective vulnerability and loss of dopamine neurons in PD, and role of dopamine in cognitive abilities, I hypothesized *Vps35* p.D620N may impair retromer-dependent recycling of specific cargos with consequent effects on dopaminergic neurotransmission. In this thesis I sought to investigate the potential for early physiological alterations and classic late-stage motor disturbances in a mouse model of VPS35 p.D620N parkinsonism, with the focus on the dopaminergic dysfunction. In this first characterization of this new mouse model I used common behavioural tests to address questions

related to motor and cognitive abilities of young and old mice, particularly focusing on early alterations seen in humans affected by PD, and behaviours related to dopamine dysfunction. For this reason I focused on tasks that may reveal alterations in the anxiety/fear-related behaviours, as well as deficits in cognitive flexibility and perseverance. Additionally I combined the use of different brain activity recording approaches, from *ex-vivo* fast scan cyclic voltammetry to *in-vivo* microdialysis, to evaluate dopamine release and function in the presence of the mutation in young and older animals. Overall I provide an extensive description of several early alterations that will be important to understand the mechanism of disease and possibly identify early markers and/or therapeutic interventions.

Chapter 2: Methods

2.1 VPS35 p.D620N knock-in mice and gene expression

Conditional and constitutive knock-in mice were generated by Ozgene PLC (Australia) using a gene targeting approach in C57Bl/6J embryo stem cells (Bruce4). Genetic engineering targeted the *VPS35* locus on murine chromosome 8 (85,260,392-85,299,802 reverse strand (GRCm38.p5); Ensemble genomic reference sequence ENSMUSG00000031696; NCBI mRNA reference sequence NM_022997.4). A floxed "mini-gene" consisting of: 1) splice acceptor, *VPS35* exon 15-17 coding sequence, a polyadenylation signal (pA), and; 2) a *PGK*-neomycin (neo)-pA selection cassette internally flanked by FRT sites, was inserted into intron 14. The 5' targeting arm spanning endogenous exon 15 was used to introduce the *VPS35* g.85,263,520 G>A (p.D620N) mutation. Conditional animals (denoted cVKI) have their endogenous gene (exons 1-14) spliced to the mini-gene cassette (exons 15-17, pA); the *PGK*-neo-pA selection cassette was removed by crossing to transgenic animals expressing FlpE-recombinase. Heterozygous cVKI mice were crossed to transgenic animals expressing Cre-recombinase to remove the floxed mini-gene cassette, enabling heterozygous constitutive VPS35 p.D620N expression (denoted VKI mice; Figure 1). Removal of the Cre transgene was achieved by selective breeding to C57Bl/6J stock in subsequent generations. Genotyping to ensure the absence of neo, FlpE- and Cre-recombinase transgenes, and to verify the presence of the *VPS35* g.85,263,520 G>A (p.D620N) mutation, was performed using a TaqMan® allelic discrimination assay on a 7900HT System (Applied Biosystems). Intron 14 - exon 15 of the modified genomic locus in homozygous VKI animals was ultimately confirmed by Sanger sequencing, using ABI 3730xls instrumentation (Applied Biosystems). The VKI strain has been deposited in Jackson Labs with open distribution supported by the Michael J Fox Foundation (*VPS35* knock-in: B6(Cg)-Vps35tm1.1Mjff/J).

2.2 Animals and tissue collection

For all experiments, only male animals were used. Wild-type (WT), heterozygous (het) and homozygous (homo) VPS35 p.D620N knock-in (VKI) mice were maintained for >5-10 generations, kept on a reverse cycle (light on from 7pm to 7am) and single-sex group-housed in enrichment cages after weaning at post-natal day 21. *Post-mortem* ear notches were taken for *post-hoc* genotyping (experimenter blind).

For protein, mRNA and cDNA analysis, mice were sacrificed by rapid decapitation. Samples of motor cortex, striatum, hippocampus, olfactory bulbs, and cerebellum were rapidly (<6min) dissected and all remaining tissue pooled as 'whole-brain'. Tissues were separately flash frozen in liquid nitrogen.

All experiments, including behaviour, perfusions and tissue collection, were performed in the morning between 8am and 11am, at time where mice are awake. The radial arm maze was the only test performed in the afternoon, so the operator could remove water from the animal cage and allow 5 hours of water deprivation before testing.

2.3 mRNA expression

To quantify *Vps35* expression, cerebellar RNA from 3 months old animals was isolated using RNeasy Kit (Qiagen) and reverse transcribed using High Capacity cDNA Kit (Applied Biosystems), according to the manufacturer's instructions. The reactions were incubated in a thermal cycler for 10 min at 25°C, 120 min at 37°C, 5 min at 85°C and then held at 4 °C. To determine the relative expression of *Vps35* we amplified by means of Real-time PCR using the 7900HT System with SYBR ® Green PCR Master Mix (Applied Biosystems) at 95°C for 10 min

followed by 40 cycles of 15 s at 95°C and 1 min at 57°C. The relative expression of mutant *VPS35* was analyzed with the ΔΔCt method, using the geometric mean of endogenous control genes, *Actb*, *Gapdh* and *Rpl19*. Primers sequences are available in Table A.1 in Appendix A .1. The fold change ($2^{-\Delta\Delta Ct}$) expression was normalized to the expression of the wild-type littermates.

2.4 Protein analysis

For Western blot analysis, dissected striatal brain tissue was lysed in HEPES buffer (20mM HEPES, 50mM KAc, 200mM Sorbitol, 2mM EDTA, 0.1% Triton X-100, 0.5% NP-40, pH 7.2; Sigma Aldrich) containing protease and phosphatase inhibitors (Roche), homogenized, and incubated (on ice, 45min, gentle agitation every 15 minutes). Lysates were cleared by centrifugation at 4000 x *g* for 12 mins at 4°C and supernatant was quantified by BCA assay (Pierce). Lysates were denatured in 1x NuPage LDS sample buffer (Thermo Fisher Scientific) and heated for 10 mins at 70 °C and 10-15 µg of protein was resolved by SDS-PAGE as described (Follett et al., 2014), or using NuPAge 4-12% Bis-Tris gel (Thermo Fisher Scientific) and transferred to PVDF membranes (EMD Millipore). Membranes blocked with 5% nonfat milk in Tris-buffered saline containing 0.1% Tween 20 (TBST) were probed overnight at 4°C with primary antibodies diluted in 3% BSA (Sigma-Aldrich) in PBS. The following day, membranes were washed in TBST (3×5 min) at room temperature (RT) followed by incubation for 1h at RT with horseradish peroxidase(HRP)-conjugated anti-mouse, rabbit, or Rat IgG (Santa-Cruz Biotechnology). Blots were washed in TBST (3×5 min) at RT, and developed using enhanced chemiluminescence plus reagent (Thermo Scientific) and imaged on a Chemi-Doc imaging system (Cell-Bio). Images were analyzed for band intensity with Image J software. The

following primary antibodies were used for WB: mouse anti-VPS35 (Abnova, H00055737-M02; 1:500); anti-GAPDH (Cell Signaling, 2118; 1:2000); anti-PSD95 (6G6-1C9, Thermofisher Scientific, MA1-045; 1:1000); anti-TH (Sigma-Aldrich, T2928; 1:2000); rabbit anti-mouse VMAT2 for WB (Phoenix Pharmaceuticals, Inc; 1:500), rat anti-DAT (EMD Millipore, MAB369; 1:500), rabbit anti-DARP-32 (Cell signaling, 2302S; 1:1000), mouse α-synuclein LB-509 (Abcam, ab27766; 1:1000), Rabbit anti-SERT (Synaptic Systems, 340 003; 1:1000), Rabbit anti-NET (Synaptic Systems, 260 003; 1:1000), and rabbit anti-D2 receptor (Millipore AB5084P; 1:1000). The detection of primary antibodies was achieved by probing membranes with Donkey anti-Rabbit or mouse IgG conjugated HRP (Santa-Cruz Biotechnology, sc-2318, sc-2313, respectively), or Rabbit anti-Rat IgG HRP (Abcam, ab6734. For *WES* analysis: lysates were probed by ProteinSimple *WES* automated capillary-based size sorting system as previously described (D. A. Beccano-Kelly et al., 2014); briefly, lysates were mixed with fluorescent master mix (ProteinSimple), heated (70°C for 10min) and loaded into manufacturer microplates containing primary antibodies (see below) and blocking reagent, wash buffer, HRP-conjugated secondary antibodies, and chemimluminescent substrate (ProteinSimple). Primary antibodies: VPS35 (Abnova H00055737-M02), VPS26 (a gift from J. Bonifacino, NICHD) and β-tubulin (Abcam ab6046). Data was analyzed on manufacturer-provided Compass software.

2.5 Immunohistochemistry

For ex-vivo imaging, mice were terminally anesthetized (sodium pentobarbital 240mg/Kg, i.p.) and intracardially perfused with PBS then 4% paraformaldehyde (PFA). Brains were extracted, post-fixed overnight (4% PFA, 4°C) then cryoprotected with increasing sucrose gradient (10%, 20%, 30% in PBS O/N, 4°C). Coronal slices (30µm) were obtained by cryostat. Where

necessary, antigen retrieval using 10mM sodium-citrate plus 0.05% Tween (pH 6; 30min, 37°C) was performed. Sections were rinsed with 0.1% Triton-X in 1x PBS (PBST; 3x10min), blocked in 3% milk in 0.03% PBST (30min, RT) followed by a second block in 10% normal goat serum (NGS) in 0.03% PBST (30min, RT). Primary antibodies: rabbit anti-synapsin1 (AB1543P, Millipore; 1:500), anti-VMAT2 (H-V008, Phoenix Pharmaceuticals; 1:500), mouse anti-PSD95 (MA-045, Thermo Scientific; 1:250), chicken anti-Tyrosine Hydroxylase (TH; ab76442 Abcam; 1:1000), goat anti-VPS35 (S-18, sc-55805, Santa Cruz; 1:250), Rat anti-DAT (N-terminal, MAB369, Millipore; 1:500), rabbit anti-DARP-32 (Cell signaling, 2302S; 1:1000), and mouse anti-α-synuclein LB-509 (Abcam, ab27766; 1:1000) were applied in 5% NGS + 0.01% NaN3 in 0.01% PBST; overnight 4°C) prior to washing (3x10min PBST) and secondary incubation with species specific Alexafluor IgG secondary antibodies (90min RT, Invitrogen; 1:1000). Tissues were washed again in 0.1% PBST (3 x 10min), then mounted using DAPI Fluoromount-G® (0100-20, SouthernBiotech). Images were acquired using a 60x oil objective on an Olympus Fluoview FV-1000 confocal laser scanning microscope (9 x 0.33um step size). Images were then stacked (three stacks of 3 individual images viewing 1um tissue depths), masked and binarized using FIJI ImageJ software (NIH, USA) and analyzed using Cell Profiler image analysis software (v.2.1.1). Individual puncta were quantified, and are defined as discrete, clearly defined, areas where the specific antibody has bound.

2.6 Stereological cell counts

For slices expressing TH-positive labelling in the SNpc, optical fractionator sampling was conducted on images acquired by confocal laser-scanning microscope (Olympus Fluoview FV1000, 60x oil) and whole-volume estimates produced from tiled images acquired on an EVOS

FL microscope, as described by stereology.info (MBF Bioscience). Dopaminergic neurons of the SNpc were identified by TH-positive immunolabeling, and reference to coronal images of The Mouse Brain in Stereotaxic Coordinates atlas (Franklin and Paxinos 3rd Ed., 2007). For our counting to encompass the full rostro-caudal extent of the relevant SNpc dopamine nuclei, a section-sampling fraction of 1/3 was used to analyze a total of ~10 sections for each brain. Average slice thickness was estimated expecting minimal shrinkage as the sections were parallel processed and mounted in aqueous medium. A guard height of 2μm was used with a counting frame height of 28μm. Counting frame size measured 159μm width (x) by 159μm height (y), which was chosen to include ~10-20 neurons per frame, and the position within the SNpc was roughly maintained across all sections in all animals sampled. The area-sampling fraction was determined by the counting frame area/SNpc area, as measured by tiled images and area measuring software on the EVOS FL microscope.

2.7 Microdialysis

Under isoflurane anesthesia, a CMA 7 microdialysis probe (1mm dialyzing membrane; Harvard Apparatus) was lowered into the mouse striatum according to the following coordinates: AP +0.5, ML +2.1 from bregma, DV -2.8 below dura as previously (Yue et al., 2015). The probe was secured to the skull by glass ionomer cement (Instech Laboratories) and a stainless steel screw. During surgery animals were given lidocaine prior to incision (30uL, s.q.), meloxicam (1mg/Kg, s.q.) and warm 0.9% saline (s.q.) at the end of the procedure. Following surgery, mice were allowed to recover and experiments were run 24h after probe implantation. Microdialysis probes were perfused at a flow rate of 1.5 uL/min with a modified Ringer's solution (in mM: NaCl 147, KCl 3, $MgCl_2.6H_2O$ 1.2 and $CaCl_2$ 1.2). Samples were collected every 15 min,

starting 2 hours after the onset of probe perfusion, into vials containing 2µL of 10mM acetic acid.

Dopamine and its metabolites (DOPAC and HVA) were measured by HPLC coupled to electrochemical detection (ALEXYS Neurotransmitter platform, Antec). Five microliters of sample were automatically injected (AS 110 Autosampler, Antec) onto an Acquity UHPLC BEH C18 analytical column (1 mm inner diameter, 10 cm length; Waters) perfused at a flow rate of 50µL/min (LC 110S pump, Antec) with a mobile phase containing 100mM phosphoric acid, 100mM citric acid, 0.1mM EDTA, 600mg/l octan sulphonic acid sodium salt and 8% acetonitrile (pH 3). Dopamine, 3,4-dihydroxyphenylacetic acid (DOPAC) and HVA were detected by means of an electrochemical detector (Decade II, Antec) with cell potential set at 0.8V vs. salt bridge. Retention times were: 2.57 ± 0.2 min for DOPAC, 3.82 ± 0.2 min for dopamine and 5.18 ± 0.2 min for HVA. Mice were euthanized after the experiment and brains collected to confirm probe placement by immunohistochemistry.

2.8 Dopamine evaluation from striatal tissue via HPLC

Striatal tissue was mechanically homogenized in a solution of 100uM EDTA and 0.1mM perchloric acid. Samples were cleared by centrifugation at 14000 x *g* for 10 mins at 4°C and supernatant separated from pellet, then dopamine and its metabolites measured by HPLC as above. Pellet was lysed in HEPES buffer (20mM HEPES, 50mM KAc, 200mM Sorbitol, 2mM EDTA, 0.1% Triton X-100, 0.5% NP-40, pH 7.2; Sigma Aldrich) containing protease and phosphatase inhibitors (Roche), homogenized, and incubated (on ice, 45min, gentle agitation every 15 minutes). Lysates were cleared by centrifugation at 4000 x *g* for 12 mins at 4°C and

supernatant was quantified by BCA assay (Pierce), to normalize monoamines levels to protein concentration.

2.9 Fast-scan cyclic voltammetry

FSCV was conducted in the dorsolateral striatum in 300μm thick coronal slices, as previously (Beccano-Kelly et al., 2015; Volta et al., 2017). Slices were perfused at RT with artificial cerebrospinal fluid [ACSF - containing in mM: 130 NaCl, 10 glucose, 26 $NaHCO_3$, 3 KCl, 1 $MgCl_2.6H_20$, 1.25 NaH_2PO_4 (monobasic monohydrate), 2 $CaCl_2$; pH 7.2-7.4, mOsm 290-310] and oxygenated (95% O_2, 5% CO_2) at RT for > 1h prior to experiments. Individual slices were then placed in a recording chamber (temperature 22-26°C), and perfused at 1-2mL/min with ACSF. Stimuli were delivered by nickel-chromium bipolar electrodes (made in house) placed in the dorsolateral striatum, optically isolated (A365, World Precision Instruments, USA) and controlled / sequenced with ClampEx software. Voltammetric responses were recorded, standardized and analyzed with an Invilog Voltammetry system and software (Invilog Research Ltd., Finland). Carbon fiber electrodes (diameter: 32μm, length: 300μm, sensitivity: >20nA/μM) were purchased prefabricated (Invilog) and placed within 100-200μm of the stimulating electrode in the dorsolateral striatum (example image in Figure A.3). Triangular waveforms (ramp from -400mV to 1200mV to -400mV, 10ms duration at 10Hz) were used to detect the oxidation and redox peaks for dopamine between 700 and 800mV (example image in Figure 3.9.E). Field activity was recorded to ensure viability of the slice during the entire duration of the experiment. Experimental paradigm shown in Figure 3.9.

Input/Output paradigms consisted of increasing single pulse stimuli (100-700μA, delivered every 2 minutes / 0.0083Hz) to determine ~70% maximum response used for the

remainder of the experiment. Three single pulses were delivered at 0.0083Hz to assess baseline stability, followed by a single paired-pulse stimulus (4 seconds inter-pules-interval, IPI). A train of stimuli (100Hz) was applied for 1 second to evaluate the maximal response at the given intensity.

Quinpirole [(-)-Quinpirole hydrochloride, Tocris Biosciences] was employed to assay pre-synaptic D2R agonism, at a concentration (50nM) to reduce dopamine response by 20-50%. During drug wash-in, single pulse stimulations were continued at 0.0083Hz for ten minutes. A repeat of the 3 single simulations, paired-pulses and train were then recorded in the drug condition. At the end of each recording session a three-point calibration of each carbon fiber electrode was conducted by injecting three concentrations of dopamine (0.1μM, 0.5μM, 1.0μM) in ACSF.

Slices were excluded from analysis if values were more than two standard deviation from average, or when an artefact was present and analysis was not possible. Additional exclusions were made depending on the shape of the voltammogram, indicating proper dopamine detection, particularly for the calibration at the end of the recording.

Additional correlation analysis were performed to exclude variability effects on genotypes. Specifically average temperature, osmolarity, pH of the solution, duration of recording and slice stimulation, were comparable across all genotypes and did not have an effect on the phenotype difference.

2.10 Behaviour

Mice undergoing experimental procedures were weighed prior to testing. All tests were performed in the morning between 8:30am and 11:30am, except for the radial arm maze (1pm to

5pm). Separate cohorts of animals were tested at 3, 6, or 18 months of age. All experimentation and analysis was conducted with the experimenter blinded to genotype. After 3-day familiarization to experimenter handling, mice underwent a combination of the following paradigms: *Open field*: mice explored an open arena (48cm x 48cm) for 15min, as previous (Volta et al., 2017). Videos were analyzed *post-hoc* with ANY-maze behavioral tracking software (Stoelting). *Objects familiarizations:* after habituating the mice to the open field arena and a 5 minutes resting period, mice were placed again in the arena. This time the arena contains two different objects. Mice are left familiarizing with the objects for 5 minutes, then moved back into their home cage. This process was repeated for 3 times to evaluate habituation or preference of a specific object. Videos were analyzed *post-hoc* with ANY-maze behavioral tracking software (Stoelting) to quantify time spent exploring each object. *Cylinder*: mice were placed in a 1L beaker and videoed for 5 minutes as previous (Volta et al., 2017). The number of rearings and forelimb wall contacts was scored manually off-line. *Rotarod*: Motor performance was evaluated using an accelerating rotarod (Model 7650, Ugo Basile). Mice were videoed during a training session to establish baseline falling latency, and in test sessions. Training consisted of six trials over two days. For each trial the rotation was set at a constant speed, but higher from trial to trial, so all mice have the ability to run at 22 revolution per minute (rpm). During the test session the rod was left accelerating from 5 to 36 rpm over 5 minutes. Fails were scored if mice (1) fell from the device, or (2) gripped the rod making a passive revolution. Videos were analysed offline and number of fails and latency to first fail were scored. *Elevated plus maze*: Mice were placed in the centre of an elevated plus-shaped apparatus (1m above ground), with two open and two enclosed arm (30.5cm each), and allowed to freely explore for 5 minutes. The number of events and time entering or exploring each arm were manually scored off-line. Open

arms exploration includes both head digging (exploring the open arm with the body still in the center or in the enclosed arm) or full body entrance (as in Wall and Messier 2001).

Alternatively mice underwent a *Radial arm maze* task: mice were given choice of a solution of 30% sucrose water and regular water in their home cage for three consecutive days to avoid fear of novelty and habituate them to sucrose. Two days post-habituation mice were tested in the RAM. The maze consisted of a central area and 8 arms originating from it. A lid was placed over the maze to avoid escape for the mouse. Spatial cues were placed in the maze and on the wall in the room, to help the mouse orientate when searching for the reward. Mice were water deprived 5 hours prior to testing (8am – 1pm), then left exploring the maze for 5 minutes. A petri-dish containing 30% sucrose-water solution was left in arm 8. Test is repeated for three consecutive days. On day 4 of testing the sucrose-water petri-dish was moved to arm 4 to evaluate flexibility in the mouse learning abilities. The test is than repeated for a fifth day. The mouse was left to rest for two days before testing again for two extra days, to test long term memory. Finally the sucrose-water solution was removed from the maze and mice were tested for two extra days to evaluate extinction of learned behaviours (as in Figure 3.24).

For all tests, objects and mazes were cleaned with 15% isopropanol and then water within each mouse or each trial, to prevent smell recognition to later the test.

2.11 Statistics and data reporting

Data are presented throughout as mean ± SEM where n is the number of animals, or else slices from the number of mice indicated in parentheses. Throughout the study, comparisons were conducted by 1-, 2-, or 3-way ANOVA with appropriate *post-hoc* tests, as detailed in the text, using Prism 6.0 (GraphPad, San Diego California USA).

Chapter 3: Results

3.1 VPS35 p.D620N knock-in (VKI) mice

To physiologically examine the effects of the *Vps35* p.D620N mutation, but avoid the confounds of random insertion and overexpression, we engineered C57Bl/6J mice to express a *Vps35* exon 15 g.85,263,520 G>A (p.D620N) nucleotide mutation (Figure 3.1.A). Successful manipulation was verified by genomic and cDNA sequencing (Figure 3.1.B). WT and mutant allele-specific *Vps35* mRNA expression was equimolar and unaltered by gene targeting in VKI animals (Figure 3.1.C, $F_{2,24} = 0.05$, $p = 0.95$). The substitution does not affect the total levels of VPS35 protein levels in the mouse brain. *WES* capillary-based protein quantification of brain lysates from 3-month-old VKI animals found no significant genotype effect on the levels of VPS35 (Figure 3.1.D.i, $F_{2,25} = 0.02$, $p = 0.97$), nor the levels of other components of the retromer complex, such as VPS26 (Figure 3.1.D.ii, $F_{2,25} = 0.31$, $p = 0.73$).

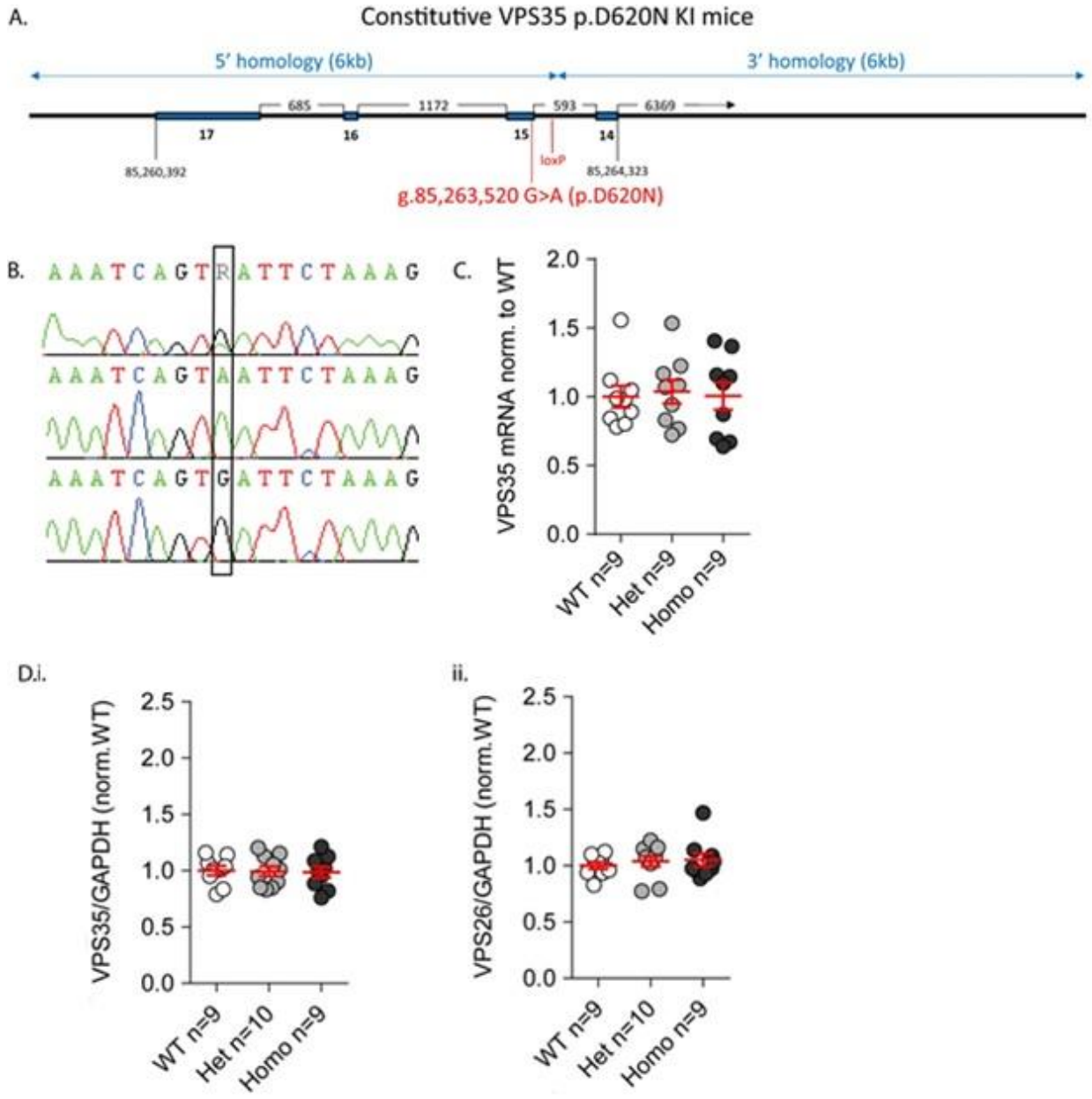

Figure 3.1. Generation of *Vps35* p.D620N knock-in mice (VKI).

A) Schematic of the targeting design showing the murine genomic sequence (Ensembl reference ENSMUSG00000031696), 5' and 3' homology arms (arrowed), exons 14-17 (blue), recombineered loxP site in intron 14, the g.85,263,520 G>A (p.D620N) mutation in exon 15 (encoding p.D620N) and endogenous stop codon in exon 17(TAA). FlpE-recombinase deletion between FRT sites removed the *PKG*-neo-pA cassette to yield the cVKI allele (not shown). Subsequent Cre-recombinase deletion between loxP sites created the VKI allele. B) cDNA sequencing in WT mice (top), heterozygous VKI (middle) and homozygous VKI (bottom), between g. 8:85263511-85263528 (GRCm38) highlighting the g.85,263,520 G>A nucleotide mutation in exon 15 that encodes the p.D620N amino acid substitution. C) Relative VPS35 mRNA (fold change) expression analysis in cerebellar tissue from 3-month-old mice using quantitative RT-PCR for. Data normalized to WT (1-way ANOVA $F_{2,24} = 0.05$, $p = 0.95$). D) Proteins in brain lysates from young VKI mice were quantified using *WES* capillary-based analysis that produces

chemiluminescence curves. Samples were loaded with antibodies against VPS35, VPS26 and GAPDH (as a loading control). Band intensities were quantified relative to loading control and normalized to WT levels. There were no significant genotype effect on protein levels of retromer components VPS35 (i, 1-way ANOVA $F_{2,25} = 0.02$, $p = 0.97$) & VPS26 (ii, 1-way ANOVA $F_{2,25} = 0.31$, $p = 0.73$).

VKI mice are viable up to 18 months, showed no evidence of overt distress, bred well and produced heterozygous and homozygous pups at expected Mendelian ratios.

Mice increase weight with age. Normally 18-month-old WT animals weigh ~50g, with some reaching ~60g. Compared to similar wild animals, laboratory mice are obese, likely due to a combination of inbreeding and an environment containing free access to food and little room for activity; variability is probably a consequence of group housing and social hierarchy. Interestingly, VKI mice did not gain as much weight with age, maintaining a stable weight past 12 months of age (2-way ANOVA interaction $F_{10,257} = 2.58$, $p < 0.01$, $F_{2,257} = 10.09$, genotype $p < 0.0001$, age (months) $F_{5,257} = 168.72$, $p < 0.0001$, *Bonferroni post-test* as shown in Figure 3.2.A and Table B.1 in Appendix B.1). Cursory necropsy suggests that VKI mice lay down less fat than WT littermates. Internal organs, for example the liver, appeared lighter (Figure 3.2.B; 1-way ANOVA $F_{2,21} = 3.03$, $p = 0.06$) albeit not statistically significant (at 95% confidence). Despite these differences, internally and externally VKI mice did not show signs of discomfort. Rather, 18-month-old VKI mice, aside lower body fat, appeared similar to their WT littermates and mice from other lines at a similar age.

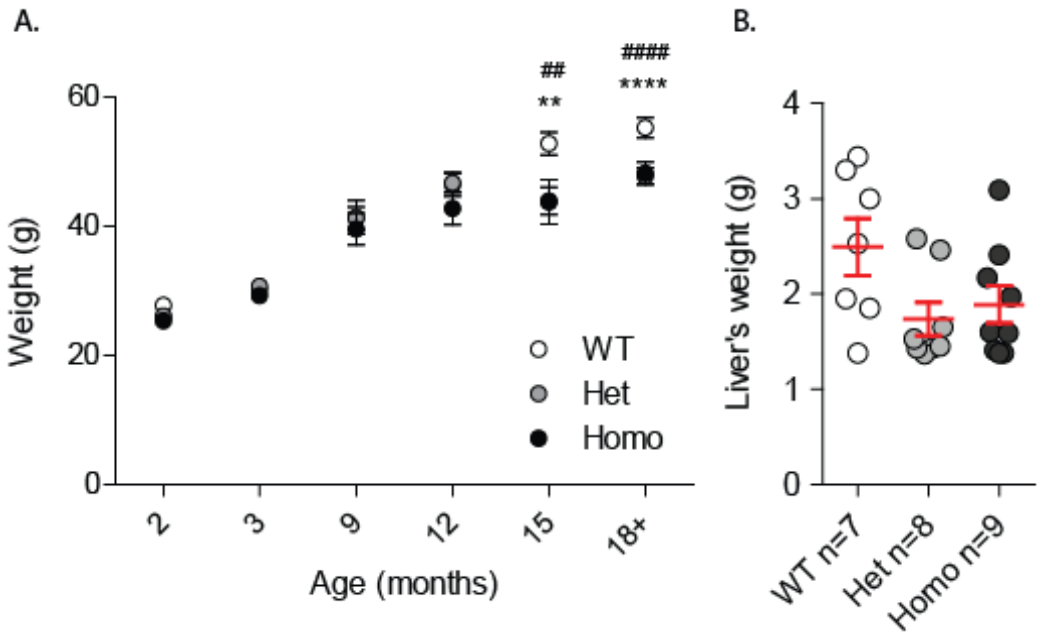

Figure 3.2 VKI mice weight
A) VKI mice weight plot by month of age. WT mice show greater weight at 15 and 18 months of age, when compared to their het and homo littermates (2-way ANOVA interaction $F_{10,257} = 2.58$, $p < 0.01$, $F_{2,257} = 10.09$, genotype $p < 0.0001$, age (months) $F_{5,257} = 168.72$, $p < 0.0001$, *Bonferroni post-test* WT vs het ###$p < 0.001$ & ####$p < 0001$, WT vs homo **$p < 0.01$, ****$p < 0.0001$, respectively). Different animals were weighed at different time points (number of animals at corresponding age point shown in Table B.1, Sub-Appendix B.1, including additional statistical information). B) Liver was collected from a cohort of 18-month-old animals, and weighed. There is a strong trend towards lighter livers in VKI mice (1-way ANOVA $F_{2,21} = 3.03$, $p = 0.06$).

3.2 Dopaminergic alterations

3.2.1 VKI mice and neuronal loss

We examined the integrity of the nigrostriatal system (striatum and SNpc), by means of confocal imaging and stereological examination in 3-month-old VKI animals. No significant differences were observed between VKI and WT littermates in the intensity of TH+ terminals innervating the dorsolateral striatum (Figure 3.3,Aii, 1-way ANOVA $F_{2,6} = 0.28$, $p = 0.75$), or gross nigral neuronal cell counts, as marked by TH (Figure 3.3.C.ii; 1-way ANOVA $F_{2,13} = 0.74$, $p = 0.49$). Consistent findings were observed by western blotting for TH in striatal lysate from 3-month-old mice (Figure 3.3.B; 1-way ANOVA $F_{2,33} = 2.86$, $p = 0.08$).

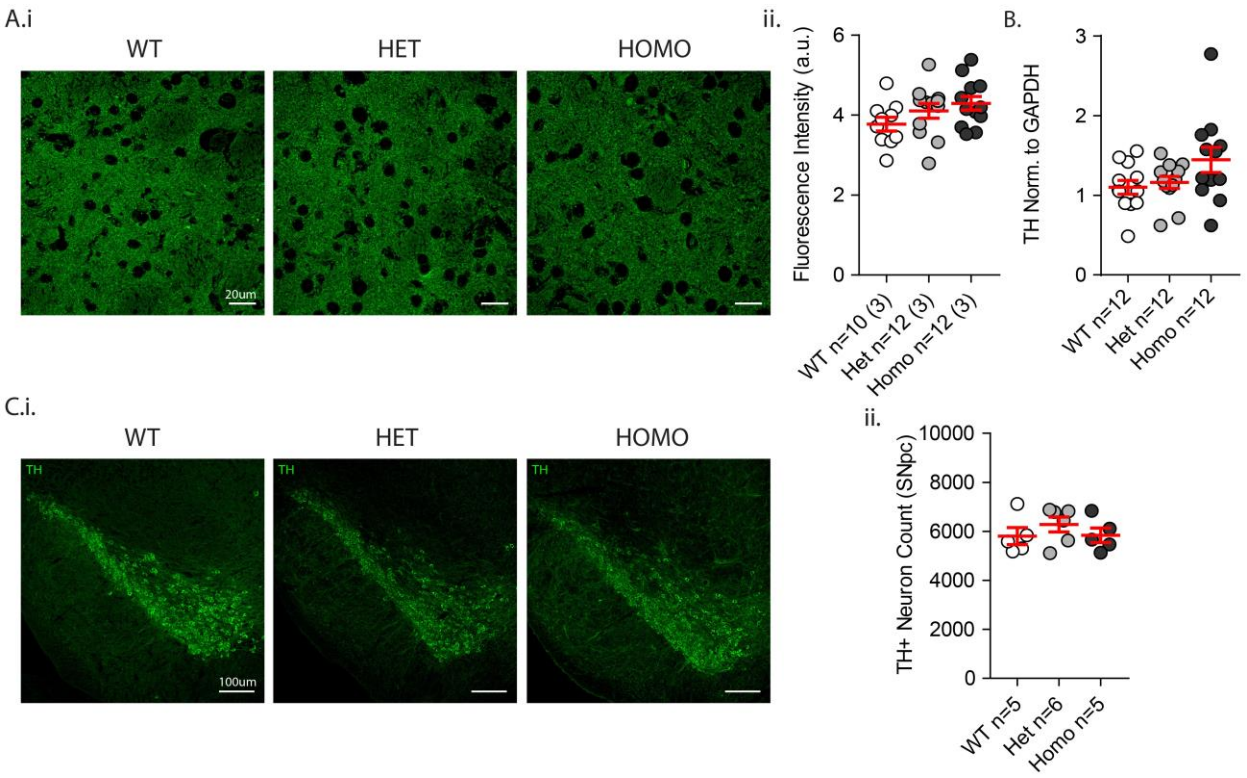

Figure 3.3 Evaluation of nigrostriatal TH positive neurons in young VKI mice
Representative images of TH (green) staining in striatal (A.i.) and nigral (C.i) sections of PFA perfused brain from VKI mice. No difference was detected in total levels of TH in the striatum (A.ii, 1-way ANOVA $F_{2,6} = 0.28$, $p = 0.75$) across genotypes, nor in the total count of TH+ neurons in the SNpc (C.ii, 1-way ANOVA $F_{2,13} = 0.74$, $p = 0.49$) of the same mice. Similarly there were no differences in total level of TH in the striatum quantified with Western blotting (B, 1-way ANOVA $F_{2,33} = 2.86$, $p = 0.08$).

Similar to young animals, preliminary data showed no differences in TH+ stereological neuronal count in the SNpc of 18-month-old mice (Figure 3.4.A; 1-way ANOVA $F_{2,5} = 0.84$, $p = 0.28$), with comparable TH protein levels in striatal tissue (Figure 3.4.B, 1-way ANOVA $F_{2,22} = 1.99$, $p = 0.15$). Combined, these results indicate that physiologic expression of VPS35 p.D620N in mice did not induce dopaminergic neurodegeneration up to 18 months of age.

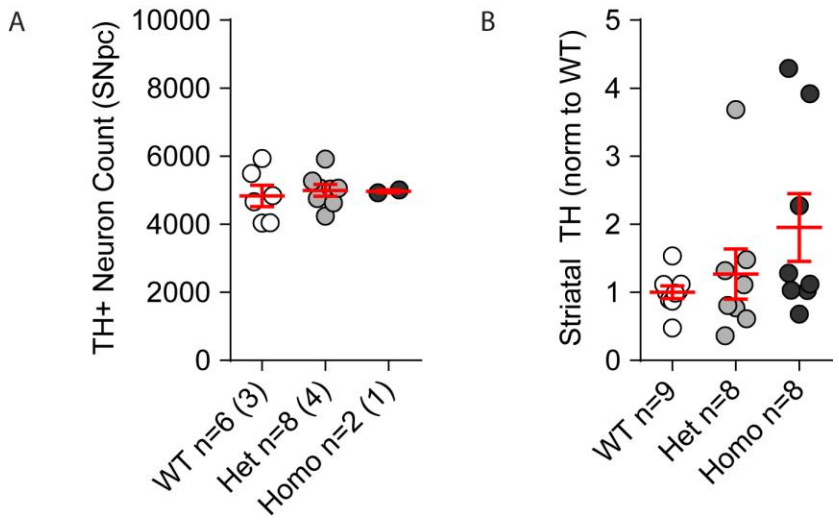

Figure 3.4 Preliminary evaluation of TH in striatal tissue and SNpc sections from old VKI mice
A) No difference was detected in total levels of TH+ neurons in the SNpc of VKI mice (1-way ANOVA $F_{2,5} = 0.84$, $p = 0.28$)). B) A trending increase was found in TH levels in striatal tissue from old VKI animals (1-way ANOVA $F_{2,22} = 1.99$, $p = 0.15$).

3.2.2 Extracellular dopamine in VKI mice

To evaluate dopamine in VKI mice, we measured extracellular levels in 3 and 18-month-old animals by *in vivo* microdialysis of awake animals. Microdialysis probes were lowered into the mouse dorsolateral striatum and four samples, one every 15 minutes, were collected as baseline to give an average extracellular dopamine level. Individual probe placements were confirmed by immunohistochemistry at the end of the experiment. No differences in basal levels of dopamine were observed in young VKI mice (Figure 3.5.B; 1-way ANOVA $F_{2,28} = 0.61$, $p = 0.54$), relative to WT littermates. However, dopamine metabolites, DOPAC and HVA, were trending towards an increase in heterozygous and homozygous VKI animals (Figure 3.5.C.i & ii, 1-way ANOVA $F_{2,28} = 2.89$, $p = 0.07$ & $F_{2,28} = 3.06$, $p = 0.06$, respectively), and produced a significantly greater metabolites/dopamine ratio in homozygous animals, suggesting increased turnover of dopamine in the presence of the mutation (Figure 3.5.C.iii, 1-way ANOVA $F_{2,28} = 6.44$, $p<0.04$; *Bonferroni post-test* WT *vs* het $t_{(20)} = 0.40$, $p = 0.99$, WT vs $t_{(20)} = 3.20$, homo $p = 0.03$).

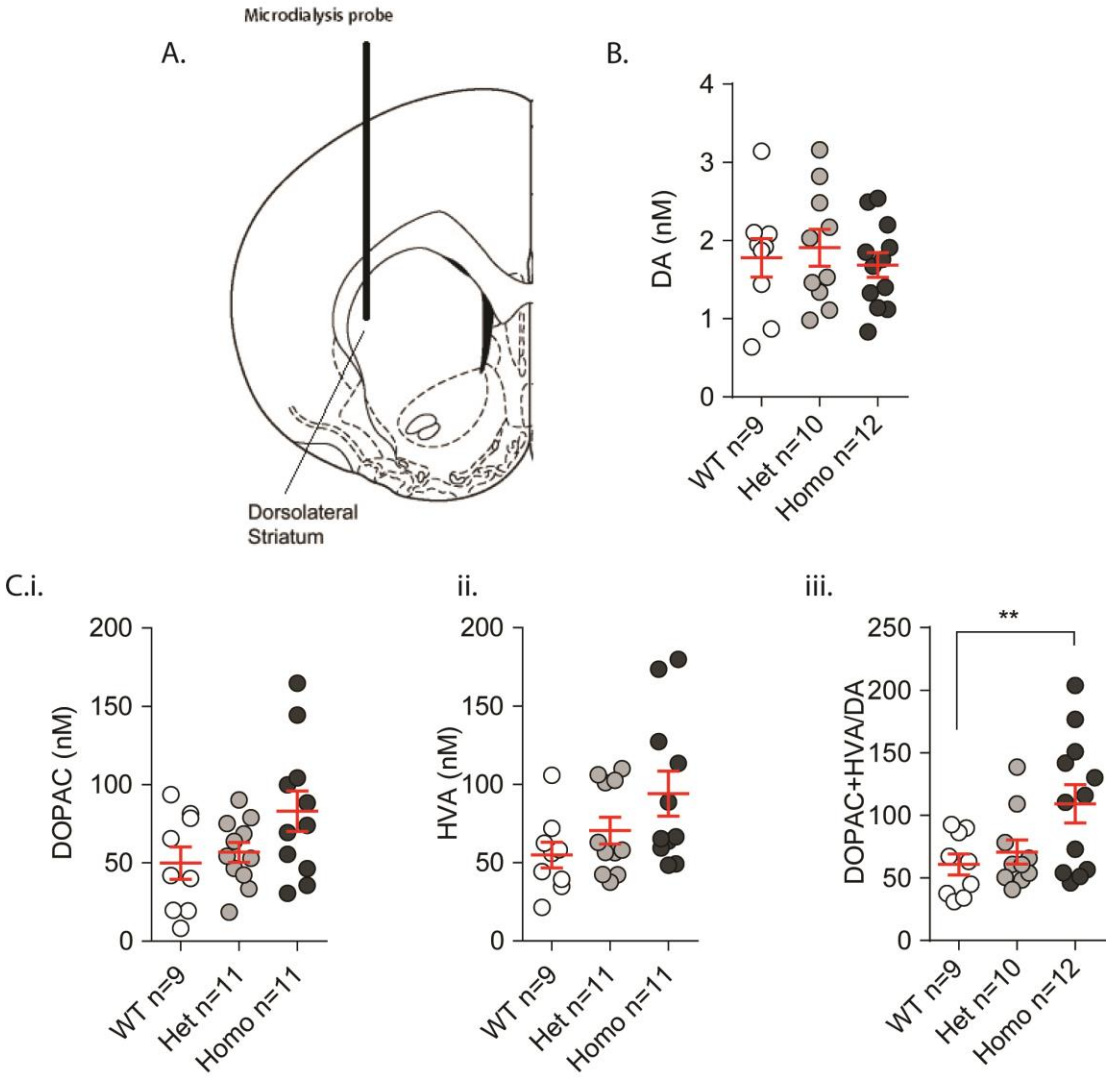

Figure 3.5 Extracellular striatal dopamine in young VKI animals
A) A schematic of the placement of the probe (co-ordinates AP +0.5, ML +2.1 DV -2.8) for *in-vivo* detection of dopamine from the dorsolateral striatum. B) Average levels from 4 dialysates collected over an hour. No difference was found in overall basal levels of dopamine (1-way ANOVA $F_{2,28} = 0.61$, $p = 0.54$). C) Dopamine metabolites total levels (DOPAC C.i & HVA C.ii) and their ratio over levels of dopamine (iii). Homo VKI mice show similar, albeit trending towards increased, levels of DOPAC and HVA (i & ii, 1-way ANOVA $F_{2,28} = 2.89$, $p = 0.07$ & $F_{2,28} = 3.06$, $p = 0.06$ respectively), with a significantly higher ratio indicating greater turnover of dopamine (iii; 1-way ANOVA $F_{2,28} = 6.44$, $p<0.04$; *Bonferroni post-test* WT *vs* het $t_{(28)} = 0.40$, $p = 0.99$, WT vs $t_{(28)} = 3.20$, homo $p = 0.03$).

When microdialysis collection was performed with 18-month-old VKI, no differences were found in total dopamine levels across all genotypes (Figure 3.6, 1-way ANOVA $F_{2,30} = 0.36$, $p = 0.69$). While metabolites were higher in levels in younger animals, there was no

obvious difference in older mice (Figure 3.6.B.i & .ii, 1-way ANOVA $F_{2,30} = 0.28$, $p = 0.77$ & $F_{2,30} = 0.14$, $p = 0.86$ respectively), nor in the metabolites/dopamine ratio (Figure 3.6.B.iii, 1-way ANOVA $F_{2,30} = 0.28$, $p = 0.75$).

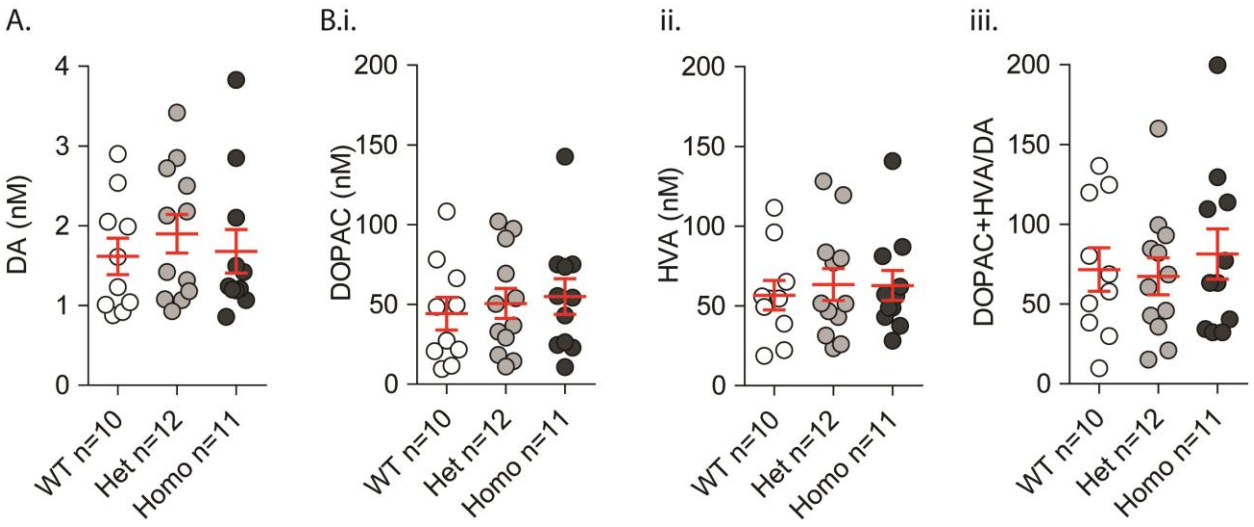

Figure 3.6 Extracellular dopamine in 18 months old VKI
A) Average levels from 4 dialysates collected over an hour. No difference was found in overall basal levels of dopamine (1-way ANOVA 1-way ANOVA $F_{2,30} = 0.36$, $p = 0.69$). B) No differences were found in VKI mice when compared to their WT littermates when measured total levels of DOPAC and HVA (i & ii; 1-way ANOVA $F_{2,30} = 0.28$, $p = 0.77$ & $F_{2,30} = 0.14$, $p = 0.86$ respectively) and their ratio over dopamine (iii; 1-way ANOVA $F_{2,30} = 0.28$, $p = 0.75$).

3.2.3 Whole tissue evaluation of monoamine levels

To measure the total content of dopamine and metabolites, we rapidly decapitated VKI mice and collected the striatum. Tissue was homogenized and supernatant was assayed by HPLC for dopamine and its metabolites. We saw no genotype differences, at either 3 or18 months of age, suggesting that total production of dopamine was not altered in VKI mice, nor overall metabolites levels (3-month-old animals in Figure 3.7, 1-way ANOVA $F_{2,15} = 0.5$, $p = 0.61$, $F_{2,15} = 0.54$ $p = 0.58$, $F_{2,15} = 0.48$ $p = 0.62$, & $F_{2,15} = 0.15$, $p = 0.85$ respectively; 18-month-old in Figure 3.8, 1-way ANOVA $F_{2,14} = 0.78$, $p = 0.47$, $F_{2,14} = 0.39$, $p = 0.68$, $F_{2,14} = 0.63$, $p = 0.54$, & $F_{2,14} = 0.31$, $p = 0.73$ respectively).

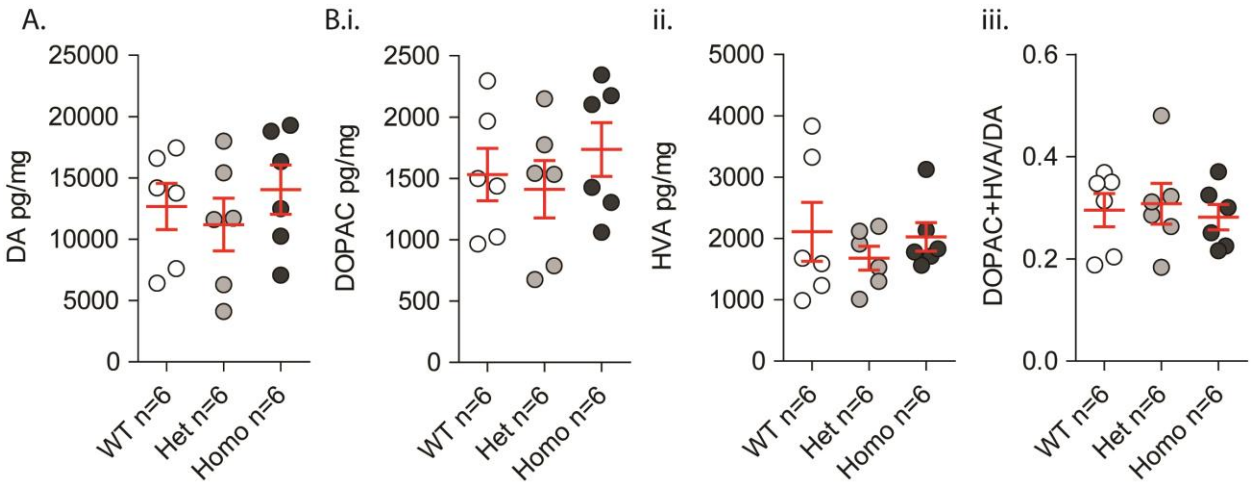

Figure 3.7 Evaluation of total levels of dopamine and metabolites in striatal tissue from young VKI animals
Striatal tissue was processed for monoamine detection by an HPLC. When compared to striata from WT mice, young VKI animals showed no differences in total levels of dopamine (A, 1-way ANOVA $F_{2,15} = 0.5$, $p = 0.61$) or metabolites (B.i & .ii, 1-way ANOVA $F_{2,15} = 0.54$ $p = 0.58$, $F_{2,15} = 0.48$ $p = 0.62$), nor their ratio (B.iii, 1-way ANOVA $F_{2,15} = 0.15$, $p = 0.85$).

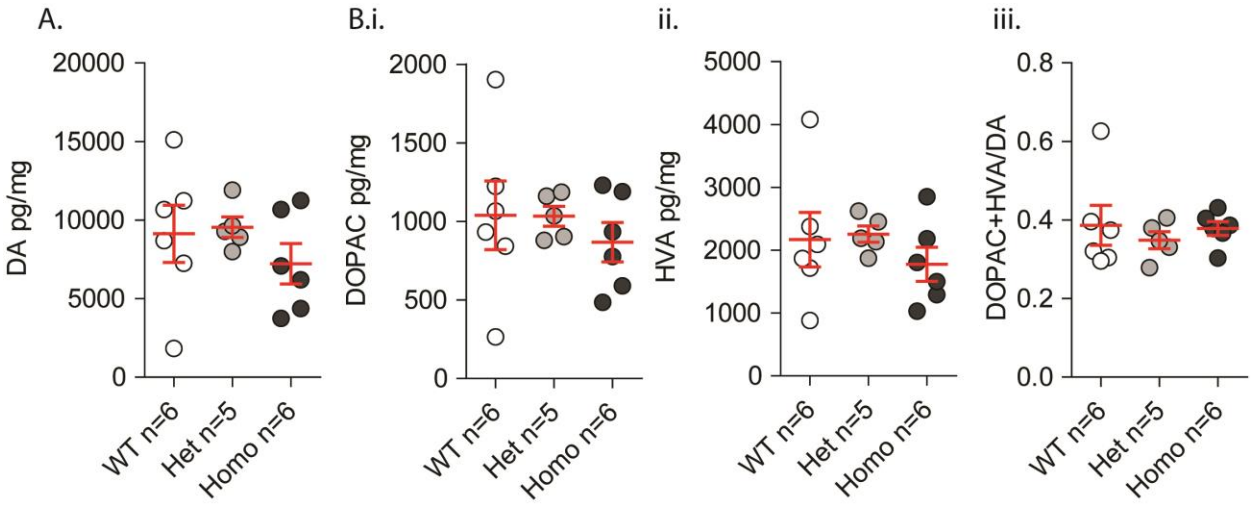

Figure 3.8 Evaluation of total levels of dopamine and metabolites in striatal tissue from old VKI animals
As above, striatal tissue was processed for monoamine detection by an HPLC. When compared to WT mice, old VKI animals showed no differences in total levels of dopamine (A, 1-way ANOVA $F_{2,14} = 0.78$, $p = 0.47$) or metabolites (B.i & .ii, 1-way ANOVA $F_{2,14} = 0.39$, $p = 0.68$, $F_{2,14} = 0.63$, $p = 0.54$ respectively), nor their ratio (B.iii, 1-way ANOVA $F_{2,14} = 0.31$, $p = 0.73$).

3.2.4 Striatal dopamine function

To assay nigrostriatal dopamine release directly, we conducted fast scan cyclic voltammetry (FSCV) in acute slices (as described in methods 2.7 and shown in Figure 3.9, with additional images in Figure A.3 in appendix A.3).

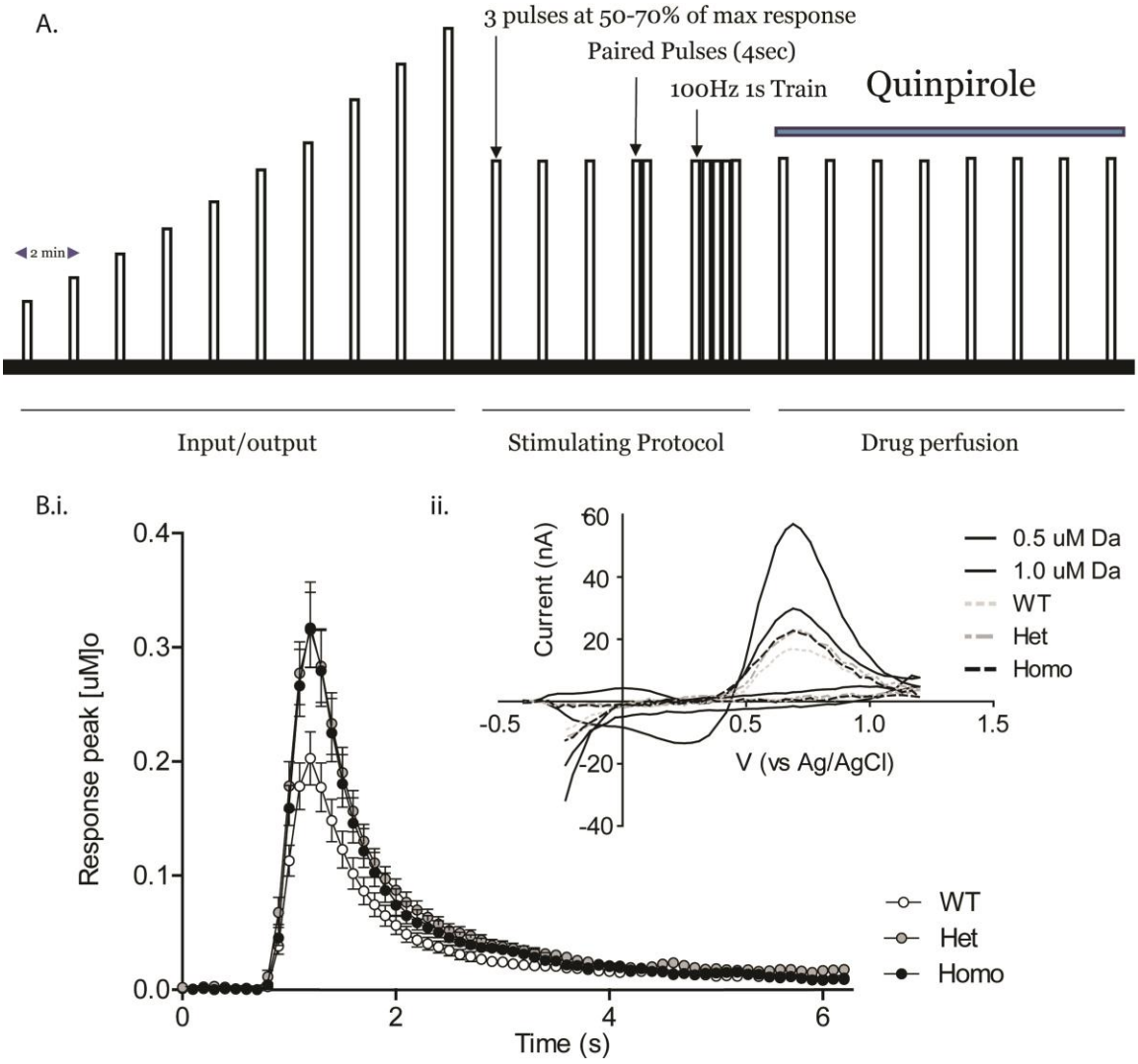

Figure 3.9 Methodological procedure for ex-vivo FSCV

A) Experimental procedure for FSCV recording. A series of stimuli was sent with 2 minutes intervals. Initially an input/output curve was generated by increasing the intensity of stimulation from 100 to 700µA (increase of 100µA at every stimulus every 2 minutes). After the input/output a series of 3 stimuli was sent at 50-70% of maximal response during input/output. Followed a paired stimulation at 50-70% of max response, with 4 seconds interval, to evaluate paired pulse ratio (PPR). Finally a train of stimuli of 100Hz for 1 second was applied. After 2 minutes recovery a solution of quinpirole was applied to the bath and a series of 8 stimuli with 2 minutes intervals was

applied to the slice, to evaluate D2 function. B) Average peak for each genotype (i), showing greater response and slower decay for mutant animals, with corresponding voltammogram in the top right corner (ii), including voltammogram for 0.5µM and 1 µM of dopamine, used for calibration of the carbon-fiber electrode at the end of each day of recording.

In the dorsolateral striatum, single stimuli elicit dopamine release and current transients, which increase with stimulus intensity (100~700µA). In young animals, 700µA was often the maximum stimulus applied given the plateau of WT slices at this intensity, although a few slices from WT, and many from het and homo mice were stimulated up to 1000µA. There was a significant genotype effect on the stimulus-response relationship, with elevated dopamine release observed in VKI slices (2-way RM-ANOVA, interaction $F_{12,378} = 4.02$, $p < 0.0001$, input $F_{6,378} = 70.20$, $p < 0.0001$, genotype $F_{2,63} = 4.09$, $p < 0.05$, subject $F_{63,378} = 34.91$, $p < 0.0001$; with *Bonferroni post-test* as indicated in Figure 3.10.A and Table A.2, also graphically shown in Figure 3.9.B). When a series of three consecutive stimuli were applied at 50-70% of the maximal response, average decay times were marginally slower in het VKI slices suggesting reduced re-uptake of the extracellular dopamine (Figure 3.10.B, 1-way ANOVA $F_{2,77} = 4.38$, $p < 0.02$, *Bonferroni post-test* $t_{(77)} = 2.92$, $p < 0.01$ & $t_{(77)} = 1.92$, $p = 0.11$ for het and homo, respectively). We then hypothesized D2 autoreceptor function may be impaired as well (Phillips et al., 2002; Rice & Patel, 2015), and conducted paired-pulse ratio experiments. Paired stimuli (4s IPI) evoked the expected depression (~80%) of the second pulse but there was no difference between genotypes (Figure 3.10.C, 1-way ANOVA $F_{2,77} = 1.36$, $p = 0.26$). Nevertheless, slices from VKI mice showed a trend towards less paired-pulse depression; of note, a second peak (P2/P1 ratio>0) was more frequently observed in homo and het VKI slices than WT. When a train of stimuli (1s duration, 100Hz) was applied to the slice, relative to single pulses, the predicted increase in response amplitude was comparable between WT, het and homo VKI mice (Figure

3.10.D, 1-way ANOVA $F_{2,70} = 1.28$, $p = 0.28$). In agreement with decay times for single pulses, we observed lower ratios of train decay versus single pulse decay in slices from het VKI mice (Figure 3.10.E, 1-way ANOVA $F_{2,87} = 3.946$, $p = 0.05$, although the result did not reach significance with *Bonferroni post-test*).

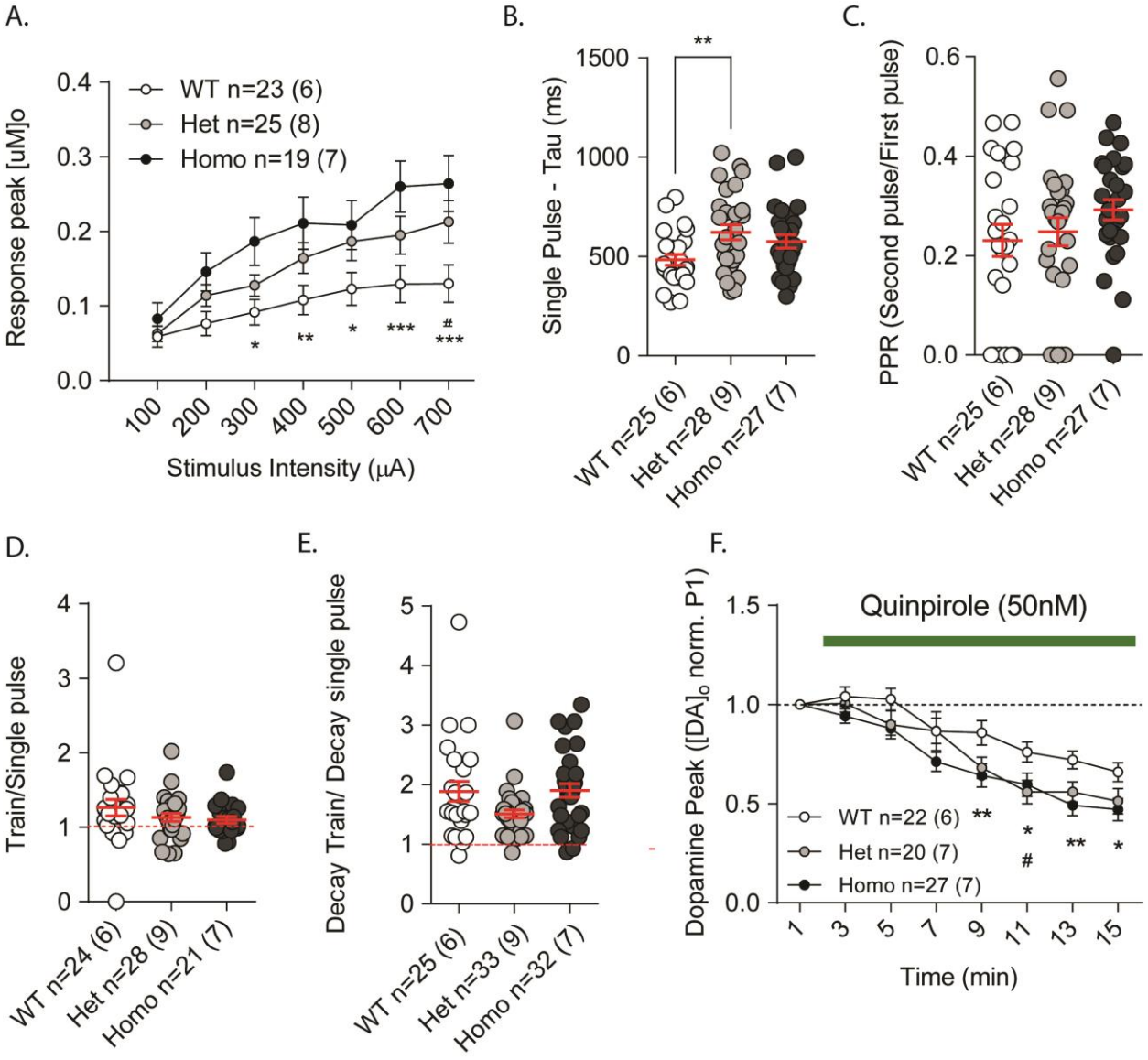

Figure 3.10 Fast scan cyclic voltammetry in young VKI mice

A) A series of increasing stimuli was applied with 2 minutes intervals to obtain an input/output curve and the maximal evoked dopamine release. VKI slices showed an increase in evoked dopamine as compared to slices from their WT littermates (2-way ANOVA interaction $F_{12,378} = 4.02$, $p < 0.0001$, input $F_{6,378} = 70.20$, $p < 0.0001$, genotype $F_{2,63} = 4.09$, $p < 0.05$, subject $F_{63,378} = 34.91$, $p < 0.0001$; *Bonferroni post-test* WT vs. Het $t_{(441)} = \#p<0.05$,

WT vs. Homo; *p<0.05, **p<0.01, ***p<0.001; additional statistical information in Table A.2 in appendix A.3). B) At stimulation intensities leading to 50-70% maximum dopamine release, based on the input/output, a series of 3 pulses was given with an interval of 2 minutes between each. With this paradigm the decay was longer in het VKI mice ($F_{2,77}$ = 4.38, p < 0.02, *Bonferroni post-test* $t_{(77)}$ = 2.92, **p < 0.01 & $t_{(77)}$ = 1.92, p = 0.11 for het and homo slices, respectively). C). In a paired-pulse paradigm with an interval of 4 seconds between the first and the second pulse, VKI slices were comparable to WT (1-way ANOVA $F_{2,77}$ = 1.36, p = 0.26). D) WT and VKI slices show a comparable release and decay in dopamine signal when a train of stimulus (100Hz, 1s) was applied, shown as a train/single pulse ratio (1-way ANOVA $F_{2,70}$ = 1.28, p = 0.28). E) Given the greater decay time in het slices, when looking at the ratio of train decay time over single pulse decay time, a greater value is shown for WT and homo slices, but not for het (1-way ANOVA $F_{2,87}$ = 3.946, p = 0.05, these data does not reach significance with post-hoc test). F) In WT slices, the D2 agonist quinpirole (50nM) infused in the slice chamber gave a 20-50% reduction in dopamine release within ~ 5 minutes from reaching the slice (drug perfusion starts at minute 0; drug reaches the slice by minute 2). A series of stimuli was applied, with 2 minutes intervals, to evoke 50-70% maximum dopamine release. VKI slices showed a more rapid, greater D2 inhibition compared to slices from WT littermates (2-way RM-ANOVA, interaction $F_{14,658}$ = 1.47, p = 0.11, time $F_{7,658}$ = 66.41, p < 0.0001, genotype $F_{2,94}$ = 4.03, p < 0.05, subjects $F_{94,658}$ = 7.04, p < 0.0001; *Bonferroni post-test* WT *vs* Het #p<0.05, WT *vs* Homo; *p<0.05, **p<0.01, as indicated in Table A.3 in Appendix A.3).

We then decided to evaluate how age would affect dopamine release. We performed FSCV in slices from 18-month-old animals. When assayed for the input/output paradigm, VKI mice showed similar dopamine release compared to their WT littermates (Figure 3.11.A, c), albeit a trend towards lower dopamine in het and homo mice would suggests at this age the system may begin to fail.

When a series of three stimuli at 50-70% of maximal response was applied to slices from old animals, the decay time was greater in older animals when compared to young age, but with no significant differences between genotypes, albeit with a trend towards smaller decay in homozygotes (Figure 3.11B, 1-way ANOVA $F_{2,76}$ = 2.81, p = 0.06), suggesting faster re-uptake when compared to WT. Similarly to young slices, the PPR stimulation did not have a different effect in slices from VKI mice, relative to slices from WT mice (Figure 3.11.C, 1-way ANOVA $F_{2,77}$ = 2.48, p = 0.09), although we saw a trend towards smaller ratio in mutant animals, and more (rather than fewer) failures for the second peak. Train stimulation did not affect VKI slices differently than slices from WT (Figure 3.11.D, 1-way ANOVA $F_{2,76}$ = 0.25, p = 0.77), nor the

ratio of the decay during train over the decay of the single pulse (Figure 3.11.E, 1-way ANOVA $F_{2,69} = 0.06$, $p = 0.93$).

We surmise D2 receptor function is largely intact in VKI mice although the efficacy of D2R negative tuning may be less in young animals. To directly investigate prolonged D2 auto-receptor activation, quinpirole, a D2R agonist was bath applied at 50nM, a concentration previously shown to reduce dopamine release by 20-50% in WT slices (Volta et al., 2017). In young animals, a series of stimuli applied at 2 minutes intervals to VKI slices showed a more rapid D2 inhibition on dopamine release when compared to slices from WT littermates (Figure 3.10.F, 2-way RM-ANOVA, interaction $F_{14,658} = 1.47$, $p = 0.11$, time $F_{7,658} = 66.41$, $p < 0.0001$, genotype $F_{2,94} = 4.03$, $p < 0.05$, subjects $F_{94,658} = 7.04$, $p < 0.0001$, *Bonferroni post-test* as in Table A.3). However, over a longer exposure to the drug (30minutes) WT slices reached the same degree of inhibition as mutant (Figure A.3). When the same paradigm was performed in slices from older animals, the effect was still notable for homozygous mice, but was not present in het slices (Figure 3.11.F, 2-way RM ANOVA interaction $F_{14,441} = 0.99$, $p = 0.46$, time $F_{7,441} = 46.64$, $p < 0.0001$, genotype $F_{2,63} = 3.68$, $p < 0.05$, subject $F_{63,441} = 7.45$, $p < 0.0001$, however this data did not reach significance with *Bonferroni post-test*). The disparity between the effects of D2R activation in paired-pulse ratios (over a period of seconds), which are grossly normal, and those augmented by D2R agonism (over a period of minutes), suggests changes to dopamine release modulated by D2R function at the synapse may be subtle and activity dependent.

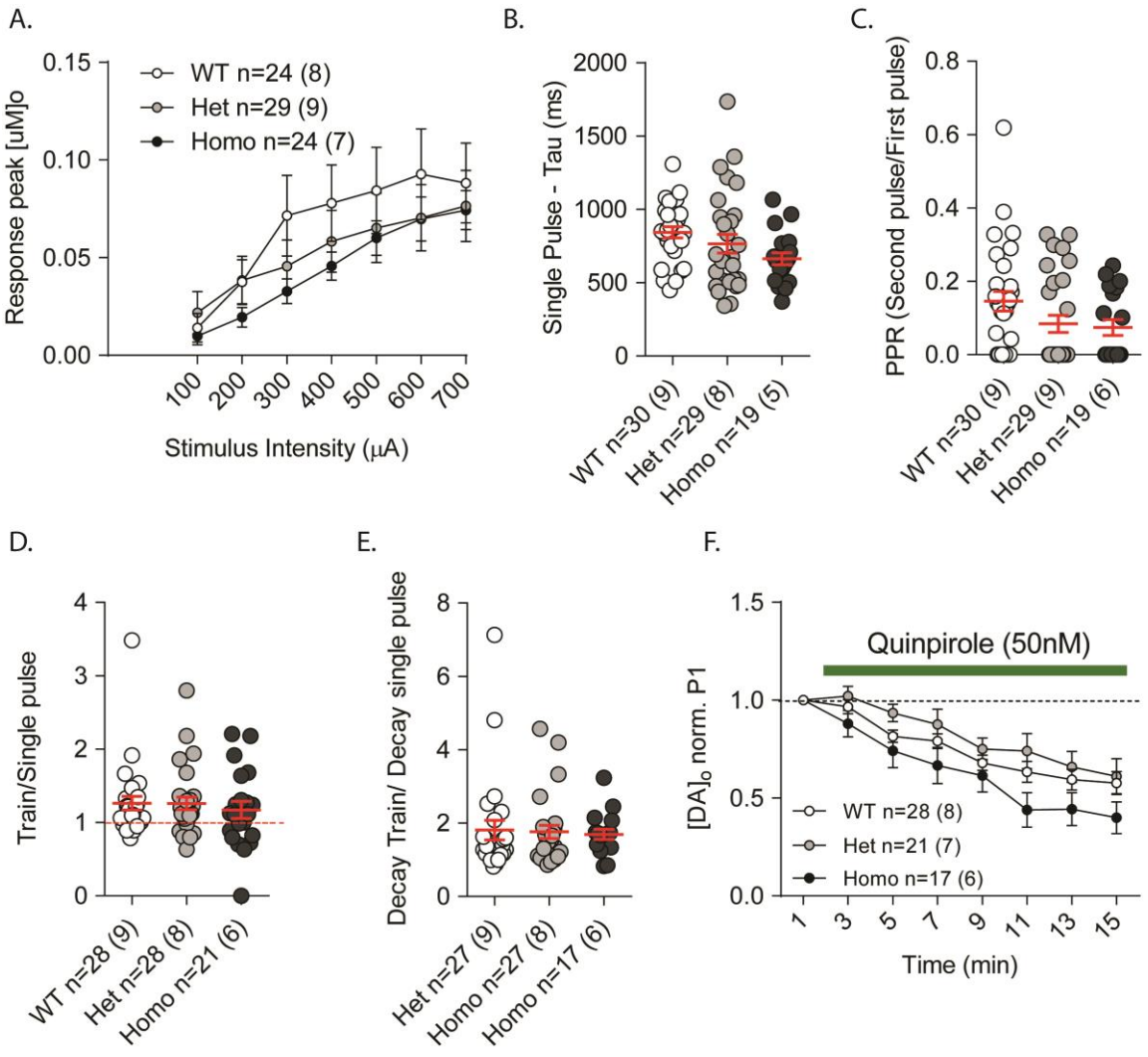

Figure 3.11 Fast scan cyclic voltammetry in old VKI

A) VKI slices showed a decrease in evoked dopamine as compared to slices from their WT littermates (2-way RM-ANOVA interaction $F_{14,658} = 1.47$, $p = 0.11$, time $F_{7,658} = 66.41$, $p < 0.0001$, genotype $F_{2,94} = 4.03$, $p < 0.05$, subjects $F_{94,658} = 7.04$, $p < 0.0001$; this data did not reach significance by *Bonferroni post-test*). B) At stimulation intensities leading to 50-70% maximum dopamine release, based on the input/output, a series of 3 pulses was given with an interval of 2 minutes between each. With this paradigm the decay was no significant difference between VKI mice and WT littermates, albeit there is a strong trend towards faster re-uptake for homozygous animals (1-way ANOVA $F_{2,76} = 2.81$, $p = 0.06$). C) In a paired-pulse paradigm with an interval of 4 seconds between the first and the second pulse, VKI slices were comparable to WT, although there was a trend towards lower ratio (1-way ANOVA $F_{2,77} = 2.48$, $p = 0.09$). D) WT and VKI slices show a comparable release and decay in dopamine signal when a train of stimulus (100Hz, 1s) was applied, shown as a train/single pulse ratio (1-way ANOVA $F_{2,76} = 0.25$, $p = 0.77$). E) Given the decay time is comparable for both single pulse and train stimulation, when looking at the ratio of train decay time over single pulse decay time there is not difference across genotype (1-way ANOVA $F_{2,69} = 0.06$, $p = 0.93$.). F) A series of stimuli was applied, with 2 minutes intervals while a solution of 50nM of quinpirole was perfusing in the bath. Slices from homozygous mice, but not het animals, showed a more rapid, greater D2 inhibition compared to slices from WT littermates (2-way RM-ANOVA, interaction $F_{14,441} = 0.99$, $p = 0.46$, time $F_{7,441} =$

46.64, $p < 0.0001$, genotype $F_{2,63} = 3.68$, $p < 0.05$, subject $F_{63,441} = 7.45$, $p < 0.0001$; this data is not significant by *Bonferroni post-test*).

3.2.5 Protein quantification of striatal synaptic proteins

To explore these alterations in dopamine release, we sought to investigate the synaptic machinery responsible for the packaging and re-uptake of dopamine. At young age, when compared to WT littermates, VKI mice displayed a significant increase in VMAT2 protein levels (Figure 3.12.A & B.i., 1-way ANOVA $F_{2,25} = 5.30$, $p < 0.01$, *Bonferroni post-test* WT *vs* het $t_{(25)} = 2.45$, $p = 0.042$, WT *vs* homo $t_{(25)} = 3.09$, $p < 0.01$). Conversely, a notable loss of total DAT protein (Figure 3.12.A & B.ii., 1-way ANOVA $F_{2,32} = 17.75$, $p < 0.0001$, *Bonferroni post-test* WT *vs* het $t_{(32)} = 3.32$, $p < 0.01$, WT *vs* homo $t_{(32)} = 5.95$, $p < 0.0001$) was observed. Results were normalised to TH for tissue specificity, but remain consistent when normalized to GAPDH (Figure A.2). These changes occurred independent of differences to levels of post-synaptic scaffold protein, PSD95 (Figure 3.14.C; 1-way ANOVA $F_{2,23} = 0.42$, $p = 0.65$) indicating that VPS35 p.D620N expression does not globally modify synapse connections in the striatum, and that alterations to VMAT2 and DAT are somewhat specific.

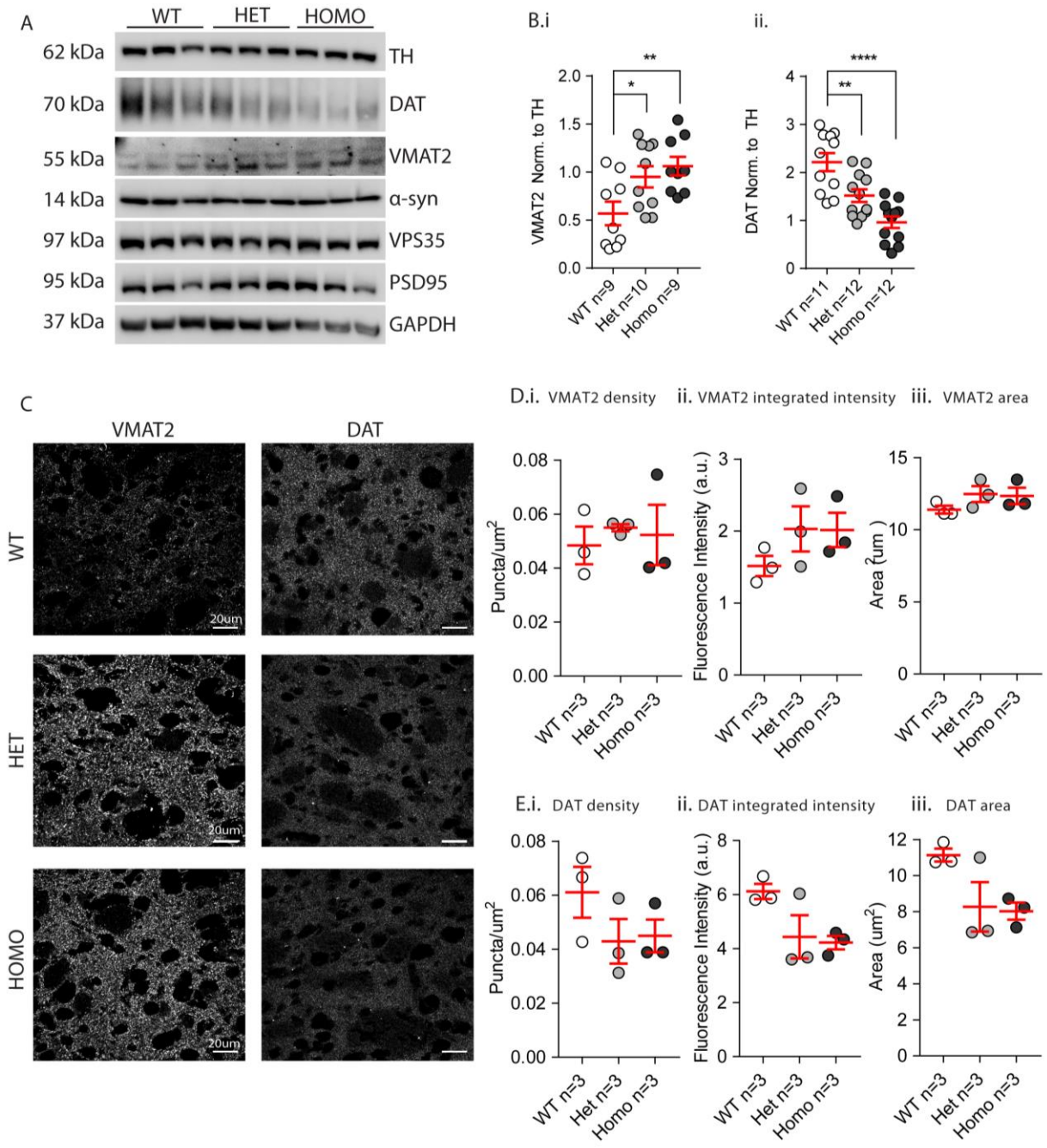

Figure 3.12 Dopaminergic markers DAT and VMAT2 in tissue and striatal slices from young VKI mice
A) Representative western blots of dopaminergic specific markers VMAT2 and DAT in VKI mice. Blots are cropped; for full-length blots see Figure A.1. B) Densitometry analysis was conducted by normalizing VMAT2 and DAT intensity to TH loading control (VMAT2, i, 1-way ANOVA $F_{2,25} = 5.30$, $p < 0.01$, *Bonferroni post-test* WT *vs* het $t_{(25)} = 2.45$, $p = 0.042$, WT *vs* homo $t_{(25)} = 3.09$, $p < 0.01$; DAT, ii, 1-way ANOVA $F_{2,32} = 17.75$, $p < 0.0001$, *Bonferroni post-test* WT *vs* het $t_{(32)} = 3.32$, $p < 0.01$, WT *vs* homo $t_{(32)} = 5.95$, $p < 0.0001$). C) Representative Confocal images of VMAT2 (left) and DAT (right) in the dorsolateral striatum of 3-month-old VKI mice. D) No changes in VMAT2 puncta density were detected (D.i, 1-way ANOVA $F_{2,8} = 0.19$, $p = 0.604$). VMAT2 puncta

integrated density and area are trending towards an increase in KI littermates when compared to WT controls (D.ii & iii, 1-way ANOVA $F_{2,8} = 1.47$, $p = 0.30$; $F_{2,8} = 1.46$, $p = 0.30$, respectively). E) DAT puncta density, integrated intensity, and area are trending towards a decrease in KI littermates when compared to WT controls (1-way ANOVA respectively: E.i, $F_{2,8} = 1.54$, $p = 0.29$, E.ii, $F_{2,8} = 4.17$, $p = 0.07$, & E.iii, $F_{2,8} = 4.03$, $p = 0.07$).

Interestingly, VMAT2 levels remain constantly higher in older animals, as shown by western blot quantification from striatal tissue from 10-month-old VKI (Figure 3.13.A, 10-month-old VKI 1-way ANOVA $F_{2,6} = 31.47$ $p < 0.001$, *Bonferroni post-test* WT *vs* het $t_{(6)} = 3.49$, $p < 0.05$ & WT *vs* homo $t_{(6)} = 7.91$, $p < 0.001$), with a slight reduction by 18 months of age (Figure 3.13.B, 18-month-old VKI, 1-way ANOVA $F_{2,7} = 5.45$, $p = 0.055$).

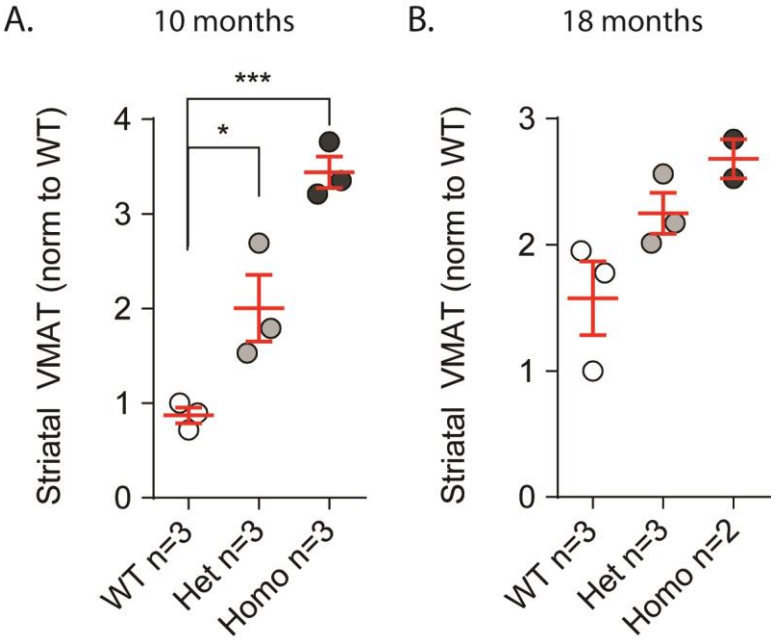

Figure 3.13 VMAT2 levels in striata from 10 and 18-month-old VKI
A) VMAT2 levels in striata from 10-month-old animals, showing greater levels of VMAT2 in VKI mice when compared to WT littermates (1-way ANOVA $F_{2,6} = 31.47$ $p < 0.001$, *Bonferroni post-test* WT *vs* het $t_{(6)} = 3.49$, $p < 0.05$ & WT *vs* homo $t_{(6)} = 7.91$, $p < 0.001$). B) VMAT2 levels in striata from 18-months-old VKI, showing a trending increase in het and homo (1-way ANOVA $F_{2,7} = 5.45$, $p = 0.055$).

To expand on these results, we employed confocal imaging in the dorsolateral striatum isolated from young VKI mice using antibodies against VMAT2 and DAT. No difference was observed between genotypes when analyzed for VMAT2 positive puncta density (Figure 3.12.C

& D.i; 1-way ANOVA $F_{2,8} = 0.19$, $p = 0.604$), and VMAT2 puncta integrated intensity and area were not significantly different compared to WT littermates (Figure 3.12.C, D.ii. & D.iii, 1-way ANOVA $F_{2,8} = 1.47$, $p = 0.30$; $F_{2,8} = 1.46$, $p = 0.30$, respectively). Consistent with western blotting, VKI het and homo mice displayed a non-significant loss in the density, integrated intensity, and area of DAT puncta within the dorsal striatum (Figure 3.12.C, 1-way ANOVA E.i, $F_{2,8} = 1.54$, $p = 0.29$, E.ii, $F_{2,8} = 4.17$, $p = 0.07$, & E.iii, $F_{2,8} = 4.03$, $p = 0.07$, respectively). Any changes appear independent of universal loss of striatal synaptic markers, as demonstrated by no observed differences in density or co-localization between the pre- and post- synaptic proteins, synapsin1 and PSD95 (Synapsin1 density 1-way ANOVA $F_{2,8} = 1.64$, $p = 0.27$, PSD95 density $F_{2,8} = 1.91$, $p = 0.22$ & synapsin1/PSD95 co-localization $F_{2,8} = 0.56$, $p = 0.59$, as shown in Figure 3.14.B.i, .ii & .iii respectively).

Given the role of VPS35 in α-synuclein processing and cathepsin D trafficking (Miura et al., 2014), and the role of α-synuclein in PD, we also evaluated α-synuclein levels in VKI mice. Immunohistochemical analysis of slices from brains from young VKI animals show no differences in α-synuclein puncta density or distribution in the SNpc (Figure 3.15.A.ii, 1-way ANOVA $F_{2,59} = 0.32$, $p = 0.72$), nor in protein levels as quantified by western blotting of striatal tissue (Figure 3.15.B, 1-way ANOVA $F_{2,33} = 0.28$, $p = 0.98$).

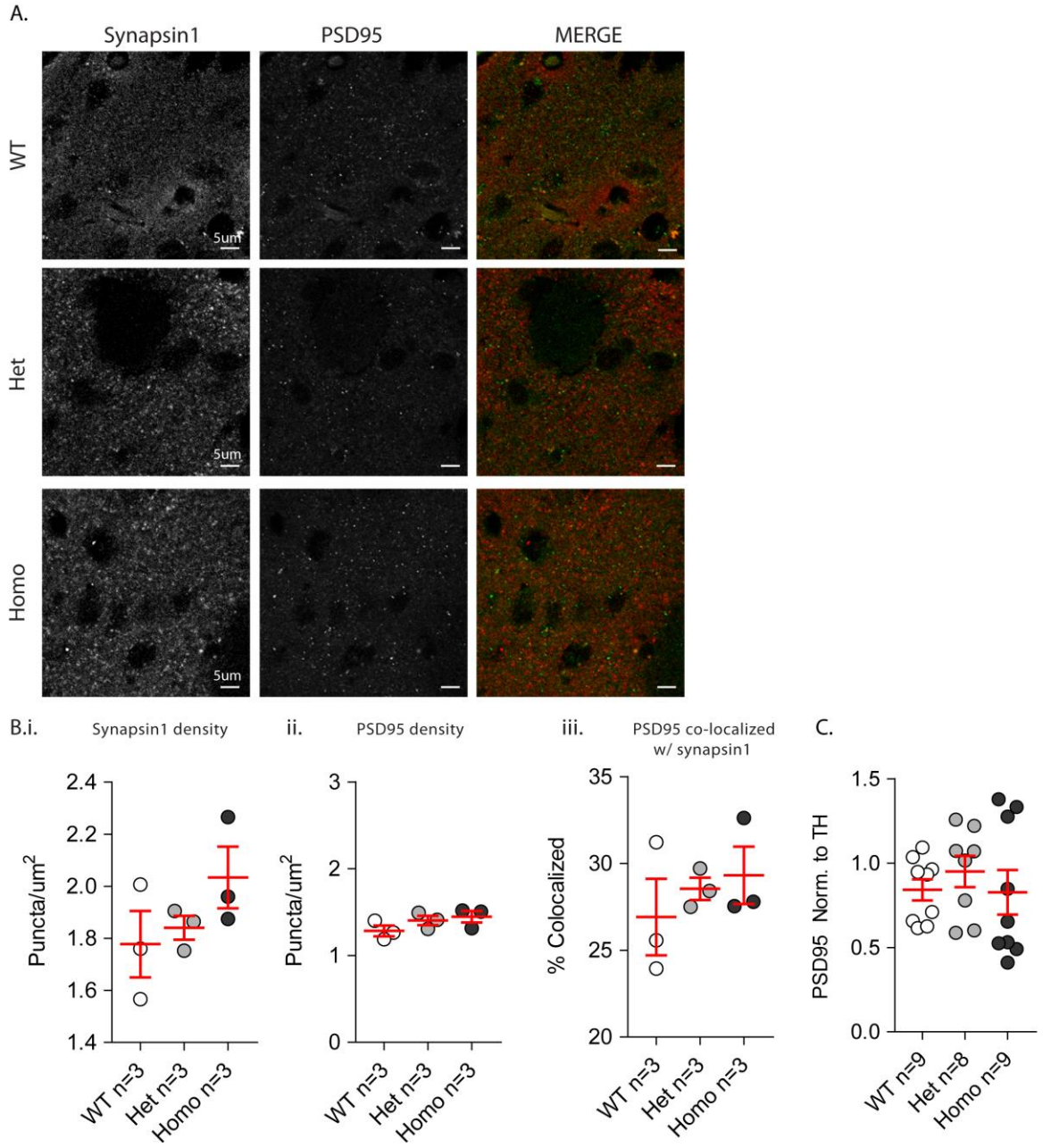

Figure 3.14 Synaptic markers synapsin1 & PSD95 in striatal tissue and slices from young VKI mice
A) Representative Confocal images of Synapsin1 (left) and PSD95 (middle), also merged (right), in the dorsolateral striatum of 3-month-old VKI mice. B) No changes in either synapsin1 (i, 1-way ANOVA $F_{2,8} = 1.64$, $p = 0.27$), or in PSD95 (ii, 1-way ANOVA $F_{2,8} = 1.91$, $p = 0.22$) puncta density were detected, nor in the percentage of synapsin1 and PSD95 co-localization (iii, 1-way ANOVA $F_{2,8} = 0.56$, $p = 0.59$). C) Densitometry analysis was conducted by normalizing PSD95 intensity to TH loading control. No difference was found in PSD95 levels (1-way ANOVA $F_{2,23} = 0.42$, $p = 0.65$).

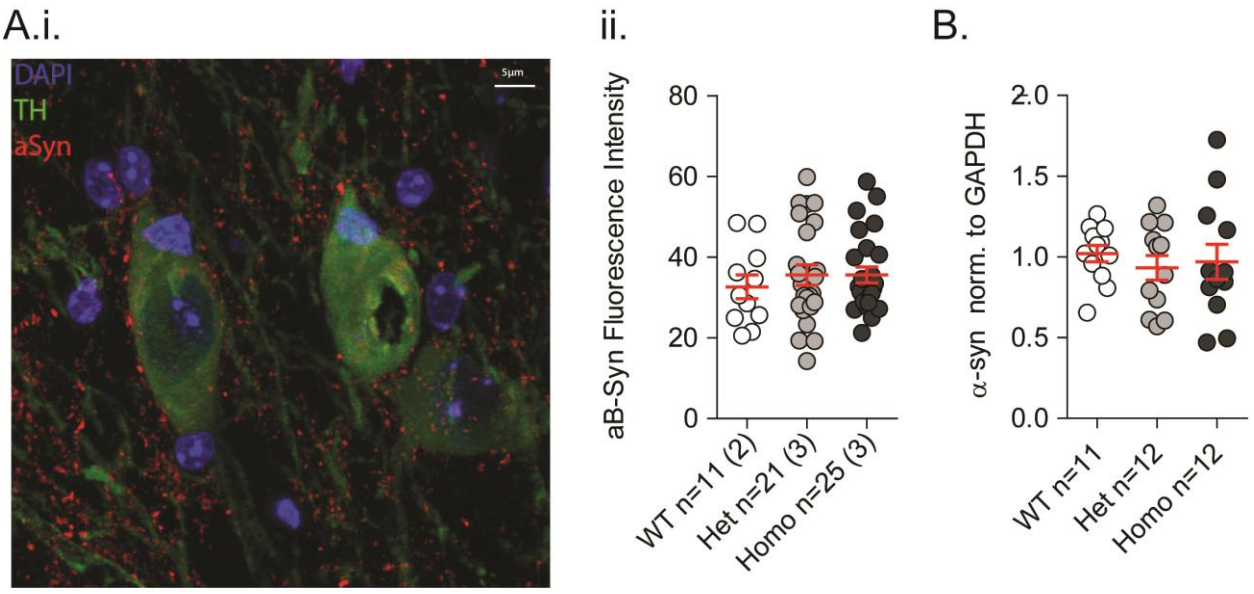

Figure 3.15 α-synuclein evaluation in striatal tissue and SNpc from young VKI mice.
A) Quantification of α-synuclein in slices from VKI mice. Representative image for α-synuclein levels in the SNpc by immunohistochemistry (i). TH+ neurons are shown in green and α-synuclein in red. α-synuclein levels in the SNpc of VKI mice and their WT littermates quantified by IHC, showing no differences in the presence of the mutation (ii, 1-way ANOVA $F_{2,59} = 0.32$, $p = 0.72$). B). α-synuclein levels in the striatum of VKI mice and their WT littermates quantified by western Blot are comparable across all genotypes (1-way ANOVA $F_{2,33} = 0.28$, $p = 0.98$).

Given such strong dopaminergic changes and the increased response to a D2R agonist, we sought to evaluate levels of D2R and its trafficking via VPS35 and the retromer. Interestingly, no difference were found in total striatal levels of D2R, nor in binding of D2R with VPS35 (Figure 3.16.B.ii, iii & iv, 1-way ANOVA $F_{2,13} = 0.60$, $p = 0.56$, $F_{2,16} = 0.45$, $p = 0.64$ & $F_{2,16} = 0.65$, $p = 0.53$, respectively). Despite no changes in D2R, we saw a significant increase in total striatal DARPP-32 levels (Figure 3.17.A, 1-way ANOVA $F_{2,16} = 8.77$, $p < 0.05$, *Bonferroni post-test* WT *vs* het $t_{(16)} = 2.82$, $p < 0.05$ & WT *vs* homo $t_{(16)} = 4.11$, $p < 0.01$), also confirmed by immunohistochemistry (Figure 3.17.B; 1-way ANOVA $F_{2,77} = 3.70$, $p < 0.05$, this data did not reach significance by *Bonferroni post-test*), although the increase was only clear in homozygous mice.

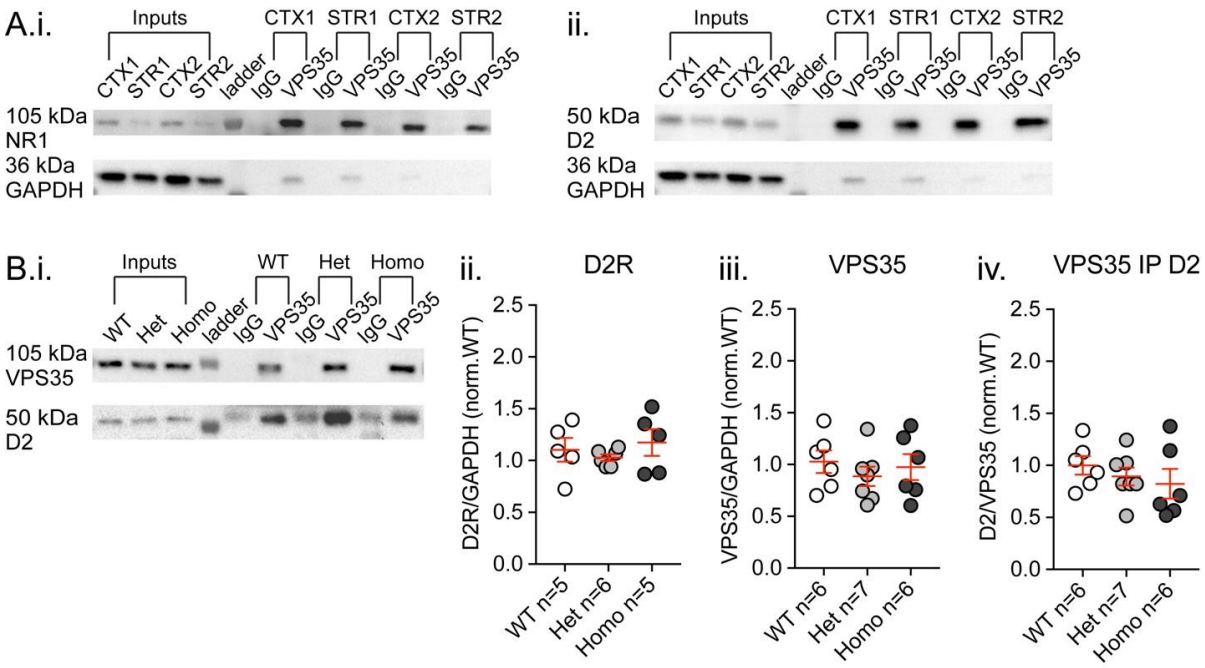

Figure 3.16 Evaluation of D2 levels and binding with VPS35 in striatum from young VKI animals
A) Co-immunoprecipitation were performed on cortical and striatal lysates from VKI mice and their littermates using anti-VPS35 to pull retromer complex and associated proteins. IPs were run on traditional western Blot and propped for VPS35 and D2R. Protein levels from IPs were normalized to the amount of VPS35 pulled. There was no genotype effect on the levels of D2R or VPS35, nor on the amount of D2R pulled by VPS35 (ii, iii, & iv, 1-way ANOVA $F_{2,15} = 0.60$, $p = 0.56$, $F_{2,18} = 0.45$, $p = 0.64$ & $F_{2,18} = 0.65$, $p = 0.53$, respectively).

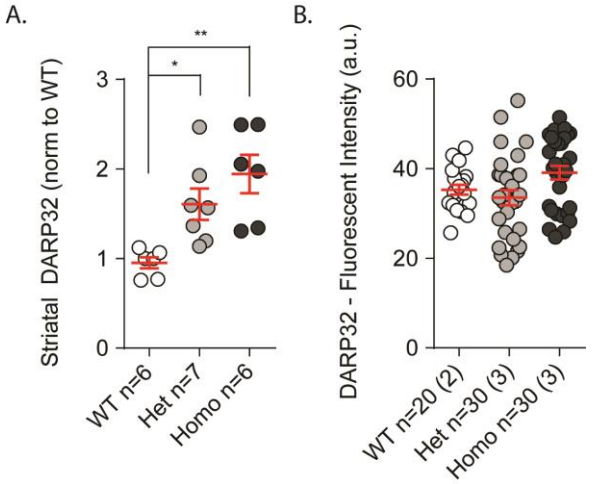

Figure 3.17 Total levels of DARP-32 in the striatum from young VKI mice
A) Total levels of DARP-32 were measured in striatal tissue collected from VKI mice and their WT littermates. Both het and homo mice show increased DARP-32 levels at 3 months of age (1-way ANOVA $F_{2,16} = 8.77$, $p < 0.05$, *Bonferroni post-test* WT *vs* het $t_{(16)} = 2.82$, $p < 0.05$ & WT *vs* homo $t_{(16)} = 4.11$, $p < 0.01$). B) Slices from 3-month-old animals were stained for DARP-32. There was an increase in DARP-32 levels in slices from homozygous

animals (1-way ANOVA $F_{2,77} = 3.70$, $p < 0.05$ although this result did not reach significance by *Bonferroni post-test*).

To evaluate whether alterations were specific to dopaminergic neurons, we assayed serotoninergic transporter (SERT) and norepinephrine transporter (NET) protein levels by western blotting in striatal tissue from young VKI. Interestingly, total striatal SERT was higher (Figure 3.18.B.i, 1-way ANOVA $F_{2,6} = 6.82$, $p < 0.05$, with *Bonferroni post-test* WT *vs* het $t_{(6)} = 3.14$, $p < 0.05$ & WT *vs* homo $t_{(6)} = 3.25$, $p < 0.05$), and NET showed a more variable trend towards being increased (Figure 3.18.B.ii, 1-way ANOVA $F_{2,6} = 2.49$, $p = 0.162$) in VKI, relative to WT littermates.

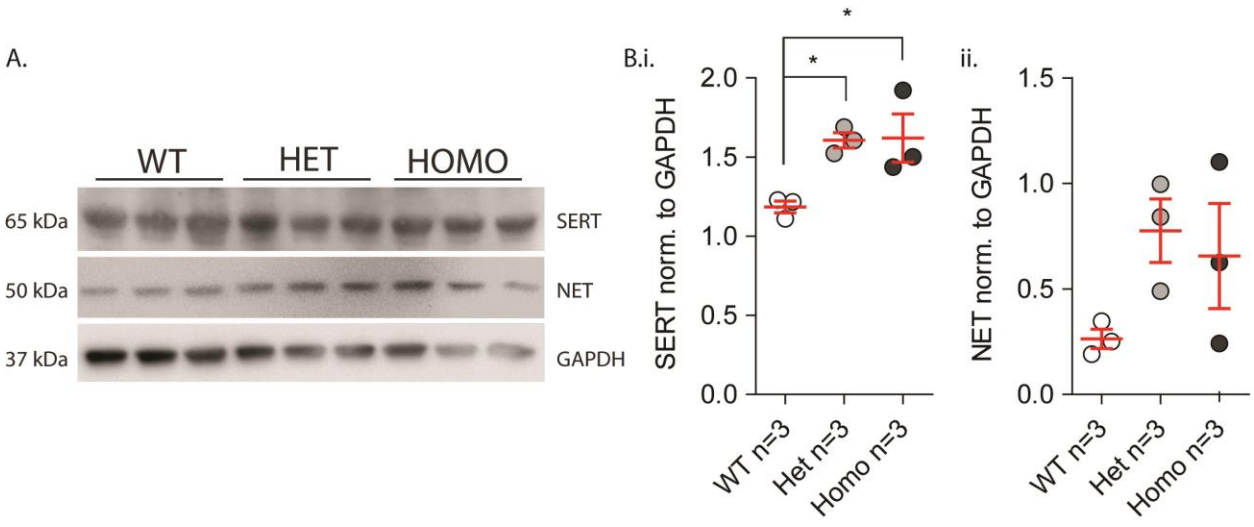

Figure 3.18 Total protein levels of SERT and NET in young VKI striata
A) Representative western blot of SERT and NET in VKI mice. B) Densitometry analysis was conducted normalizing SERT and NET intensity to GAPDH loading control. There was a significant increase in total SERT levels in the striatum of VKI mice (i, 1-way $F_{2,6} = 6.82$, $p < 0.05$, with *Bonferroni post-test* WT *vs* het $t_{(6)} = 3.14$, $p < 0.05$ & WT *vs* homo $t_{(6)} = 3.25$, $p < 0.05$), and a strong trend towards increased levels of NET in mutant animals when compared to WT (ii, 1-way ANOVA $F_{2,6} = 2.49$, $p = 0.162$).

3.3 VKI mice behaviour

3.3.1 VKI mice locomotor function and exploratory behavior

At young ages, motor function was normal in VKI as compared to WT littermates. There were no changes in locomotion in an open field, as measured by total distance traveled and moving time (Figure 3.19.A.i&ii, 1-way ANOVA $F_{2,116} = 0.39$, $p = 0.67$ & $F_{2,116} = 0.71$, p=0.49 respectively). Open field exploration was also comparable as shown by the percentage time spent in the center of the arena (Figure 3.19.A.iii, 1-way ANOVA $F_{2,116} = 0.06$, $p = 0.93$).

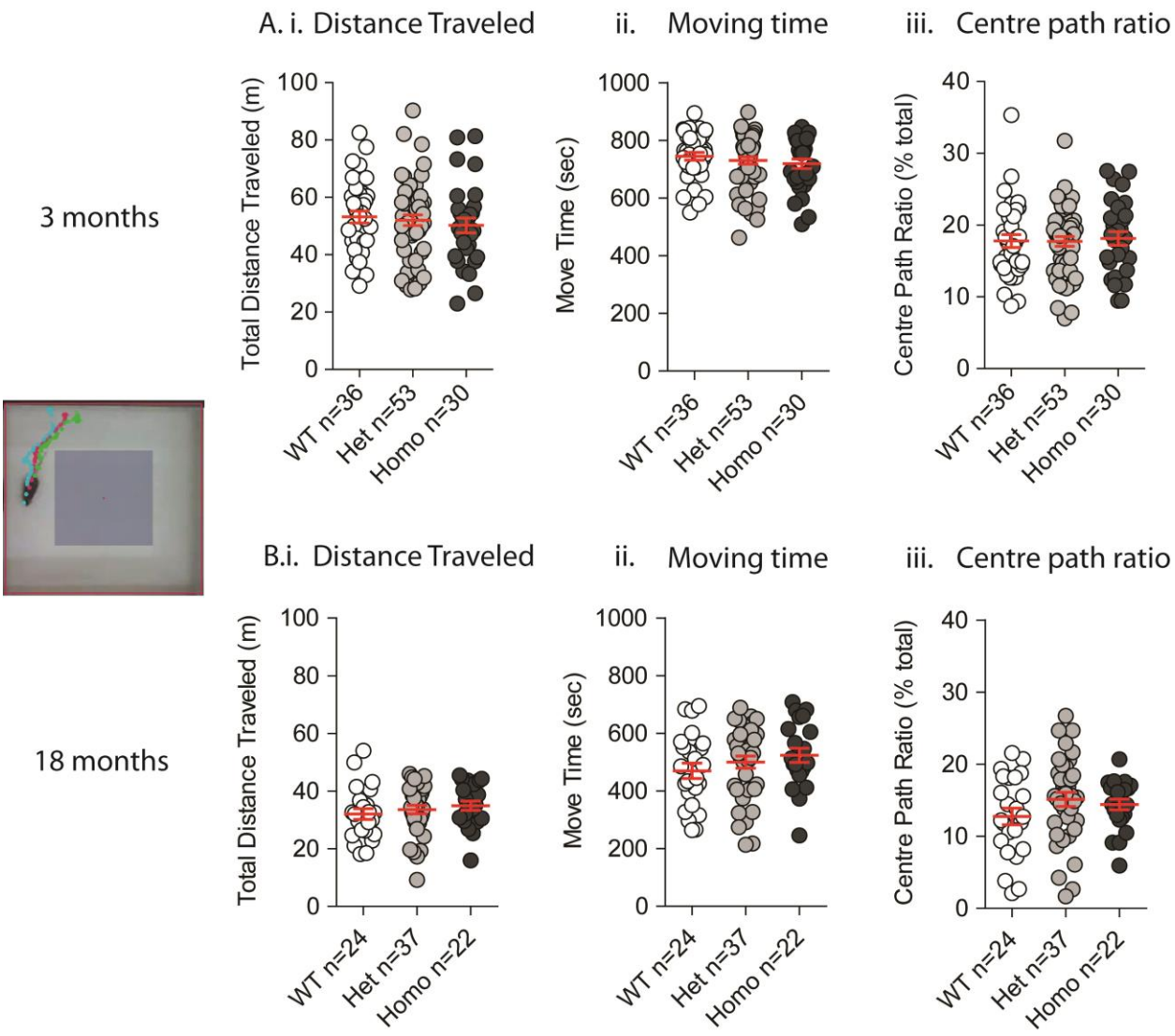

Figure 3.19 Open field test in young and old VKI mice
Young (A) and old (B) mice were placed in an open field arena and video recorded as they explored their new environment for 15 minutes. A) Total distance traveled (i) and moving time (ii) was not different across genotypes (1-way ANOVA $F_{2,116} = 0.39$, $p = 0.67$ & $F_{2,116} = 0.71$, p=0.49 respectively). Percentage of central path exploration was also similar across genotypes (iii, 1-way ANOVA $F_{2,116} = 0.06$, p=0.94). B) Older mice also show no difference in total distance traveled or moving time (i & ii; 1-way ANOVA $F_{2,80} = 0.62$, $p = 0.54$ & $F_{2,80} = 1.07$, $p = 0.35$ respectively). There was no difference in the center path ratio between genotypes (iii, 1-way ANOVA $F_{2,80} = 1.46$, $p = 0.23$, albeit a small trend towards increased distance in the center for VKI mice).

When mice were placed in a 1L cylinder, total number of rearing events was not different in VKI mice compared to het and homo (Figure 3.21.A.i, 1-way ANOVA $F_{2,109} = 0.33$, $p = 0.71$). Grooming events and time were also measured showing no differences across all genotypes (Figure 3.21.A.ii & iii, 1-way ANOVA $F_{2,109} = 0.61$, $p = 0.54$ & $F_{2,109} = 1.79$, $p = 0.17$ respectively). Motor performance on an accelerating rotarod was evaluated. After 2 days of training mice were tested on the rotarod and number of failing events was counted whit an increasing acceleration of the rod. All animals needed two days of training to achieve the ability to run on the accelerating rod, with no difference in total number of fail events over the two days between WT and VKI mice (Figure 3.19.A.i, 1-way ANOVA $F_{2,100} = 1.27$, $p = 0.28$). When tested all mice performed similarly, with comparable increasing number of fail events as the acceleration was increasing (Figure 3.20.Aii., 2-way ANOVA interaction $F_{18,882} = 1.73$, $p < 0.05$, RPM $F_{9,882} = 104.9$, $p < 0.0001$, genotype $F_{2,98} = 1.28$, $p = 0.28$, subjects $F_{98,882} = 2.58$, $p < 0.0001$, also shown as total number of fail events over the 5 minutes of testing in Figure 3.20.A.iii, $F_{2,100} = 1.45$, $p = 0.24$).

With ageing, all mice showed a reduced distance traveled and moving time in the open field (2-way ANOVA distance traveled: interaction $F_{2,195} = 0.83$, $p = 0.43$, genotype $F_{2,195} = 0.038$, $p = 0.96$, age $F_{1,195} = 115.2$, $p < 0.0001$, with *Bonferroni post-test* for WT, het, and homo respectively: $t_{(195)} = 6.86$, $p < 0.0001$; $t_{(195)} = 7.48$, $p < 0.0001$; $t_{(195)} = 4.67$, $p < 0.0001$; moving

time: interaction $F_{2,195} = 1.93$, $p = 0.15$, genotype $F_{2,195} = 0.24$, $p = 0.78$, age $F_{1,195} = 224.6$, $p < 0.0001$, with *Bonferroni post-test* for WT, het, and homo respectively: $t_{(195)} = 9.85$, $p < 0.0001$; $t_{(195)} = 10.07$, $p < 0.0001$; $t_{(195)} = 6.56$, $p < 0.0001$; data not shown), but no significant difference was found between VKI and their WT littermates at 18 months of age (Figure 3.19.B.i & ii, 1-way ANOVA $F_{2,80} = 0.62$, $p = 0.54$ & $F_{2,80} = 1.07$, $p = 0.35$ respectively). Comparable to younger animals, there was not difference in center path ratio by older VKI animals compared to WT (Figure 3.19.B.iii, 1-way ANOVA $F_{2,80} = 1.46$, $p = 0.23$). However, WT show a significant decrease in percentage distance covered in the center, homozygous mice showed a much smaller decrease, while heterozygous mice show a similar percentage exploring the center in young and old age (2-way ANOVA interaction $F_{2,195} = 1.19$, $p = 0.30$, genotype $F_{2,195} = 0.81$, $p = 0.44$, age $F_{1,195} = 24.41$, $p < 0.0001$, with *Bonferroni post-test* for WT, het, and homo respectively: $t_{(195)} = 3.74$, $p < 0.001$; $t_{(195)} = 2.13$, $p > 0.05$; $t_{(195)} = 2.61$, $p < 0.05$). Similarly, the performance in the rotarod test worsen with age, with a much longer training period (5 days versus 2 days at young age) and a much higher number of fail events during testing, but no difference was found between het, homo and WT littermates (Figure 3.20.B.i-iii, 1-way ANOVA $F_{2,45} = 1.004$, $p = 0.37$, 2-way ANOVA interaction $F_{18,360} = 1.83$, $p < 0.05$, RPM $F_{18,360} = 68.45$, $p < 0.0001$, genotype $F_{2,40} = 0.03$, $p = 0.97$, subjects $F_{40,360} = 3.09$, $p < 0.0001$, & 1-way ANOVA $F_{2,45} = 0.03$, $p = 0.97$ respectively), indicating that gross motor skills are not affected in VKI mice.

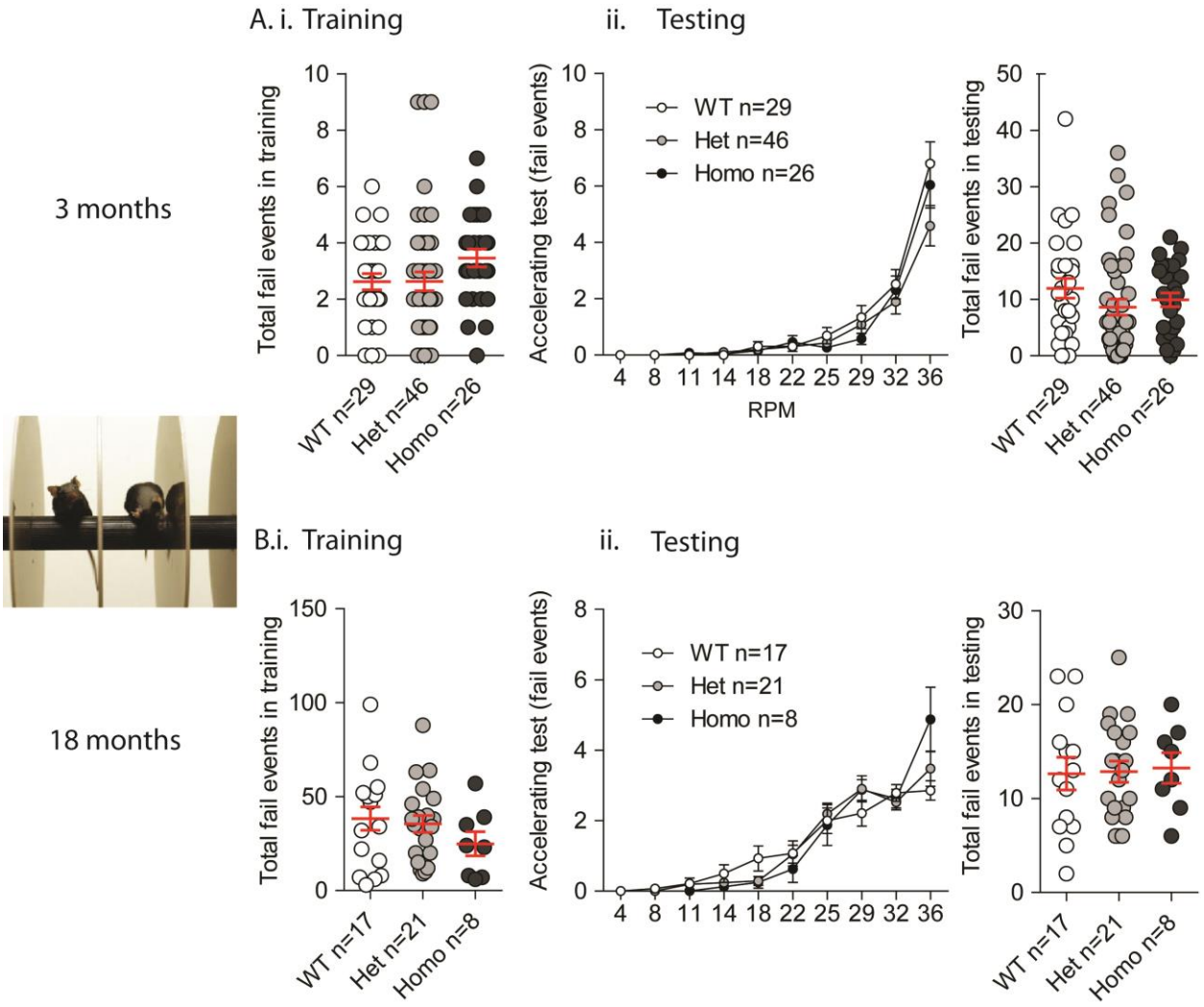

Figure 3.20 Rotarod performance in young and old VKI

Mice were placed on an accelerating rotarod (from 4 to 36 RPM) for 5 minutes. Every time the mouse fell or held on to the rotarod was considered a fail event. A) During training there was no difference between VKI mice and their WT littermates (i, 1-way ANOVA $F_{2,100} = 1.27$, $p = 0.28$) VKI mice show no differences in their performance when compared with their WT littermates (ii, fail per acceleration: 2-way ANOVA interaction $F_{18,882} = 1.73$, $p = 0.03$, RPM $F_{9,882} = 104.9$, $p < 0.0001$, genotype $F_{2,98} = 1.28$, $p = 0.28$, subjects $F_{98,882} = 2.58$, $p < 0.0001$, & total fails during testing: 1-way ANOVA $F_{2,100} = 1.45$, $p = 0.24$, respectively). B) Older mice were also tested for their rotarod performance. Training was longer in old animals (5 days to reach the ability to perform the test), but no difference was found in number of fails for VKI mice compared to WT littermates (i, 1-way ANOVA $F_{2,45} = 1.004$, $p = 0.37$). When tested for the accelerating rotarod VKI mice performed similarly to WT animals (ii, 2-way ANOVA 2-way ANOVA interaction $F_{18,360} = 1.83$, $p < 0.05$, RPM $F_{18,360} = 68.45$, $p < 0.0001$, genotype $F_{2,40} = 0.03$, $p = 0.97$, subjects $F_{40,360} = 3.09$, $p < 0.0001$, & 1-way ANOVA $F_{2,45} = 0.03$, $p = 0.97$ respectively).

Reduced rearings are also noted in older animals. Surprisingly, homozygous animals, but not heterozygous mice, show an increased number of rearings (1-way ANOVA $F_{2,79} = 2.97$, $p =$

0.057) albeit not significant, while both het and homo mice trend towards agreater number of grooming events and total grooming time, that is significant different for homozygous animals (1-way ANOVA grooming events: $F_{2,79} = 2.67$, $p = 0.08$ & grooming time: $F_{2,79} = 5.45$, $p < 0.01$, with *Bonferroni post-test* WT vs het $t_{(79)} = 1.77$, $p = 0.16$ & homo $t_{(79)} = 3.3$, $p < 0.01$).

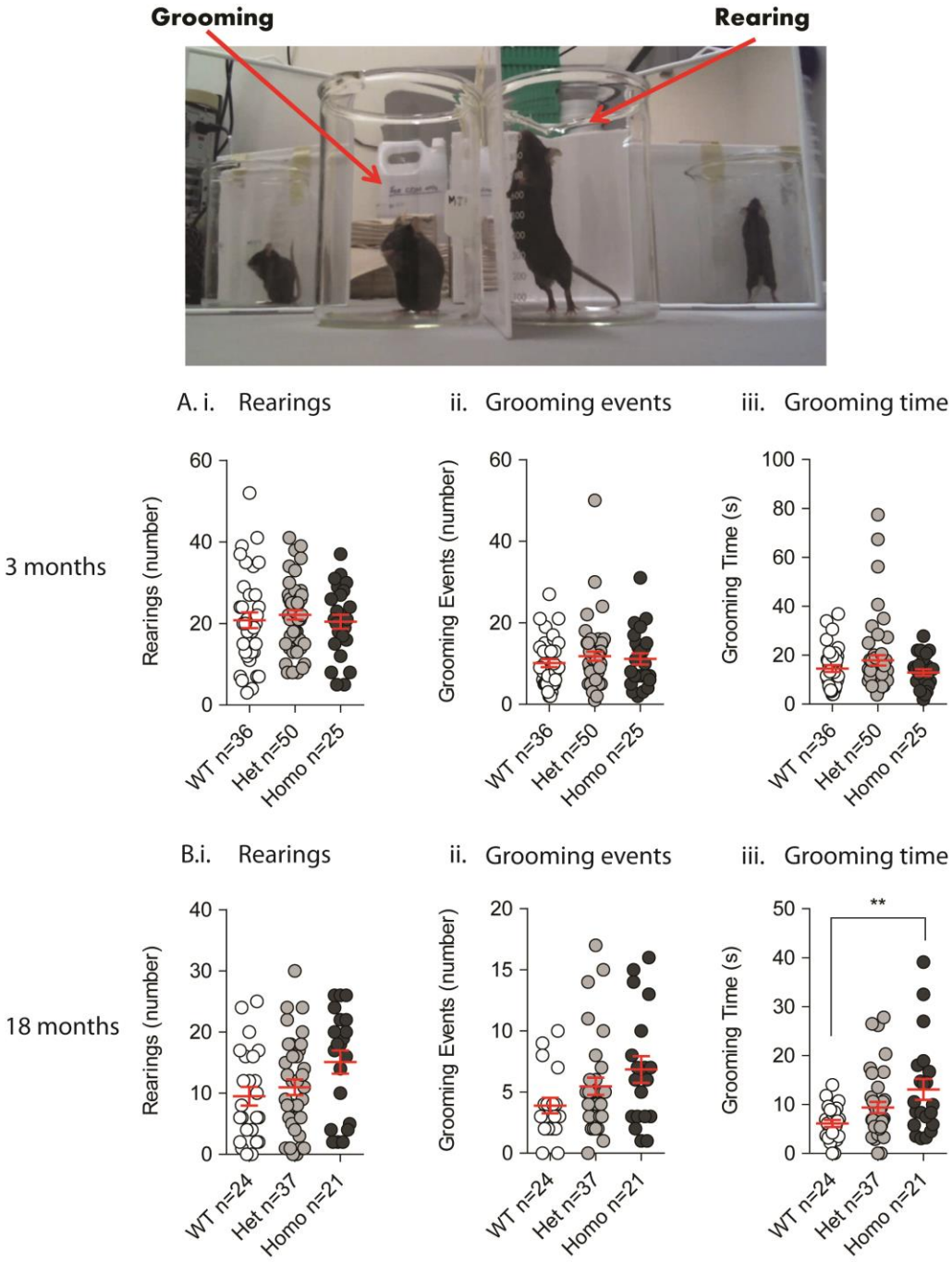

Figure 3.21 Cylinder test activity in young and old VKI mice

Mice were video recorded after being placed in a 1L-glass beaker for 5 minutes. The number of rearings and grooming activity was scored off-line by an experimenter blinded to genotype. A) Mice show no significant difference in novelty-induced exploration (rearing; 1-way ANOVA $F_{2,109} = 0.33$, $p = 0.71$). Similarly, there was no differences in total number of grooming events and total duration of grooming (ii & iii, 1-way ANOVA $F_{2,109} = 0.61$, $p = 0.54$ & $F_{2,109} = 1.79$, $p = 0.17$ respectively) B) In older age VKI mice show increased number of rearings (i, 1-way ANOVA $F_{2,79} = 2.97$, $p = 0.057$), and higher number of grooming events, with significantly more time

spent grooming (1-way ANOVA grooming events, ii: $F_{2,79} = 2.67$, $p = 0.08$ & grooming time, iii: $F_{2,79} = 5.45$, $p < 0.01$, with *Bonferroni post-test* WT vs het $t_{(79)} = 1.77$, $p = 0.16$ & homo $t_{(79)} = 3.3$, $p < 0.01$).

When tested in an elevated plus maze, young VKI mice explored both enclosed and open arms less than WT littermates (shown as number of total entrances events in all arms in Figure 3.22.A, 1-way ANOVA $F_{2,101} = 6.28$, $p < 0.01$, with *Bonferroni post-test* WT vs het $t_{(101)} = 2.54$, $p < 0.05$ & homo $t_{(101)} = 3.46$, $p < 0.01$ for het and homo VKI mice respectively). Interestingly, VKI mice spent significantly less time exploring the open arms (Figure 3.22.B, 1-way ANOVA $F_{2,101} = 6.56$, $p < 0.01$, with *Bonferroni post-test* WT vs het $t_{(101)} = 2.88$, $p < 0.01$ & homo $t_{(101)} = 3.41$, $p < 0.01$ for het and homo mice, respectively). At 3 months, while general locomotion and locomotor learning appear unaltered, the motivation for exploration in stressful and anxiogenic environments is reduced.

With ageing all mice reduce exploration of the maze, reducing number of entrances in all arms (Figure 3.22.A, 2-way ANOVA interaction $F_{2,179} = 5.54$, $p < 0.01$, age $F_{1,179} = 143.7$, $p < 0.0001$, genotype $F_{2,179} = 2.29$, $p = 0.104$, *Bonferroni post-test* young vs old $t_{(101)} = 9.08$, $p < 0.0001$ for WT; $t_{(101)} = 8.119$, $p < 0.0001$ for het; $t_{(101)} = 4.04$, $p < 0.001$ for homo). Interestingly, while all animals reduced the time spent exploring the open, a significant reduction is shown in WT, while there is a smaller decrease in het animals and no difference between young and old homo mice (Figure 3.22.B, 2-way ANOVA interaction $F_{2,179} = 6.64$, $p < 0.01$, age $F_{1,179} = 32.19$, $p < 0.0001$, genotype $F_{2,179} = 0.82$, $p = 0.44$, *Bonferroni post-test* young vs old $t_{(101)} = 5.99$, $p < 0.0001$ for WT; $t_{(101)} = 3.11$, $p < 0.01$ for het; $t_{(101)} = 0.84$, $p > 0.05$ for homo). This data would suggest the explorative behaviour to be altered at both ages, with a tendency towards an anxiety-like behaviour in young age. This would be in agreement with higher grooming time for 18-

month-old VKI, in the cylinder test, suggesting older animals trend towards anxiolytic-like behaviour.

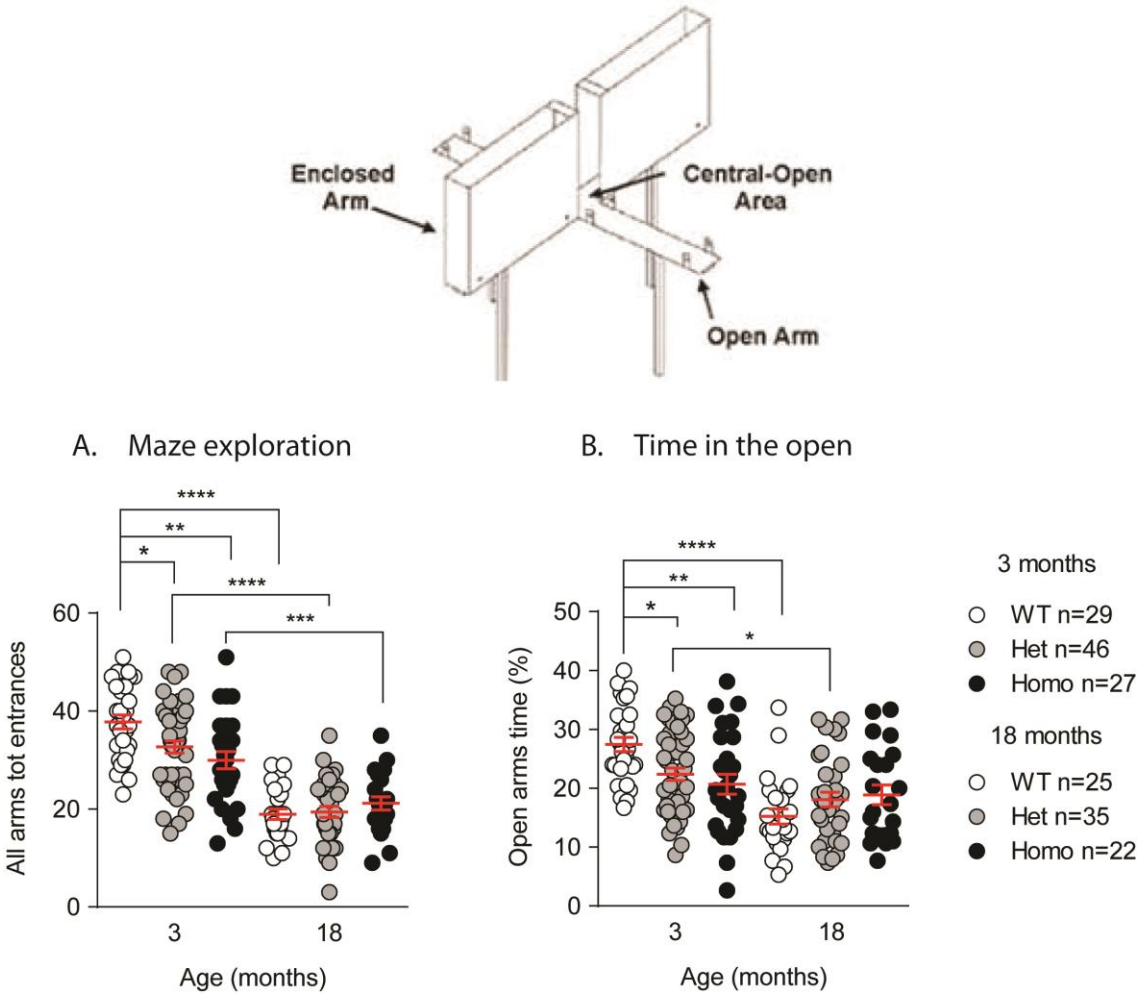

Figure 3.22 Exploratory behaviour in an elevated plus maze in young and old VKI
Mice were left exploring an elevated plus maze for 5 minutes. Number of entrance in each arm was counted and total time spent exploring the open arms was measured. A) 3-months-old animals show fewer total number of entrances in all arms, indicating lower exploration of the maze (1-way ANOVA $F_{2,101} = 6.28$, $p < 0.01$, with *Bonferroni post-test* WT vs het $t_{(101)} = 2.54$, $p < 0.05$ & homo $t_{(101)} = 3.46$, $p < 0.01$ for het and homo mice respectively). All mice decreased exploration with age with no differences across all genotypes (2-way ANOVA interaction $F_{2,179} = 5.54$, $p < 0.01$, age $F_{1,179} = 143.7$, $p < 0.0001$, genotype $F_{2,179} = 2.29$, $p = 0.104$, *Bonferroni post-test* young vs old $t_{(101)} = 9.08$, $p < 0.0001$ for WT; $t_{(101)} = 8.119$, $p < 0.0001$ for het; $t_{(101)} = 4.04$, $p < 0.001$ for homo). B) Young mice show lower percentage of time spent exploring the open arms (1-way ANOVA $p<0.0002$, *Bonferroni post-test* $p<0.04$, $p<0.002$ for het and homo mice respectively). With age WT mice reduce their percentage of time spent exploring the open, while this reduction is smaller in het animals and absent in homo mice (2-way ANOVA interaction $F_{2,179} = 6.64$, $p < 0.01$, age $F_{1,179} = 32.19$, $p < 0.0001$, genotype $F_{2,179} = 0.82$, $p = 0.44$, *Bonferroni post-test* young vs old $t_{(101)} = 5.99$, $p < 0.0001$ for WT; $t_{(101)} = 3.11$, $p < 0.01$ for het; $t_{(101)} = 0.84$, $p > 0.05$ for homo).

Not all mice underwent the same experiments. A detailed list of experiments and the order they were performed, for each cohort, is shown in Table B.3 in Appendix B.2. The first cohort of young animals to be tested underwent open field without being tested for elevated plus maze.

We then looked further in the exploratory activity of VKI mice during the open field. We re-analyzed two cohorts of mice tested in the open field, and divided the arena into four different zones. The analysis on a 6-months-old cohort of VKI mice, naive to experiments prior to open field, showed reduced time in the two zones closer to the examiner, for heterozygous animals, while WT littermates uniformly covered the entirety of the arena (Figure 3.23.B; 1-way ANOVA $F_{3,15} = 0.89$, $p = 0.86$ & $F_{3,15} = 3.03$, $p = 0.07$, respectively for WT and het). Unfortunately, the number of animals was low and quite variable and this data did not reach significance. When a separate cohort of 3-month-old VKI mice, previously exposed to elevated plus maze prior to open field, was analyzed for zone preference, there was no apparent change in percentage of time spent exploring each zone (Figure 3.23.C; 1-way ANOVA $F_{3,19} = 2.53$, $p = 0.56$, $F_{3,28} = 0.81$, $p = 0.49$, & $F_{3,16} = 0.67$, $p = 0.57$ for WT, het, and homo, respectively).

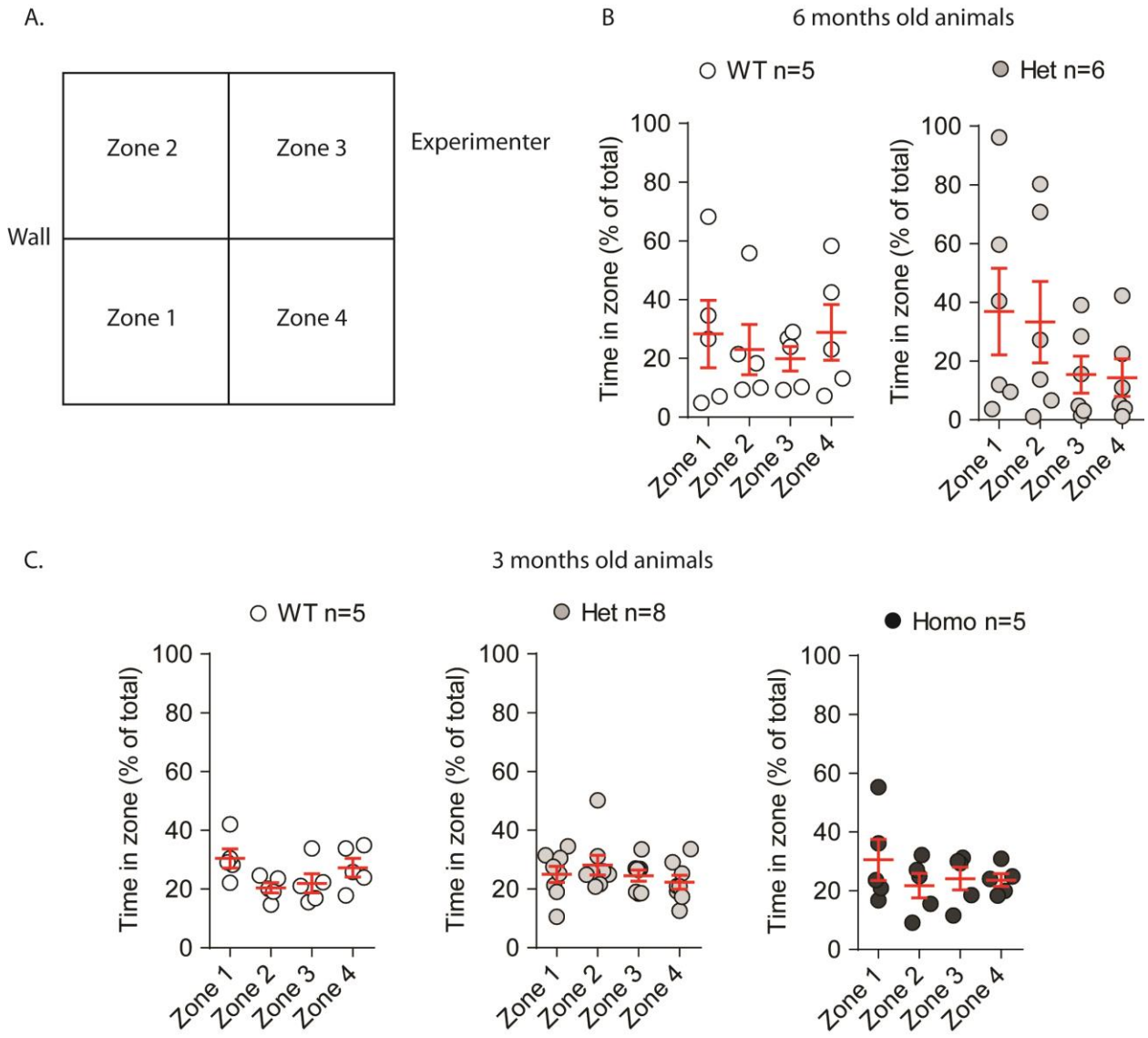

Figure 3.23 Zone preference in an open field in 6 months old VKI

Open field experiment was re-analyzed for a cohort of 6-month-old animals naive to testing, and a cohort of 3-month-old animals that experienced the elevated plus maze before the open field. For analysis, the open field arena was divided into 4 zones. A) Areas 1 and 2 were distant from the experimenter and closer to a wall. Zones 3 and 4 were instead closer to the experimenter and further away from the wall. B) In the naive group, WT mice (left) uniformly explored all zones in both groups (1-way ANOVA $F_{3,15} = 0.89$, $p = 0.86$), while het animals show a trend towards greater exploration in zones 1 and 2 (1-way ANOVA $F_{3,15} = 3.03$, $p = 0.07$). C) In the group previously exposed to elevated plus maze, no difference was found between time spent in the 4 zones across all genotypes (1-way ANOVA $F_{3,19} = 2.53$, $p = 0.56$, $F_{3,28} = 0.81$, $p = 0.49$, & $F_{3,16} = 0.67$, $p = 0.57$ for WT, het, and homo, respectively).

3.3.2 Cognitive evaluation

To evaluate cognition in VKI mice we used a radial arm maze paradigm. Usually the radial arm maze is used to evaluate spatial memory. In our case we did not suspect alteration in memory function, particularly in young animals; therefore we modified the paradigm to better assess set-shifting, perseveration, and outcome evaluation.

We used here a radial arm maze consisting of a central area and 8 arms (maze shown in Figure 3.24). Mice were first habituated for 3 days to a solution of 30% sucrose in regular water. As expected, given a choice of regular water and 30% sucrose-water in their home cage (bottle holder as shown in Figure B.5), all mice preferred sucrose-water and did not consume regular water. The amount of liquid consumption was also increased compared to average (normally around 3-4mL of water per day). Unfortunately mice were no single housed, nor separated by genotype, so it was not possible to distinguish whether some mice have been drinking more sucrose-water than others, or if certain mice had a stronger preference towards sucrose-water compared to regular water.

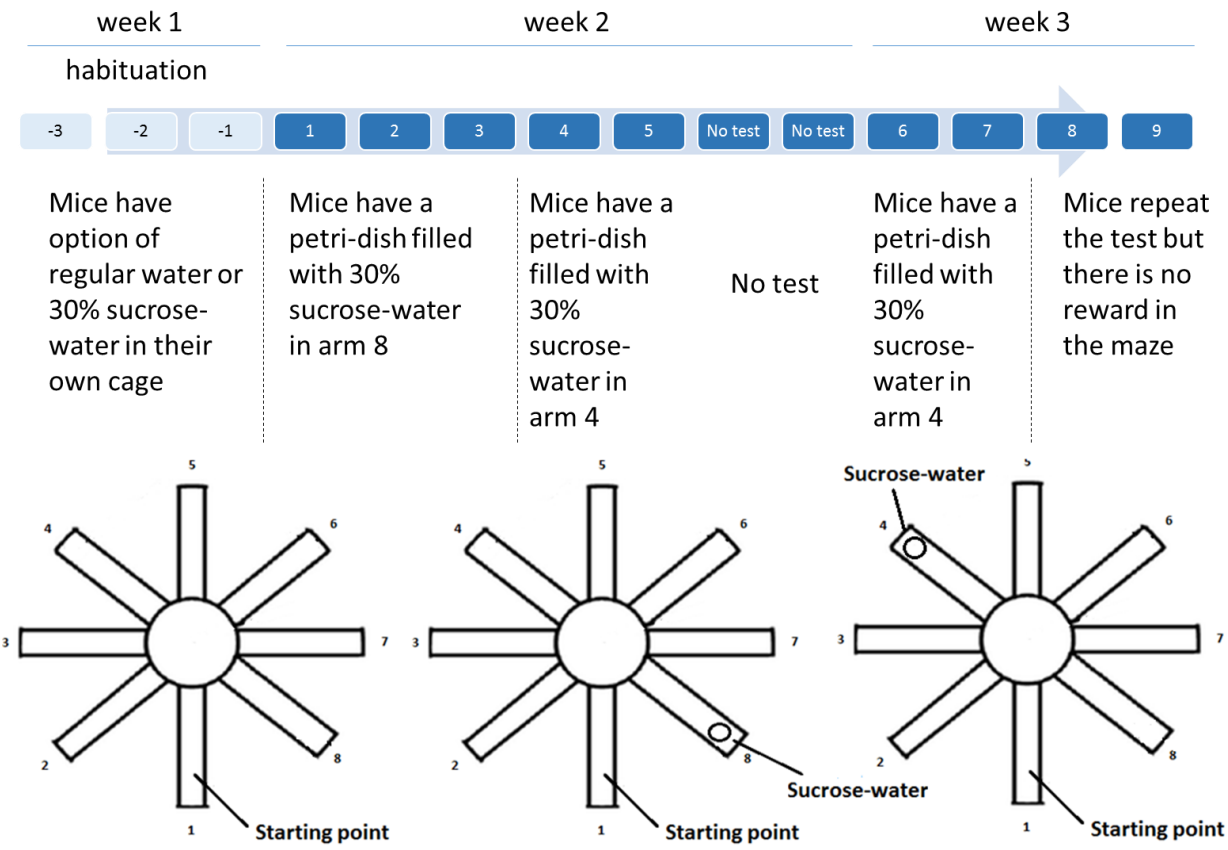

Figure 3.24 Experimental set up for radial arm maze test
Time line for the radial arm maze test. Mice were habituated to a 30% sucrose-water solution for 3 days prior to testing. On day 1 mice testing begins. Mice were left exploring the maze for 5 minutes with a petri-dish containing sucrose-water in arm 8. The test was repeated for the 2 following days. On day 4 the solution was moved to arm 4. After day 5 there was a 2-days period in which mice were not tested. On day 6 the solution was still in arm 4. Sucrose-water was then removed from the maze on day 8 and the test was repeated for two days (day 8 and 9).

After three days of habituation, mice were tested and left exploring the maze for 5 minutes each day for 9 consecutive days.

For the first three days of testing, a petri-dish filled with the sucrose-water solution was placed in arm 8 (as shown in Figure 3.24 and discussed in the method section 2.10). At all ages (3 and 18-months) all mice showed preference for arm 8 over other arms, quantified in percentage of time spent in arm 8 over total time exploring all arms (Figure 3.25.A, B, & C; while equal exploration of arm would require ~12.5% of time in each arm, exploration of arm 8

is ~25%). On day 4 of testing, the sucrose solution was moved to arm 4. As expected, WT mice showed a significant decrease in time spent in arm 8 and a significant increase in time spent in arm 4. While there was a small increase in the time spent in arm 4, het and homo animals did not show any reduction in time spent exploring arm 8, now lacking the reward. Instead VKI mice perseverated on spending time in arm 8, despite the absence of the reward in that arm (Figure 3.25.C, 3-way ANOVA $F_{2,58} = 3.861$, $p < 0.05$, *post-test* WT $t_{(57)} = 3.52$, $p < 0.001$, het $t_{(57)} = 0.79$, $p = 0.12$, & homo $t_{(57)} = 0.97$, $p = 0.99$).

After day 5, mice were left resting and tested again after two days (day 6). All young mice were able to find sucrose fairly quickly and increased the time spent in the arm containing sucrose. On day 8, sucrose was removed from the maze and the test was repeated. All young animals decreased the time spent in arm 4 and increased the time spent in arm 8. This behaviour suggests that in the absence of sucrose all mice go back to the first location of sucrose, the strongest association with the reward.

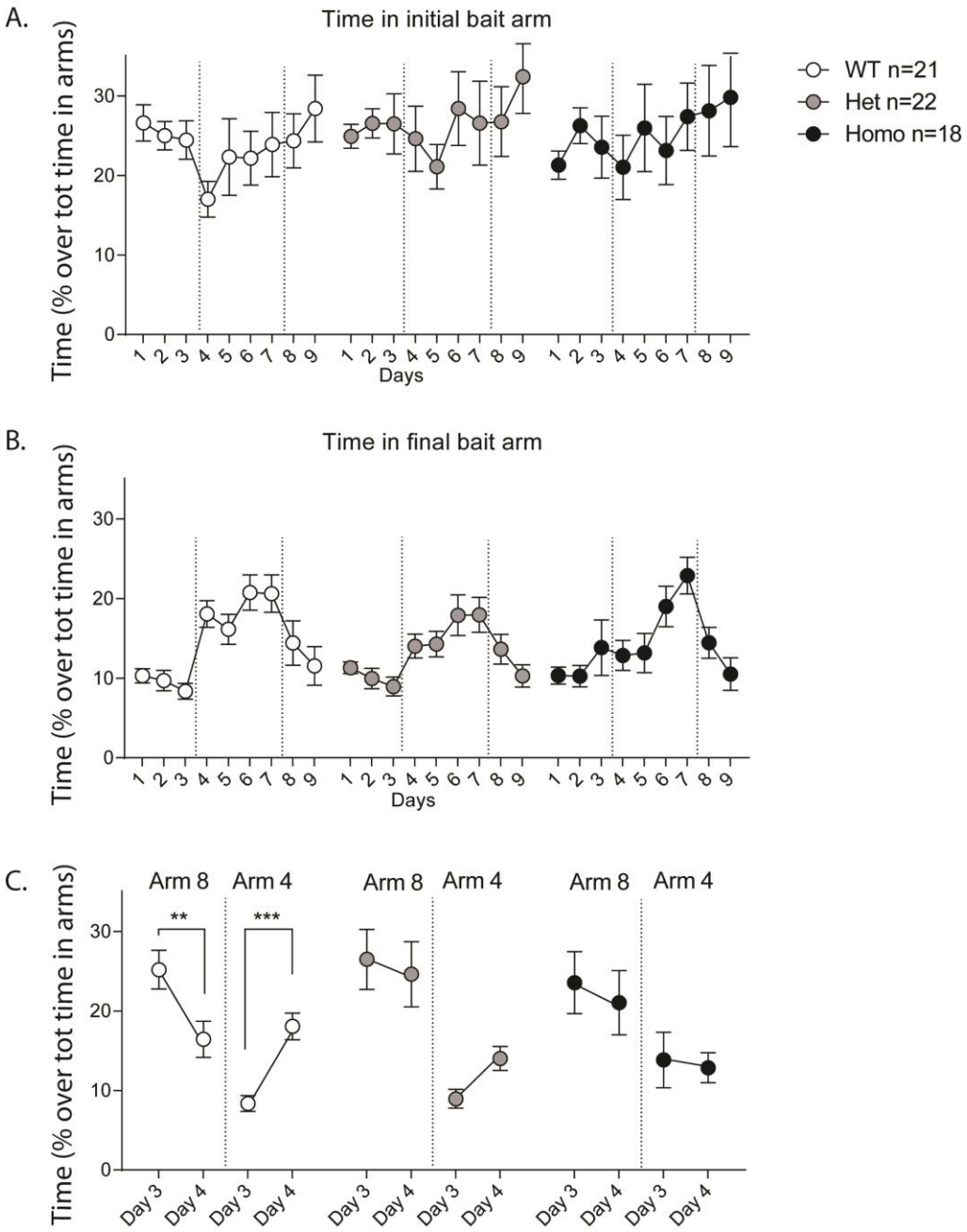

Figure 3.25 Radial arm maze in 3-months-old VKI

A) Percentage of time spent in arm 8 over the 9 days of testing. WT (white) reduced time spent in arm 8 when sucrose was moved to arm 4 (day 4), while het (grey) and homo (black) did not show this change. B) Percentage time spent in arm 4, indicating increased time on day 4 for WT and het animals, but not homozygous mice. C) Summary of Figure 3.25.A&B, showing the change in time spent in either arm 8 and 4 when sucrose was moved from arm 8 to arm 4 between day 3 and day 4 of testing (3-way ANOVA $F_{2,58} = 3.861$, $p < 0.05$, *post-test* WT $t_{(57)} = 3.52$, $p < 0.001$, het $t_{(57)} = 0.79$, $p = 0.12$, & homo $t_{(57)} = 0.97$, $p = 0.99$).

When 18-month-old were tested on the same paradigm, on day 4 of testing WT mice showed a similar phenotype to younger animals, significantly decreasing the time spent in arm 8 and increasing the time spent in arm 4. While old het and homo animals increased the time spent in arm 4, there was no reduction in time spent in arm 8 (Figure 3.26.C; although these data did not reach significance by 3-way ANOVA $F_{2,38} = 1.375$, $p < 0.26$). Older mutant mice are showed a similar persistent phenotype to young VKI mice, only less pronounced. Similarly to younger animals, once the sucrose solution was removed from the maze, the time spent in arm 8 did not change compared to the day before, as all mice went back to the original arm containing sucrose throughout the entire experiment (Figure 3.26.D). As with young animals, older WT and het mice decreased the time spent in arm 4. Interestingly, 18-month-old homo mice did not show the same reduction, suggesting that the perseverative phenotype was worsening with age, although this did not reach significance (Figure 3.26.D, 3-way ANOVA $F_{2,38} = 0.27$, $p < 0.20$).

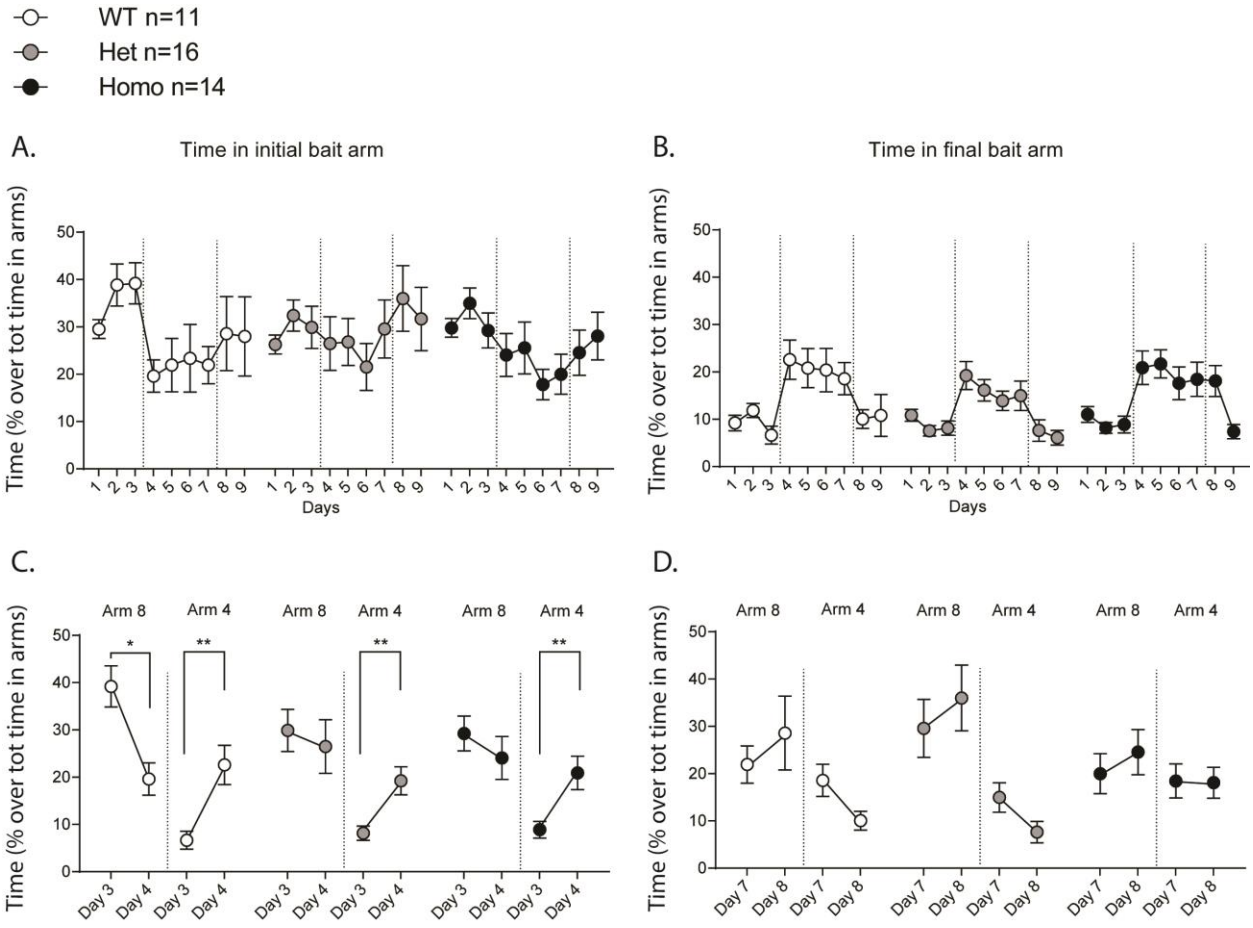

Figure 3.26 Radial arm maze in 18-months-old VKI

A) Percentage of time spent in arm 8 over the 9 days of testing. WT (white) reduced time spent in arm 8 when sucrose was moved to arm 4 (day 4), while het (grey) and homo (black) did not show this change. B) Percentage time spent in arm 4, indicating increased time on day 4 for WT and het animals, but not homozygous mice. C) Summary of Figure 3.26.A&B, showing the change in time spent in either arm 8 and 4 when sucrose was moved from arm 8 to arm 4 between day 3 and day 4. This difference was not apparent in het and homo mice (3-way ANOVA $F_{1,38} = 1.375$, $p < 0.26$). D) Summary of Figure 3.26.A&B, showing the change in time spent in either arm 8 and 4 when sucrose was moved away from the maze between day 7 and day 8 of testing. This change was obvious in WT and het mice, but absent in homozygous animals (3-way ANOVA $F_{2,38} = 0.27$, $p < 0.20$, although this data did not reach significance).

We then sought to evaluate spatial and memory recognition in young animals using a novel object recognition and a novel object location paradigm. We tried first to identify a pair of objects for which our mice would not show any preference that would alter the result of the test; many were used, in different shapes, texture, and colour. Unfortunately we were unable to

identify objects that were suitable for the test, and could not guarantee that the zone preference would not affect the test. Despite not being able to perform novel object location or novel object recognition tasks, we investigated mouse behaviour during the familiarization process preceding the test itself with a specific pair of objects. After the open field paradigm, mice were left exploring the same arena but in the presence of two different novel objects for 5 minutes (specific objects used for this task shown in Figure B.6). This assay was performed three times with 5 minutes resting time intervals in which the mice were put back in their home cage. The time spent exploring either object was quantified using the same Anymaze tracking system as for the open field. For all WT there was a strong preference towards one of the 2 objects, and several familiarization trials were not able to reduce this preference (Figure 3.27.A, 1-way ANOVA $F_{5,27} = 8.17$, $p < 0.001$, *Bonferroni post-test* familiarization 1 $t_{(22)} = 2.36$, $p = 0.08$, familiarization 2 $t_{(22)} = 2.91$, $p < 0.05$, & familiarization 3 $t_{(22)} = 5.18$, $p < 0.0001$). Interestingly, VKI mice showed no preference in the first familiarization trial, but eventually built up a preference during trial 2, which seemed to become stronger during trial 3 but without reaching significance (Figure 3.27, 1-way ANOVA $F_{5,27} = 1.11$, $p = 0.38$),. What caused this increasing preference would need further investigation, but showed consistently different exploratory behaviour and cognitive abilities for VKI mice.

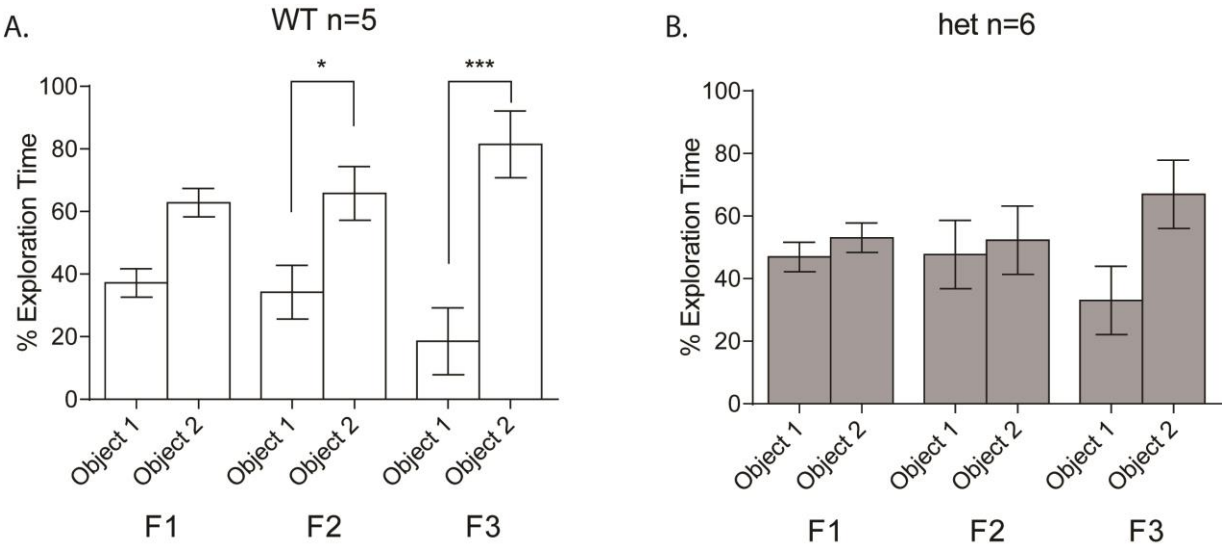

Figure 3.27 Object preferences in 6-month-old VKI
Exploration for the 2 objects for the three familiarization trials (F1, F2, and F3). WT mice showed greater exploration of object 2, particularly in F2 and F3 (A, 1-way ANOVA $F_{5,27} = 8.17$, $p < 0.001$, *Bonferroni post-test* familiarization 1 $t_{(22)} = 2.36$, $p = 0.08$, familiarization 2 $t_{(22)} = 2.91$, $p < 0.05$, & familiarization 3 $t_{(22)} = 5.18$, $p < 0.0001$), while het mice only showed a trending preference during the last familiarization trial (B, 1-way ANOVA $F_{5,27} = 1.11$, $p = 0.38$).

3.4 Pathological assessment

Pathological evaluation of brain tissue from 18-month-old VKI mice was performed in collaboration with Heather Melrose's group at Mayo clinic. Brains were fixed via intra-cardiac perfusion with 4% PFA, then collected and shipped to Melrose's lab for histology. Brain slices were stained for canonical PD pathological markers, such as α-synuclein and tau. While the greatest portion of the pathology evaluation is still ongoing a few images have been analyzed and showed a much stronger phospho-tau staining signal in slices from brains from 18-month-old homozygous animals when compared to slices from WT of the same age (Figure 3.28).

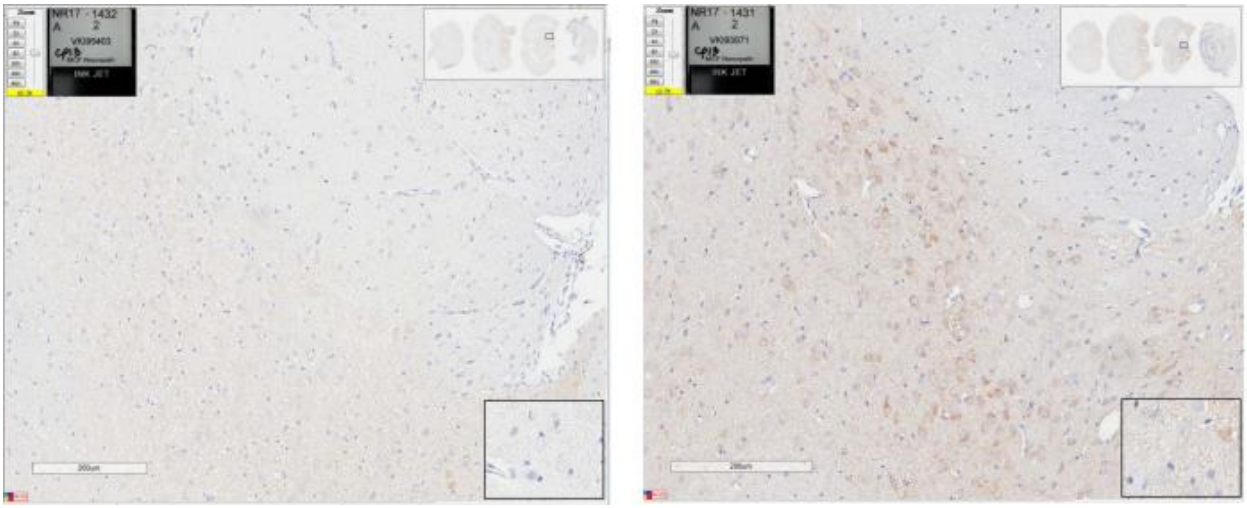

Figure 3.28 Example images of tau staining in brain slices from VKI.
Brains from 18-month-old VKI animals were extracted. 5µm slices were obtained by cryostat and stained for phospho-tau (Ser202, CP13). Here shown two example images of midbrains from WT (left) and homozygous (right) mice, showing greater staining in the midbrain from homozygous animal.

Chapter 4: Discussion

In this work we aimed to characterize a novel mouse model of parkinsonism. Prof. Farrer's lab developed a mouse carrying the point mutation p.D620N of the VPS35 protein, recently linked with PD. The mutant mouse is viable and shows no alteration in the physiological levels of the protein. In my work I evaluated alterations in the dopaminergic system and attempted to correlate behavior, in the presence of the mutation. My goal was to understand early deficits in PD and explore a possible mechanism for disease.

4.1 Dopaminergic dysfunction

In VKI mice there was no overt loss of TH+ dopaminergic innervation to the striatum or loss of nigral neurons. However, striatal immunohistochemistry and protein biochemistry revealed a major increase in VMAT2 (albeit similar puncta number, with greater intensity and area) and significant decrease in DAT (also trending by immunohistochemistry with less puncta, intensity, and area). Remarkably, striatal tissue from young VKI showed an increased capacity to evoke dopamine release by *ex-vivo* FSCV, which was gene dose-dependent. In heterozygous animals, there was also a modest increase in dopamine decay time consistent with elevated evoked dopamine and impaired re-uptake. A similar increase in the duration of dopamine release transients was shown in a *Lrrk2* pG2019S knock-in mouse model we recently published, phenomenon that persisted in the absence of DAT re-uptake (Volta et al., 2017).

While DAT levels appeared to be reduced in young het and homo mice, the re-uptake by FSCV was only significantly affected in het animals. This would suggest het and homo dopaminergic neurons compensate slightly differently, or homozygous animals have more than one impairment, which diminishes this phenotype. Regardless, levels of DAT do not necessary

relate to its function, or its expression on the membrane. Preliminary data suggest that DAT is indeed trafficked by VPS35, shown by co-immunoprecipitation of DAT with VPS35. Future studies should investigate whether differential activity and/or surface expression is seen in het and homo VKI animals.

D2R levels were not different and autoreceptors appeared to function normally on short-term scales (attenuating further dopamine release within seconds during paired-pulse stimulation), albeit the efficacy of D2R negative tuning may be less in VKI slices. However, bath application of quinpirole, a selective D2R agonist, had a more immediate inhibitory effect on dopamine release in VKI slices over a longer time-frame (~10 minutes), at both ages. No differences in D2R binding with VPS35 suggests that trafficking to the surface is not altered, although it would be interesting to assay whether there are more D2R on the cell surface. The increase in DARPP-32 is in agreement with greater response to quinpirole treatment in VKI slices, suggesting that altered D2R effect is likely due to altered D2R downstream signaling cascades (and possibly also D1R), rather than D2R levels per-se.

Though basal levels of extracellular dopamine appeared normal by *in-vivo* microdialysis, dopamine metabolism was significantly elevated in young homozygous animals, indicating that in 3-month-old animals the excess of dopamine is likely compensated by metabolism. As microdialysate collection was over an hour the amount of dopamine and metabolites also reflects clearance from the synaptic cleft, either by diffusion, metabolism or re-uptake. Further investigation of the enzymatic activity of MAO and COMT in VKI striatal tissue may provide more insight. Additionally, total levels of dopamine and metabolites in VKI striata were comparable across genotypes, suggesting, together with normal TH levels, that production and availability of dopamine was not affected, rather release is increased.

Interestingly, total protein levels of SERT were also increased in striata from VKI mice, with NET levels trending towards increased, possibly to compensate for dopaminergic dysfunction. Indeed, serotoninergic neurons can uptake dopamine through SERT, often linked to motor complication during PD treatment (Nishijima & Tomiyama, 2016).

In older animals dopamine release appeared decreased in comparison to WT animals, although this data was not significant. At this age, TH+ neuron loss was still not apparent. Nevertheless, while VMAT2 was still greater in old VKI mice, the increase was diminished. Additionally, no changes are found in total levels of dopamine and its metabolites in old animals, while decay time in *ex-vivo* recording was slightly faster.

In support of our results here, an independent line of *Vps35* p.D620N knock mice was reported to also have normal basal levels of dopamine and metabolites, by *in vivo* microdialysis (Ishizu et al., 2016). However, depolarization-induced dopamine release, with 120mM potassium chloride, was significantly decreased in homozygous animals compared to WT. In comparison to Ishizu's work, experimental animals were older, at 20-28 weeks, while the sample size was modest and included both sexes, FSCV was not performed, nor was evaluation of VMAT2 or DAT, thus further comparative assessment in both line is warranted.

Despite the different experimental design, the data of Ishizu and colleagues and ours suggest that retromer may be responsible for recycling of dopaminergic vesicles or proteins important for vesicles formation, docking, and/or release. Together, the quantitative analysis of striatal proteins related to dopamine storage and re-uptake, with *ex-vivo* and *in-vivo* physiological investigations of basal and evoked dopamine release, demonstrates that *Vps35* p.D620N mutation functionally impairs dopaminergic neurotransmission.

Pre-synaptic dopamine synthesis, storage, and exo-/endo-cytosis are regulated by the combinatory action of TH-mediated production, VMAT2 packaging and DAT reuptake (Meiser et al., 2013). Dopamine homeostasis is also balanced by dopamine D2/D3 autoreceptors, trace amine receptor signaling, molecular chaperones and metabolism (Meiser et al., 2013). The process by which VMAT2 and DAT are actively recycled, and how they influence each other's localization, remains unknown. Recent studies suggested DAT is recycled via VPS35-positive endosomes (Wu et al., 2017). VPS35 D620N may directly affect retromer selection of DAT as a cargo, although such DAT recycling mechanism may only be important in the small subset of actively releasing dopaminergic terminals (Pereira et al., 2016). Nevertheless, chronic DAT reduction will disrupt the balance of extra- to intracellular dopamine with consequent effects on signaling and homeostasis (Lohr, Masoud, Salahpour, & Miller, 2017). In contrast, overexpression of DAT more readily causes midbrain cell loss, possibly through accumulation of dopamine inside the neuron (Lohr et al., 2017). Whereas VMAT2 deficiency is lethal, mice expressing low levels of VMAT2 show deficits in vesicular packaging leading to depletion of dopamine levels, with consequent behavioural alterations and α-synuclein aggregation (Lohr et al., 2017). Curiously, results in VKI (and LRRK2) mice are reminiscent of BAC-transgenic VMAT2-overexpressing mice that have increased vesicular capacity to store dopamine and increased evoked release (Lohr et al., 2014; Volta et al., 2017), and which are insensitive to methamphetamine-induced dopaminergic neurodegeneration relative to WT (Lohr et al., 2015). However, a fundamental and intriguing difference in VKI mice, despite increased propensity to dopamine release and more VMAT2 protein, is that there is no more intracellular dopamine stored compared to WT littermates. An ultrastructural study of synaptic vesicle and endosomal compartments may be informative in this regard. Ongoing work is investigating the number, size,

and distribution of synaptic vesicles in brains from young and old VKI animals. These data will surely help us understand the mechanism of dopamine regulation, and the dysfunction we see in the VPS35 knock-in mouse dopamine system. While extracellular dopamine is normalized via compensatory systems, the effect on D2R is still notable and could lead to subtle behavioural alterations. Of note, DAT knock-out mice show a complete loss of D2R auto-inhibition (Gainetdinov, Jones, & Caron, 1999).

Presynaptic dopaminergic phenotypes observed in VKI mice may require molecular and/or network compensation to mask dysfunction, which may fail with age. Similar neurotransmission phenotypes have been reported in other models of mutations linked to late-onset parkinsonism (Chesselet et al., 2012; Yue et al., 2015). Many of these proteins affect the endosome recycling system and functionally converge about receptor recycling and neurotransmission (Volta, Milnerwood, & Farrer, 2015). For example, in human LRRK2 p.G2019S carriers, initial elevations in serotonin and dopamine function decline with age as symptoms manifest (Sossi et al., 2010; Wile et al., 2016), similar to results garnered in G2019S knock-in mice (Volta et al., 2017). Notably, VPS35-deficiency is lethal, but in surviving cells impairs AMPA receptor trafficking, impedes dendritic spine maturation, and decreases glutamatergic transmission (Tian et al., 2015). In contrast, AMPA receptor cluster intensity appears increased in human inducible pluripotent stem cell-derived dopaminergic neurons from *Vps35* p.D620N heterozygotes (Munsie et al., 2015). Such network effects, involving excitatory and inhibitory neurotransmission, may place excessive demand on synaptic proteostasis, ATP metabolism, mitochondria and autophagy. With time, chronic dysfunction challenges compensatory systems, and may lead to the insidious loss of dopaminergic neurons.

In PD the selective vulnerability of dopaminergic neurons in the SNpc is multifaceted (Surmeier, 2007), but includes differential expression of VMAT2 and DAT in SNpc compared to VTA (Uhl, 1998). This body of work suggests that, in our mouse, mutant VPS35 is altering trafficking of DAT to the surface, therefore reducing dopamine reuptake and leading to increased VMAT2 at terminals. The outcome is increased evoked dopamine release, possibly compensated via dopamine metabolism (COMT and MAO) or diffusion (proposed model in Figure 4.1). With ageing, while higher VMAT2 protein levels may lead to increased dopamine packaging, dopamine release appear smaller, possibly indicating terminals may be lost at this age, with surviving neurons compensating via faster re-uptake of dopamine, and greater TH levels.

Analysis of striatal tissue also suggests there is no difference in dopamine concentration between genotypes; hence VKI mice are likely to provide fundamental insights into dopaminergic regulation.

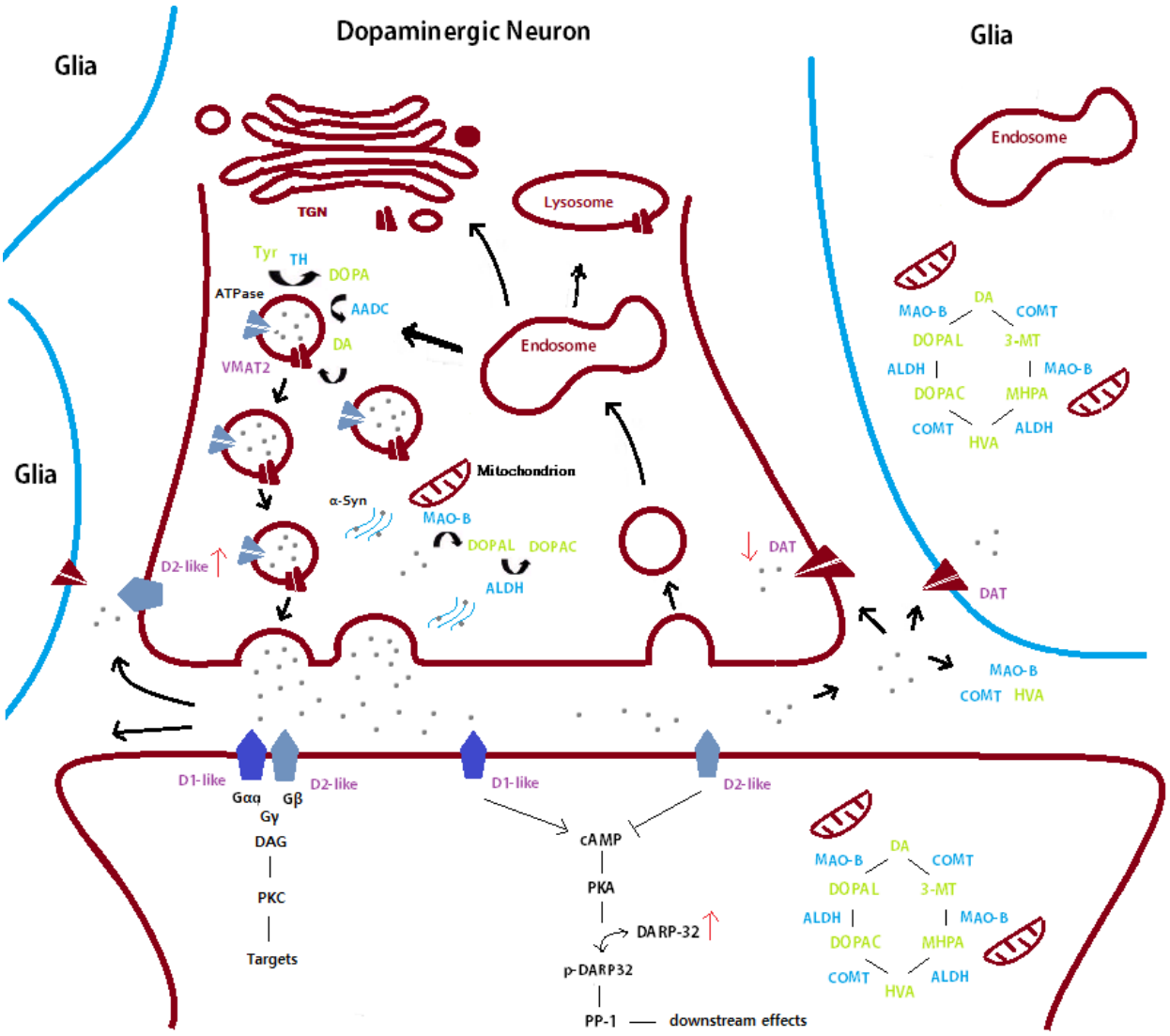

Figure 4.1 Proposed model of dopaminergic dysfunction in VKI mice

Dopaminergic neuron in the presence of a p.D620N mutation in VPS35. Vesicles and proteins machinery necessary for vesicles formation are taken from the membrane, then recycled and quickly placed in the releasable pool, rather than degraded via lysosomes. An increase in the number and/or kinetics of readily-recycling vesicle leads to increased release of dopamine, causing increased D1R & D2R signaling, and compensatory mechanisms such as decreased DAT expression on the surface. DAT decrease may be directly dependent on dysfunctional retromer trafficking and the increased temporal retention in endosomes, leading to more DAT being degraded. Extracellular dopamine is quickly metabolized, possibly via increased MAO & COMT function. Glia may play a role in extracellular dopamine clearance. Of note, altered dopamine transmission may be balanced by excitatory glutamate signaling as VPS35 p.D620N also impairs AMPA recycling (Munsie et al., 2015). Overall the system is functional and compensates quite well for altered release. Higher dopamine function can lead to additional oxidative stress in the cytosol and consequent metabolic demand for lipids and proteins turnover, and possibly α-synuclein (and tau) oligomerization.

4.2 Behavioural evaluation

At 3 months of age VKI animals are grossly normal in regards to survival and weight, and exhibit no signs of motor dysfunction. With ageing, WT mice show a substantial increase in body weight. This is not seen in VKI mice, despite an overall healthy look. In this study we did not investigate the changes in whole body composition, but cursory post-mortem evaluation suggested that organs are lighter in VKI mice, and that fat accumulation may be decreased. This difference could be dependent on increased metabolism in the presence of the mutation, whether via increased use of energy or lower accumulation. Parkinson's patients are similar in this regard, tending towards a lower body mass index with disease progression, and despite their relative immobility (J. C. Sharma & Lewis, 2017).

While it would be of interest to measure gastro-intestinal activity and food consumption, our results in the radial arm maze would suggest that sucrose consumption was not different, although the test was performed after water deprivation, and the amount of sucrose-water consumed may be dependent on the level of de-hydration of each mouse. Parallel testing with a solution of regular water could be informative. VPS35 is highly expressed in several secretory systems, including pancreas and thyroid. A role of the protein in these organs and the hormonal effects on the whole body require investigation, and could explain the altered behaviour under stress we observed.

Mice spend a good portion of their home cage time grooming. When tested in a cylinder test they usually spend the first couple of minutes exploring the cylinder and trying to escape, but eventually reach a certain level of comfort and start grooming. The amount of grooming time and number of grooming events has been used in the past as a measure of anxiety as it can be modulated by anxiolytic drugs, although grooming is a much more complex behaviour

(Smolinsky et al., 2009). Showing greater number of grooming time and events could suggest a lower level of fear or anxiety in VKI mice at 18 months of age, or could be an indication of altered explorative behaviour. Different weight could also be a factor.

Indeed, while gross locomotion is not affected, despite normalizing to body weight, exploration appears altered in VKI mice. Young animals presented preference for more protected environment, and show sign of distress with the experimenter. Eventually with habituation to the experimenter and to the task itself, these subtle alterations disappeared and VKI mice behaved similar to their WT littermates. Indeed, it is important to consider that the elevated plus maze has always been the first test performed in all cohorts, followed by the open field on the same day, the cylinder test on the following day, and finally the rotarod test at the end of the week. One cohort of young mice was not tested on the elevated plus maze, and showed clear fear-related behaviour avoiding the center of the cage during the open field. Similarly, a cohort of 6-months-old mice, which was only tested for the open field, showed preference of a side of the cage further away from the experimenter. Following cohorts of young animals, when tested on the open field after the elevated plus maze did not show this phenotype, although still apparent for the elevated plus maze. This suggests the phenotype is quite subtle, and that exposure to the experiment's room and possibly adjustments to testing itself can reduce this altered behaviour. Further evaluation might measure exploration in separate cohorts for each one of these tests, or change the order of the tests to see if it affects the results.

Interestingly, while young VKI showed increased fear-related behaviour in the elevated plus maze, this normalized to WT with age. This concurs with dopamine release being increased in young and decreased in older mice, suggesting dopamine may play a role in such behaviour. 18-month-old VKI show no difference in the open field test, always the second test of the series

after the elevated plus maze), but show higher activity during a cylinder test (usually performed after elevated plus maze and open field). At this stage is hard to attribute this difference in behaviour to lower fear or anxiety. Instead greater activity in the cylinder test could be dependent on different body mass at old age. Nevertheless, a lower ability to value the danger of the situation is not to be excluded, given the dopaminergic alterations present at both ages.

Possibly the alteration in the dopaminergic system can slow the process of adaptation to a new situation or new rules in a behavioural task. Indeed, in a radial arm maze with sucrose-water, VKI mice show a more perseverative behaviour, but eventually are capable of performing the task. This phenotype worsens with age.

Considering the aforementioned dopaminergic alterations, as the motor performance of VKI animals is not impaired, and synaptic connectivity and dopamine neuron counts are comparable to WT, compensation must be considered. Cognitive alterations are present, albeit only seen under specific challenges, and are somewhat similar to those seen in humans, often prior to motor dysfunction. People affected by PD do not show memory alteration, at least not initially. Rather, they exhibit a lack of cognitive flexibility and adaptation to a new task, or new rules while performing action (Boller & Grafman, 2000; Kehagia, Barker, & Robbins, 2010). Dopamine in the basal ganglia is very important to modulate these behaviours, modulating the value of an action. When dopamine is reduced (or possibly increased in early stages) the firing pattern may be altered. Indeed, in PD and other dopaminergic related syndromes often reward and punishment are not recognized properly, leading to addictive behaviour, gambling and in general poor decision making.

The role of dopamine in cognitive ability and fear/risk related behaviour is controversial. Some data suggest increased dopamine signaling is responsible for risk-taking behaviours,

including those seen in PD patients treated with dopaminergic drugs (Clark & Dagher, 2014). A study on DAT knock-down mice shows increased hyperactivity and mania-like behaviour reversible with D1R antagonists (Milienne-Petiot, Groenink, Minassian, & Young, 2017). In contrast, low concentrations of dopamine are necessary to avoid negative outcomes. Frank and his group proposed a model in which phasic dopamine bursts following rewards promote positive reinforcement while reductions in tonic dopamine levels lead to negative reinforcement, each controlled by the D1R/direct pathway and the D2R/indirect pathway, respectively (Cohen & Frank, 2009). This computational model suggests that the dopamine signal promotes learning from positive outcomes via stimulation of D1R, whereas learning to avoid negative outcomes is mediated via disinhibition of indirect pathway striatal neurons secondary to a reduction of D2R stimulation during dopamine pauses (Cohen & Frank, 2009).

Future work will establish whether the behaviour described here is dependent on dopaminergic dysfunction, or whether other systems are in play. Regardless, the VKI mouse (in comparison to littermates) provides useful system in which to understand the dopamine system, under normal and pathophysiological states. Further study of VKI mice may elucidate the ontology and pathology of *Vps35* p.D620N parkinsonism and may even provide much needed insight into imaging biomarkers and disease-modifying interventions for genetically-defined and idiopathic PD.

Chapter 5: Conclusion

5.1 Summary and conclusion: Implications for the field

The loss of dopaminergic markers, prior to neuronal degeneration, suggests that altered synaptic function may precede the onset of clinical symptoms in patients. Current therapies offer alleviation of motor symptoms, but none prevent onset or halt disease progression and non-motor symptoms remain problematic. Thus, new therapeutic strategies are necessary.

To address the effects of the p.D620N mutation on VPS35 and help us understand mechanism of disease, we developed a VPS35 p.D620N knock-in mouse model to preserve the endogenous regulation and stoichiometry of the retromer complex. We hypothesized that VPS35 p.D620N affects a subset of retromer functions, namely synaptic-endosomal function and neurotransmission, through impaired recycling of monoamine transporters, a novel class of retromer cargo.

In this thesis, I characterize VKI animals on different aspects, from motor behaviour, to cognition, to the nigrostriatal system and dopamine release, including a pathological evaluation of older VKI mice. Characterization of VKI mice at 3 months of age revealed an increase in nigrostriatal dopamine release and impaired recycling of dopaminergic synaptic machinery, albeit in the absence of nigral neuronal loss or motor dysfunction. With ageing VKI mice show lower fat accumulation and possible metabolic dysfunction. Older VKI present lower dopamine release, despite a consistent increase in VMAT2 levels, indicating the system is beginning to fail at this age. Nevertheless, alterations in DAT may still be present and could affect VMAT2 levels. Despite initial reduction in dopamine release, extracellular levels of dopamine and its metabolites are normal at this age, and no neuronal loss is present. Interestingly, old VKI animals begin to show pathological markers of parkinsonism, such as tau alterations. Our findings

suggest that physiologic expression of VPS35 D620N causes dysfunction of synaptic dynamics, reminiscent of early stage PD, with later alteration that replicate the ageing process seen in humans.

In PD, motor symptoms are preceded by a lengthy prodromal / pre-motor phase which can occur years if not decades prior to clinical diagnosis and loss of nigral neurons (Goldman & Postuma, 2014). Successful modeling of PD should take into consideration the subtle and prolonged nature of disease progression, as neuroprotective treatments targeted prior to neuronal loss could prove most beneficial.

Further characterization of VKI animals, including additional TH-immunoreactivity and nigral neuronal stereology, will be important to revisit at later time-points. Pharmacological investigations of dopamine release/reuptake may be especially insightful in the biology of addiction and reward, whereas electron microscopy studies may reveal ultrastructural or synaptic vesicles alterations apparent in VKI mice.

5.2 Limitations and future directions

Despite sharing many similarities with humans, mice are not quite the same and can respond differently to disease stresses. For instance, there is a notion that PD is a disease of 'accelerating ageing' and that most people would develop PD if given sufficiently long lives. The mouse lifespan is very short, two years on average in a laboratory. Neurons may need a longer period to degenerate to the same extent they do in humans.

Moreover, genetic effects can sometimes be different between humans and mice. One important mutation linked with PD is the p.A53T substitution of α-synuclein, which is the physiological form in the mouse. This main difference may help protect the mouse from

synuclein pathology, at least in the same form it appears in humans. Instead tau appears to be commonly present in several of the previously studied genetic mouse models, and the model described in this work. Tau often presents an alternative or parallel pathological marker in PD patients, suggesting in some parts we can replicate the human disease in the mouse, and possibly understand what leads to pathology. More importantly, understanding the differences between species and models can be also informative to mechanisms of disease. Future work should focus on understanding the connection between PD-linked proteins and tau, taking into account the interaction with dopamine. Given that tau is important in other neurodegenerative diseases, the role of other neurotransmitters and additional cognitive evaluation should also be taken into consideration.

Monogenic forms of PD, whether alpha-synuclein as a vesicular chaparone of presynaptic SNAREs/exocytosis, LRRK2 in Rab activation, or GBA in ceremide metabolism, all suggest perturbations in synaptic-endosomal trafficking, in lipid and membrane-associated protein turnover, are the primary event in the etiology and pathogenesis of PD. Such deficits place major demands on chaparones, ATP and mitiochondrial function, proteostasis and endosomal-autophagy, and gene dysfunction highlighted in more atypical forms parkinonism. Whether the DNAJ 'C' family, DNAJC5, DNAJC6, DNAJC12, DNAJC13, DNAJC26 of chaparones, or PINKI and Parkin in mitochondrial maintenance/ATP production, DCTN1 or MAPT in trafficking, or RAB39B, SMPD1, and most recently SLC17A5, ASAH1, and CTSD in lysosome function (Robak et al., 2017). VPS35 adds to this literature but more closely resembles the phenotype of late-onset, idiopathic Parkinson's disease. Clearly, further inquiry in synaptic-endosomal dysfunction, and in dopaminergic neurons, should be a primary concern.

Because PD is age-dependent, we sought to examine our mice to 18 months, considered an advanced age for mice. Unfortunately ageing mice to over 18 months can be challenging, particularly because of natural death of the mice prior to experimentation, but more so due to cost (asides, many mice live to >26 months). This limitation reduced the power for certain experiments and made it problematic to replicate all assays used in young animals. It is important to further investigate how early changes develop in old age, and what, if any, compensation occurs or eventually fails. Alternatively, we should seek to discover whether additional mechanisms of diseases appear in later stages. For instance, the influence of the immune system upon disease processes is well established, and we should determine whether mutant VPS35 affects immune function, and whether alterations, if present, appear early or are a consequence of parallel dysfunction in other systems. Similarly, mitochondria are likely to be affected by an over-working dopaminergic system, yet may be a primary cause of dysfunction. Electron-microscopy images from young VKI mice are now under analysis for mitochondrial (as well as endosomal) structures. Studying these systems at different age points can be helpful in understanding the progression of disease, and at which stages interventions are necessary.

Despite many similarities and homologous organisation, the human brain is more complex than the mouse brain, and the same structures likely function differently. For instance, the number of dopaminergic neurons appears to be different in the human SNpc *vs* the VTA, while in rodents this difference is not apparent. Instead the number of dopaminergic neurons in the mouse SN are equivalent to the number in the VTA (Vogt Weisenhorn et al., 2016). This could partially account for the differential behaviour in mouse models, often showing cognitive alterations more than motor. Nevertheless, mice are useful in understanding how modulation of dopamine affects cognitive abilities in certain conditions. Indeed, the decision making system is

very similar among mammals. Simple tasks can show a deficit that can then be easily modified by therapeutics or drugs that modulate the system of interest. It would be interesting to modulate dopamine in young and old VKI mice, and see if the phenotype can be reversed, or exaggerated. For example, use of dopaminergic drugs, e.g. as reserpine, to modulate VMAT2-dependent packaging of vesicle, could help understand whether the increase in dopamine release is due to more dopamine being packaged in vesicles. Additionally, pharmacological treatment can help understanding whether increased dopamine release is the cause of the perseveration phenotype shown in the radial arm maze. Similarly, altered dopamine function could be the main cause of the altered explorative behaviour, keeping VKI mice in a constant state of fear, possibly by reducing 'evaluation' of the situation. GBR 12909, a DAT blocker, and similar drugs, could also be informative in understanding the effect of reduced DAT expression in VKI mice, and consequently altered dopamine re-uptake.

The importance of physiological levels of dopamine for proper cognitive function has been extensively studied. Whether the behavioural phenotype seen in our mice in the presence of increased dopamine are linked with the actual amount of extracellular dopamine at any given point, or the post-synaptic response to dopamine signal, is yet to be understood. Future studies would evaluate the dopamine receptors signaling and expression of the receptors themselves on the cell surface, and whether such altered responses are related to the described behaviour.

Dopamine may not be the only neurotransmitter affected by mutations on VPS35. Serotonin dysfunction could explain the fear-related behaviour and together with norepinephrine may explain the alterations in total body weight. Indeed, SERT and NET levels appear increased, possibly affecting consequent release of serotonin and norepinephrine. Stress hormones could also be key to understand both the behaviour and overall alterations in VKI mice.

Differences in mouse vs human should also take in account the controlled and protected experimental environment, which may affect the mouse behaviour. Despite this valuable consideration, is very important to consider standardized test to allow replicability of the experiments across facilities. In the presence of changes from published protocols there should be a valid justification for the modification. Particularly some behavioural paradigms could be improved to provide additional information. In our case order of test performance could be affecting the mouse behaviour. The open field could be performed prior to the elevated plus maze to investigate whether the phenotype is associated to first exposure to behavioural testing, or rather dependent on the test. Similarly the cylinder test should be performed on an isolated group of animals, particularly at young age, given that the phenotype could be lost because of habituation to testing. Additionally, further testing in the radial arm maze should explore whether odour or spatial memory are playing a role in the mouse behaviour. The same test should be performed without the spatial cues, and parallel tests could use a sweetened solution without odour, as well as a control with the use of regular water to pars out the effect of de-hydration, rather than seeking of sucrose.

An important non-motor alterations present in the model described is lower weight in older age. An extensive analysis of gastro-intestinal function and hormone activity would be worthwhile, including the possible role of dopamine in food intake.

Despite some limitations, this model represents an important tool to understand the mechanism(s) that may lead to dopaminergic dysfunction, whether in PD or other related syndromes. Along the way, we may possibly understand more of how dopamine regulates mouse behaviour, in health and disease state, and how this may relate to humans.

Bibliography

Aasly, J. O., Toft, M., Fernandez-Mata, I., Kachergus, J., Hulihan, M., White, L. R., & Farrer, M. (2005). Clinical features ofLRRK2-associated Parkinson's disease in central Norway. *Annals of Neurology*, *57*(5), 762–765. http://doi.org/10.1002/ana.20456

Alim, M. A., Ma, Q.-L., Takeda, K., Aizawa, T., Matsubara, M., Nakamura, M., … Uéda, K. (2004). Demonstration of a role for alpha-synuclein as a functional microtubule-associated protein. *Journal of Alzheimer's Disease : JAD*, *6*(4), 435-42–9. Retrieved from http://www.ncbi.nlm.nih.gov/pubmed/15345814

Anitei, M., Wassmer, T., Stange, C., & Hoflack, B. (2010). Bidirectional transport between the trans-Golgi network and the endosomal system. *Molecular Membrane Biology*, *27*(8), 443–56. http://doi.org/10.3109/09687688.2010.522601

Appel-Cresswell, S., Vilarino-Guell, C., Encarnacion, M., Sherman, H., Yu, I., Shah, B., … Farrer, M. J. (2013). Alpha-synuclein p.H50Q, a novel pathogenic mutation for Parkinson's disease. *Movement Disorders*, *28*(6), 811–813. http://doi.org/10.1002/mds.25421

Aristieta, A., Azkona, G., Sagarduy, A., Miguelez, C., Ruiz-Ortega, J. Á., Sanchez-Pernaute, R., & Ugedo, L. (2012). The Role of the Subthalamic Nucleus in L-DOPA Induced Dyskinesia in 6-Hydroxydopamine Lesioned Rats. *PLoS ONE*, *7*(8), e42652. http://doi.org/10.1371/journal.pone.0042652

Arkadir, D., Bergman, H., & Fahn, S. (2014). Redundant dopaminergic activity may enable compensatory axonal sprouting in Parkinson disease. *Neurology*, *82*(12), 1093–8. http://doi.org/10.1212/WNL.0000000000000243

Arranz, A. M., Delbroek, L., Van Kolen, K., Guimarães, M. R., Mandemakers, W., Daneels, G., … Moechars, D. (2015). LRRK2 functions in synaptic vesicle endocytosis through a

kinase-dependent mechanism. *Journal of Cell Science*, *128*(3), 541–52. http://doi.org/10.1242/jcs.158196

Attar, N., & Cullen, P. J. (2010). The retromer complex. *Advances in Enzyme Regulation*, *50*(1), 216–236. http://doi.org/10.1016/j.advenzreg.2009.10.002

Beal, F. (2010). Parkinson's disease: a model dilemma. *Nature*, (Outlooks), S8-10. http://doi.org/10.1038/466S8a

Beccano-Kelly, D. A., Kuhlmann, N., Tatarnikov, I., Volta, M., Munsie, L. N., Chou, P., … Milnerwood, A. J. (2014). Synaptic function is modulated by LRRK2 and glutamate release is increased in cortical neurons of G2019S LRRK2 knock-in mice. *Frontiers in Cellular Neuroscience*, *8*(September), 301. http://doi.org/10.3389/fncel.2014.00301

Beccano-Kelly, D. A., Volta, M., Munsie, L. N., Paschall, S. A., Tatarnikov, I., Co, K., … Milnerwood, A. J. (2015). LRRK2 overexpression alters glutamatergic presynaptic plasticity , striatal dopamine tone , postsynaptic signal transduction , motor activity and memory. *Human Molecular Genetics*, *24*(5), 1336–1349. http://doi.org/10.1093/hmg/ddu543

Beccano-Kelly, D. a, Volta, M., Munsie, L. N., Paschall, S. a, Tatarnikov, I., Co, K., … Milnerwood, A. J. (2014). LRRK2 overexpression alters glutamatergic presynaptic plasticity, striatal dopamine tone, postsynaptic signal transduction, motor activity and memory. *Human Molecular Genetics*, (October), 1–14. http://doi.org/10.1093/hmg/ddu543

Betarbet, R., Sherer, T. B., MacKenzie, G., Garcia-Osuna, M., Panov, A. V., & Greenamyre, J. T. (2000). Chronic systemic pesticide exposure reproduces features of Parkinson's disease. *Nature Neuroscience*, *3*(12), 1301–1306. http://doi.org/10.1038/81834

Bezard, E., Tronci, E., Pioli, E. Y., Li, Q., Porras, G., Björklund, A., & Carta, M. (2013). Study

of the antidyskinetic effect of eltoprazine in animal models of levodopa-induced dyskinesia. *Movement Disorders*, *28*(8), 1088–1096. http://doi.org/10.1002/mds.25366

Blesa, J., Phani, S., Jackson-Lewis, V., & Przedborski, S. (2012). Classic and new animal models of Parkinson's disease. *Journal of Biomedicine and Biotechnology*, *2012*. http://doi.org/10.1155/2012/845618

Bolam, J. P., & Pissadaki, E. K. (2012). Living on the edge with too many mouths to feed: why dopamine neurons die. *Movement Disorders : Official Journal of the Movement Disorder Society*, *27*(12), 1478–83. http://doi.org/10.1002/mds.25135

Boller, F., & Grafman, J. (2000). *Handbook of neuropsychology*. Elsevier.

Bonifacino, J. S., & Hurley, J. H. (2008). Retromer. *Current Opinion in Cell Biology*, *20*(4), 427–436. http://doi.org/10.1016/j.ceb.2008.03.009

Bonifati, V., Breedveld, G. J., Squitieri, F., Vanacore, N., Brustenghi, P., Harhangi, B. S., … Heutink, P. (2002). Localization of autosomal recessive early-onset parkinsonism to chromosome 1p36 (PARK7) in an independent dataset. *Annals of Neurology*, *51*(2), 253–6. Retrieved from http://www.ncbi.nlm.nih.gov/pubmed/11835383

Bonifati, V., Rohe, C. F., Breedveld, G. J., Fabrizio, E., De Mari, M., Tassorelli, C., … Italian Parkinson Genetics Network. (2005). Early-onset parkinsonism associated with PINK1 mutations: Frequency, genotypes, and phenotypes. *Neurology*, *65*(1), 87–95. http://doi.org/10.1212/01.wnl.0000167546.39375.82

Bové, J., Prou, D., Perier, C., & Przedborski, S. (2005). Toxin-induced models of Parkinson's disease. *NeuroRx : The Journal of the American Society for Experimental NeuroTherapeutics*, *2*(3), 484–494. http://doi.org/10.1602/neurorx.2.3.484

Braak, H., Sandmann-Keil, D., Gai, W., & Braak, E. (1999). Extensive axonal Lewy neurites in

Parkinson's disease: a novel pathological feature revealed by alpha-synuclein immunocytochemistry. *Neuroscience Letters*, *265*(1), 67–9. Retrieved from http://www.ncbi.nlm.nih.gov/pubmed/10327208

Braak, H., Tredici, K. Del, Rüb, U., de Vos, R. A. ., Jansen Steur, E. N. ., & Braak, E. (2003). Staging of brain pathology related to sporadic Parkinson's disease. *Neurobiology of Aging*, *24*(2), 197–211. http://doi.org/10.1016/S0197-4580(02)00065-9

Brice, A. (2005). Genetics of Parkinson's disease: LRRK2 on the rise. *Brain*, *128*(12), 2760–2762. http://doi.org/10.1093/brain/awh676

Brichta, L., & Greengard, P. (2014). Molecular determinants of selective dopaminergic vulnerability in Parkinson's disease: an update. *Frontiers in Neuroanatomy*, *8*, 152. http://doi.org/10.3389/fnana.2014.00152

Brück, A., Aalto, S., Nurmi, E., Bergman, J., & Rinne, J. O. (2005). Cortical 6-[18F]fluoro-l-dopa uptake and frontal cognitive functions in early Parkinson's disease. *Neurobiology of Aging*, *26*(6), 891–898. http://doi.org/10.1016/j.neurobiolaging.2004.07.014

Calabresi, P., Picconi, B., Tozzi, A., Ghiglieri, V., & Di Filippo, M. (2014). Direct and indirect pathways of basal ganglia: a critical reappraisal. *Nature Neuroscience*, *17*(8), 1022–1030. http://doi.org/10.1038/nn.3743

Cenci, M. A., & Lundblad, M. (2007). Ratings of L -DOPA-Induced Dyskinesia in the Unilateral 6-OHDA Lesion Model of Parkinson's Disease in Rats and Mice. In *Current Protocols in Neuroscience* (Vol. Chapter 9, p. Unit 9.25). Hoboken, NJ, USA: John Wiley & Sons, Inc. http://doi.org/10.1002/0471142301.ns0925s41

Chartier-Harlin, M.-C., Kachergus, J., Roumier, C., Mouroux, V., Douay, X., Lincoln, S., … Destée, A. (2004). α-synuclein locus duplication as a cause of familial Parkinson's disease.

The Lancet, *364*(9440), 1167–1169. http://doi.org/10.1016/S0140-6736(04)17103-1

Chen, H., Zhang, S. M., Hernán, M. A., Willett, W. C., & Ascherio, A. (2003). Weight loss in Parkinson's disease. *Annals of Neurology*, *53*(5), 676–679. http://doi.org/10.1002/ana.10577

Cheng, H. C., Ulane, C. ., & Burke, R. . (2010). Clinical progression in Parkinson's disease and the neurobiology of Axons. *Annals of Neurology*, *67*(6), 715–725. http://doi.org/10.1002/ana.21995.Clinical

Chesselet, M. F., Richter, F., Zhu, C., Magen, I., Watson, M. B., & Subramaniam, S. R. (2012). A Progressive Mouse Model of Parkinson's Disease: The Thy1-aSyn ("Line 61") Mice. *Neurotherapeutics*, *9*(2), 297–314. http://doi.org/10.1007/s13311-012-0104-2

Choy, R. W.-Y., Park, M., Temkin, P., Herring, B. E., Marley, A., Nicoll, R. A., & von Zastrow, M. (2014). Retromer Mediates a Discrete Route of Local Membrane Delivery to Dendrites. *Neuron*, *82*(1), 55–62. http://doi.org/10.1016/j.neuron.2014.02.018

Chung, C. Y., Seo, H., Sonntag, K. C., Brooks, A., Lin, L., & Isacson, O. (2005). Cell type-specific gene expression of midbrain dopaminergic neurons reveals molecules involved in their vulnerability and protection. *Human Molecular Genetics*, *14*(13), 1709–25. http://doi.org/10.1093/hmg/ddi178

Clark, C. A., & Dagher, A. (2014). The role of dopamine in risk taking: a specific look at Parkinson's disease and gambling. *Frontiers in Behavioral Neuroscience*, *8*, 196. http://doi.org/10.3389/fnbeh.2014.00196

Coelho, M., & Ferreira, J. J. (2012). Late-stage Parkinson disease. *Nature Reviews Neurology*, *8*(8), 435. http://doi.org/10.1038/nrneurol.2012.126

Cohen, M. X., & Frank, M. J. (2009). Neurocomputational models of basal ganglia function in learning, memory and choice. *Behavioural Brain Research*, *199*(1), 141–56.

http://doi.org/10.1016/j.bbr.2008.09.029

Compta, Y., Parkkinen, L., Kempster, P., Selikhova, M., Lashley, T., Holton, J. L., … Revesz, T. (2014). The significance of α-synuclein, amyloid-β and tau pathologies in Parkinson's disease progression and related dementia. *Neuro-Degenerative Diseases*, *13*(2–3), 154–6. http://doi.org/10.1159/000354670

Cotzias, G. C., Papavasiliou, P. S., & Gellene, R. (1969). Modification of Parkinsonism — Chronic Treatment with L-Dopa. *New England Journal of Medicine*, *280*(7), 337–345. http://doi.org/10.1056/NEJM196902132800701

de Lau, L. M., & Breteler, M. M. (2006). Epidemiology of Parkinson's disease. *The Lancet Neurology*, *5*(6), 525–535. http://doi.org/10.1016/S1474-4422(06)70471-9

Deng, H., Gao, K., & Jankovic, J. (2013). The *VPS35* gene and Parkinson's disease. *Movement Disorders*, *28*(5), 569–575. http://doi.org/10.1002/mds.25430

Deutschländer, A., Ross, O. A., & Wszolek, Z. K. (2017). *VPS35-Related Parkinson Disease*. *GeneReviews(®)*. University of Washington, Seattle. Retrieved from http://www.ncbi.nlm.nih.gov/pubmed/28796472

Dhungel, N., Eleuteri, S., Li, L.-B., Kramer, N. J., Chartron, J. W., Spencer, B., … Gitler, A. D. (2015). Parkinson's disease genes VPS35 and EIF4G1 interact genetically and converge on α-synuclein. *Neuron*, *85*(1), 76–87. http://doi.org/10.1016/j.neuron.2014.11.027

Dickson, D. W. (2012). Parkinson's disease and parkinsonism: neuropathology. *Cold Spring Harbor Perspectives in Medicine*, *2*(8). http://doi.org/10.1101/cshperspect.a009258

Didier, E. S., MacLean, A. G., Mohan, M., Didier, P. J., Lackner, A. A., & Kuroda, M. J. (2016). Contributions of Nonhuman Primates to Research on Aging. *Veterinary Pathology*, *53*(2), 277–90. http://doi.org/10.1177/0300985815622974

Djarmati, A., Hedrich, K., Svetel, M., Schäfer, N., Juric, V., Vukosavic, S., … Kostic, V. (2004). Detection of *Parkin* (*PARK2*) and *DJ1* (*PARK7*) mutations in early-onset Parkinson disease: *Parkin* mutation frequency depends on ethnic origin of patients. *Human Mutation*, *23*(5), 525–525. http://doi.org/10.1002/humu.9240

Duka, T., Duka, V., Joyce, J. N., & Sidhu, A. (2009). -Synuclein contributes to GSK-3 -catalyzed Tau phosphorylation in Parkinson's disease models. *The FASEB Journal*, *23*(9), 2820–2830. http://doi.org/10.1096/fj.08-120410

Ehringer, H., & Hornykiewicz, O. (1960). Verteilung Von Noradrenalin Und Dopamin (3-Hydroxytyramin) Im Gehirn Des Menschen Und Ihr Verhalten Bei Erkrankungen Des Extrapyramidalen Systems. *Klinische Wochenschrift*, *38*(24), 1236–1239. http://doi.org/10.1007/BF01485901

Enochs, W. S., Sarna, T., Zecca, L., Riley, P. A., & Swartz, H. M. (1994). The roles of neuromelanin, binding of metal ions, and oxidative cytotoxicity in the pathogenesis of Parkinson's disease: a hypothesis. *Journal of Neural Transmission. Parkinson's Disease and Dementia Section*, *7*(2), 83–100. Retrieved from http://www.ncbi.nlm.nih.gov/pubmed/7710667

Farrer, M., Chan, P., Chen, R., Tan, L., Lincoln, S., Hernandez, D., … Langston, J. W. (2001). Lewy bodies and parkinsonism in families withparkin mutations. *Annals of Neurology*, *50*(3), 293–300. http://doi.org/10.1002/ana.1132

Farrer, M., Gwinn-Hardy, K., Hutton, M., & Hardy, J. (1999). The genetics of disorders with synuclein pathology and parkinsonism. *Human Molecular Genetics*, *8*(10), 1901–1905. http://doi.org/10.1093/hmg/8.10.1901

Farrer, M. J., Milnerwood, A. J., Follett, J., & Guella, I. (2017). TMEM230 is not a gene for

Parkinson disease. *bioRxiv*, 97030. http://doi.org/10.1101/097030

Farrer, M., Kachergus, J., Forno, L., Lincoln, S., Wang, D. S., Hulihan, M., … Langston, J. W. (2004). Comparison of Kindreds with Parkinsonism and α-Synuclein Genomic Multiplications. *Annals of Neurology*, *55*(2), 174–179. http://doi.org/10.1002/ana.10846

Feany, M. B., & Bender, W. W. (2000). A Drosophila model of Parkinson's disease. *Nature*, *404*(6776), 394–398. http://doi.org/10.1038/35006074

Ferreira, M., & Massano, J. (2017). An updated review of Parkinson's disease genetics and clinicopathological correlations. *Acta Neurologica Scandinavica*, *135*(3), 273–284. http://doi.org/10.1111/ane.12616

Follett, J., Norwood, S. J., Hamilton, N. a, Mohan, M., Kovtun, O., Tay, S., … Teasdale, R. D. (2014). The Vps35 D620N mutation linked to Parkinson's disease disrupts the cargo sorting function of retromer. *Traffic (Copenhagen, Denmark)*, *15*(2), 230–44. http://doi.org/10.1111/tra.12136

Forno, L. S. (1996). Neuropathology of Parkinson's disease. *Journal of Neuropathology and Experimental Neurology*, *55*(3), 259–72. Retrieved from http://www.ncbi.nlm.nih.gov/pubmed/8786384

Franssens, V., Bynens, T., Van den Brande, J., Vandermeeren, K., Verduyckt, M., & Winderickx, J. (2013). The benefits of humanized yeast models to study Parkinson's disease. *Oxidative Medicine and Cellular Longevity*, *2013*, 760629. http://doi.org/10.1155/2013/760629

Freeman, C. L., Hesketh, G., & Seaman, M. N. J. (2014). RME-8 coordinates the WASH complex with the retromer SNX-BAR dimer to control endosomal tubulation. *Journal of Cell Science*, jcs.144659. http://doi.org/10.1242/jcs.144659

Frost, J. J., Rosier, A. J., Reich, S. G., Smith, J. S., Ehlers, M. D., Snyder, S. H., … Dannals, R. F. (1993). Positron emission tomographic imaging of the dopamine transporter with11C-WIN 35,428 reveals marked declines in mild Parkinson's disease. *Annals of Neurology*, *34*(3), 423–431. http://doi.org/10.1002/ana.410340331

Gainetdinov, R. R., Jones, S. R., & Caron, M. G. (1999). Functional hyperdopaminergia in dopamine transporter knock-out mice. *Biological Psychiatry*, *46*(3), 303–311. http://doi.org/10.1016/S0006-3223(99)00122-5

Gallon, M., & Cullen, P. J. (2015). Retromer and sorting nexins in endosomal sorting. *Biochemical Society Transactions*, *43*(1), 33–47. http://doi.org/10.1042/BST20140290

Galvin, J. E., Lee, V. M.-Y., Baba, M., Mann, D. M. A., Dickson, D. W., Yamaguchi, H., … Trojanowski, J. Q. (1997). Monoclonal antibodies to purified cortical lewy bodies recognize the mid-size neurofilament subunit. *Annals of Neurology*, *42*(4), 595–603. http://doi.org/10.1002/ana.410420410

Gasser, T. (2009). Mendelian forms of Parkinson's disease. *Biochimica et Biophysica Acta (BBA) - Molecular Basis of Disease*, *1792*(7), 587–596. http://doi.org/10.1016/J.BBADIS.2008.12.007

Giannandrea, M., Bianchi, V., Mignogna, M. L., Sirri, A., Carrabino, S., D'Elia, E., … D'Adamo, P. (2010). Mutations in the Small GTPase Gene RAB39B Are Responsible for X-linked Mental Retardation Associated with Autism, Epilepsy, and Macrocephaly. *The American Journal of Human Genetics*, *86*(2), 185–195. http://doi.org/10.1016/j.ajhg.2010.01.011

Giasson, B. I., Covy, J. P., Bonini, N. M., Hurtig, H. I., Farrer, M. J., Trojanowski, J. Q., & Van Deerlin, V. M. (2006). Biochemical and pathological characterization of Lrrk2. *Annals of*

Neurology, *59*(2), 315–322. http://doi.org/10.1002/ana.20791

Giasson, B. I., Forman, M. S., Higuchi, M., Golbe, L. I., Graves, C. L., Kotzbauer, P. T., … Lee, V. M.-Y. (2003). Initiation and Synergistic Fibrillization of Tau and Alpha-Synuclein. *Science*, *300*(5619), 636–640. http://doi.org/10.1126/science.1082324

Gilsbach, B. K., & Kortholt, A. (2014). Structural biology of the LRRK2 GTPase and kinase domains: implications for regulation. *Frontiers in Molecular Neuroscience*, *7*, 32. http://doi.org/10.3389/fnmol.2014.00032

Gitler, A. D., Bevis, B. J., Shorter, J., Strathearn, K. E., Hamamichi, S., Su, L. J., … Lindquist, S. (2008). The Parkinson's disease protein alpha-synuclein disrupts cellular Rab homeostasis. *Proceedings of the National Academy of Sciences of the United States of America*, *105*(1), 145–50. http://doi.org/10.1073/pnas.0710685105

Goedert, M., Spillantini, M.-G., Del Tredici, K., & Braak, H. (2013). Goedert 2013_100_years_of_Lewy_pathology.PDF, 1–12.

Goldman, J. G., & Postuma, R. (2014). Premotor and non-motor features of Parkinson's disease. *Current Opinion in Neurology*, *27*(4), 434–441. http://doi.org/10.1016/j.biotechadv.2011.08.021.Secreted

Greene, J. G., Dingledine, R., & Greenamyre, J. T. (2005). Gene expression profiling of rat midbrain dopamine neurons: implications for selective vulnerability in parkinsonism. *Neurobiology of Disease*, *18*(1), 19–31. http://doi.org/10.1016/j.nbd.2004.10.003

Greggio, E., Jain, S., Kingsbury, A., Bandopadhyay, R., Lewis, P., Kaganovich, A., … Cookson, M. R. (2006). Kinase activity is required for the toxic effects of mutant LRRK2/dardarin. *Neurobiology of Disease*, *23*(2), 329–341. http://doi.org/10.1016/j.nbd.2006.04.001

Grundke-Iqbal, I., Iqbal, K., Tung, Y. C., Quinlan, M., Wisniewski, H. M., & Binder, L. I.

(1986). Abnormal phosphorylation of the microtubule-associated protein tau (tau) in Alzheimer cytoskeletal pathology. *Proceedings of the National Academy of Sciences of the United States of America*, *83*(13), 4913–7. Retrieved from http://www.ncbi.nlm.nih.gov/pubmed/3088567

Guttman, M., Seeman, P., Reynolds, G. P., Riederer, P., Jellinger, K., & Tourtellotte, W. W. (1986). Dopamine D2 receptor density remains constant in treated Parkinson's disease. *Annals of Neurology*, *19*(5), 487–492. http://doi.org/10.1002/ana.410190510

Hatano, Y., Li, Y., Sato, K., Asakawa, S., Yamamura, Y., Tomiyama, H., … Hattori, N. (2004). NovelPINK1 mutations in early-onset parkinsonism. *Annals of Neurology*, *56*(3), 424–427. http://doi.org/10.1002/ana.20251

Healy, D. G., Falchi, M., O'Sullivan, S. S., Bonifati, V., Durr, A., Bressman, S., … International LRRK2 Consortium. (2008). Phenotype, genotype, and worldwide genetic penetrance of LRRK2-associated Parkinson's disease: a case-control study. *The Lancet Neurology*, *7*(7), 583–590. http://doi.org/10.1016/S1474-4422(08)70117-0

Healy, D. G., Falchi, M., O'Sullivan, S. S., Bonifati, V., Durr, A., Bressman, S., … Wood, N. W. (2008). Phenotype, genotype, and worldwide genetic penetrance of LRRK2-associated Parkinson's disease: a case-control study. *The Lancet Neurology*, *7*(7), 583–590. http://doi.org/10.1016/S1474-4422(08)70117-0

Herzig, M. C., Kolly, C., Persohn, E., Theil, D., Schweizer, T., Hafner, T., … Shimshek, D. R. (2011). LRRK2 protein levels are determined by kinase function and are crucial for kidney and lung homeostasis in mice. *Human Molecular Genetics*, *20*(21), 4209–4223. http://doi.org/10.1093/hmg/ddr348

Hinkle, K. M., Yue, M., Behrouz, B., Dächsel, J. C., Lincoln, S. J., Bowles, E. E., … Melrose, H.

L. (2012). *LRRK2 knockout mice have an intact dopaminergic system but display alterations in exploratory and motor co-ordination behaviors. Molecular neurodegeneration* (Vol. 7). http://doi.org/10.1186/1750-1326-7-25

Hirth, F. (2010). Drosophila melanogaster in the study of human neurodegeneration. *CNS & Neurological Disorders Drug Targets*, *9*(4), 504–23. http://doi.org/10.2174/187152710791556104

Hornykiewicz, O. (1993). Parkinson's disease and the adaptive capacity of the nigrostriatal dopamine system: possible neurochemical mechanisms. *Advances in Neurology*, *60*, 140–7. Retrieved from http://www.ncbi.nlm.nih.gov/pubmed/8420131

Hornykiewicz, O. (1998). Biochemical aspects of Parkinson's disease. *Neurology*, *51*(Issue 2, Supplement 2), S2–S9. http://doi.org/10.1212/WNL.51.2_Suppl_2.S2

Hornykiewicz, O. (2006). The discovery of dopamine deficiency in the parkinsonian brain. *J Neural Transm*, *70*, 9–15. Retrieved from http://eknygos.lsmuni.lt/springer/340/1.Pathology/12 Item.pdf

Hu, F., Padukkavidana, T., Vægter, C. B., Brady, O. A., Zheng, Y., Mackenzie, I. R., … Strittmatter, S. M. (2010). Sortilin-mediated endocytosis determines levels of the frontotemporal dementia protein, progranulin. *Neuron*, *68*(4), 654–67. http://doi.org/10.1016/j.neuron.2010.09.034

Ibáñez, P., Bonnet, A.-M., Débarges, B., Lohmann, E., Tison, F., Agid, Y., … Pollak, P. (2004). Causal relation between α-synuclein locus duplication as a cause of familial Parkinson's disease. *The Lancet*, *364*(9440), 1169–1171. http://doi.org/10.1016/S0140-6736(04)17104-3

Ikeda, K., Ikeda, S., Yoshimura, T., Kato, H., & Namba, M. (1978). Idiopathic Parkinsonism with Lewy-type inclusions in cerebral cortex. A case report. *Acta Neuropathologica*, *41*(2),

165–8. Retrieved from http://www.ncbi.nlm.nih.gov/pubmed/205083

Iranzo, A., Lomeña, F., Stockner, H., Valldeoriola, F., Vilaseca, I., Salamero, M., … Santamaria, J. (2010). Decreased striatal dopamine transporter uptake and substantia nigra hyperechogenicity as risk markers of synucleinopathy in patients with idiopathic rapid-eye-movement sleep behaviour disorder: a prospective study. *The Lancet Neurology*, *9*(11), 1070–1077. http://doi.org/10.1016/S1474-4422(10)70216-7

Iranzo, A., Valldeoriola, F., Lomeña, F., Molinuevo, J. L., Serradell, M., Salamero, M., … Tolosa, E. (2011). Serial dopamine transporter imaging of nigrostriatal function in patients with idiopathic rapid-eye-movement sleep behaviour disorder: a prospective study. *The Lancet Neurology*, *10*(9), 797–805. http://doi.org/10.1016/S1474-4422(11)70152-1

Ishizu, N., Yui, D., Hebisawa, A., Aizawa, H., Cui, W., Fujita, Y., … Watase, K. (2016). Impaired striatal dopamine release in homozygous Vps35 D620N knock-in mice. *Human Molecular Genetics*, *0*(0), ddw279. http://doi.org/10.1093/hmg/ddw279

Izpisua Belmonte, J. C., Callaway, E. M., Caddick, S. J., Churchland, P., Feng, G., Homanics, G. E., … Zhang, F. (2015). Brains, genes, and primates. *Neuron*, *86*(3), 617–31. http://doi.org/10.1016/j.neuron.2015.03.021

Jankovic, J., & Aguilar, L. G. (2008). Current approaches to the treatment of Parkinson's disease. *Neuropsychiatric Disease and Treatment*, *4*(4), 743–57. Retrieved from http://www.pubmedcentral.nih.gov/articlerender.fcgi?artid=2536542&tool=pmcentrez&rendertype=abstract

Kehagia, A. A., Barker, R. A., & Robbins, T. W. (2010). Neuropsychological and clinical heterogeneity of cognitive impairment and dementia in patients with Parkinson's disease. *The Lancet Neurology*, *9*(12), 1200–1213. http://doi.org/10.1016/S1474-4422(10)70212-X

Kitada, T., Shimizu, N., Asakawa, S., Hattori, N., Matsumine, H., Yamamura, Y., … Mizuno, Y. (1998). Mutations in the parkin gene cause autosomal recessive juvenile parkinsonism. *Nature*, *392*(6676), 605–608. http://doi.org/10.1038/33416

Klein, C., & Westenberger, A. (2012). Genetics of Parkinson's disease. *Cold Spring Harbor Perspectives in Medicine*, *2*(1), a008888. http://doi.org/10.1101/cshperspect.a008888

Korolchuk, V. I., Schütz, M. M., Gómez-Llorente, C., Rocha, J., Lansu, N. R., Collins, S. M., … O'Kane, C. J. (2007). Drosophila Vps35 function is necessary for normal endocytic trafficking and actin cytoskeleton organisation. *Journal of Cell Science*, *120*(Pt 24), 4367–76. http://doi.org/10.1242/jcs.012336

Kravitz, A. V, Tye, L. D., & Kreitzer, A. C. (2012). Distinct roles for direct and indirect pathway striatal neurons in reinforcement. *Nature Neuroscience*, *15*(6), 816–8. http://doi.org/10.1038/nn.3100

Krüger, R., Kuhn, W., Leenders, K. L., Sprengelmeyer, R., Müller, T., Woitalla, D., … Przuntek, H. (2001). Familial parkinsonism with synuclein pathology: clinical and PET studies of A30P mutation carriers. *Neurology*, *56*(10), 1355–62. Retrieved from http://www.ncbi.nlm.nih.gov/pubmed/11376188

Kuhar, M. J., Ritz, M. C., & Boja, J. W. (1991). The dopamine hypothesis of the reinforcing properties of cocaine. *Trends in Neurosciences*, *14*(7), 299–302. http://doi.org/10.1016/0166-2236(91)90141-G

Kurosinski, P., Guggisberg, M., & Götz, J. (2002). Alzheimer's and Parkinson's disease--overlapping or synergistic pathologies? *Trends in Molecular Medicine*, *8*(1), 3–5. http://doi.org/10.1016/S1471-4914(01)02246-8

Kuusisto, E., Parkkinen, L., & Alafuzoff, I. (2003). Morphogenesis of Lewy bodies: dissimilar

incorporation of alpha-synuclein, ubiquitin, and p62. *Journal of Neuropathology and Experimental Neurology*, *62*(12), 1241–53. Retrieved from http://www.ncbi.nlm.nih.gov/pubmed/14692700

Kuzuhara, S., Mori, H., Izumiyama, N., Yoshimura, M., & Ihara, Y. (1988). Lewy bodies are ubiquitinated. A light and electron microscopic immunocytochemical study. *Acta Neuropathologica*, *75*(4), 345–53. Retrieved from http://www.ncbi.nlm.nih.gov/pubmed/3364159

Lago, T., Davis, A., Grillon, C., & Ernst, M. (2017). Striatum on the anxiety map: Small detours into adolescence. *Brain Research*, *1654*(Pt B), 177–184. http://doi.org/10.1016/j.brainres.2016.06.006

Lam, H. a., Wu, N., Cely, I., Kelly, R. L., Hean, S., Richter, F., … Maidment, N. T. (2011). Elevated tonic extracellular dopamine concentration and altered dopamine modulation of synaptic activity precede dopamine loss in the striatum of mice overexpressing human α-synuclein. *Journal of Neuroscience Research*, *89*(7), 1091–1102. http://doi.org/10.1002/jnr.22611

Lammel, S., Hetzel, A., Häckel, O., Jones, I., Liss, B., & Roeper, J. (2008). Unique properties of mesoprefrontal neurons within a dual mesocorticolimbic dopamine system. *Neuron*, *57*(5), 760–73. http://doi.org/10.1016/j.neuron.2008.01.022

Lang, A. E., Lozano, A. M., Montgomery, E., Duff, J., Tasker, R., & Hutchinson, W. (1997). Posteroventral Medial Pallidotomy in Advanced Parkinson's Disease. *New England Journal of Medicine*, *337*(15), 1036–1043. http://doi.org/10.1056/NEJM199710093371503

Langston, J. W. (2006). The Parkinson's complex: parkinsonism is just the tip of the iceberg. *Annals of Neurology*, *59*(4), 591–6. http://doi.org/10.1002/ana.20834

Langston, J. W. (2017). The MPTP Story. *Journal of Parkinson's Disease*, *7*(s1), S11–S22. http://doi.org/10.3233/JPD-179006

Langston, J. W., Ballard, P., Tetrud, J. W., & Irwin, I. (1983). Chronic Parkinsonism in humans due to a product of meperidine-analog synthesis. *Science (New York, N.Y.)*, *219*(4587), 979–80. Retrieved from http://www.ncbi.nlm.nih.gov/pubmed/6823561

Lasiecka, Z. M., & Winckler, B. (2011). Mechanisms of polarized membrane trafficking in neurons -- focusing in on endosomes. *Molecular and Cellular Neurosciences*, *48*(4), 278–87. http://doi.org/10.1016/j.mcn.2011.06.013

Lee, M. K., Stirling, W., Xu, Y., Xu, X., Qui, D., Mandir, A. S., … Price, D. L. (2002). Human -synuclein-harboring familial Parkinson's disease-linked Ala-53 -> Thr mutation causes neurodegenerative disease with -synuclein aggregation in transgenic mice. *Proceedings of the National Academy of Sciences*, *99*(13), 8968–8973. http://doi.org/10.1073/pnas.132197599

Lefaucheur, J.-P. (2005). Motor cortex dysfunction revealed by cortical excitability studies in Parkinson's disease: influence of antiparkinsonian treatment and cortical stimulation. http://doi.org/10.1016/j.clinph.2004.11.017

Lesage, S., Anheim, M., Letournel, F., Bousset, L., Honoré, A., Rozas, N., … French Parkinson's Disease Genetics Study Group. (2013). G51D α-synuclein mutation causes a novel Parkinsonian-pyramidal syndrome. *Annals of Neurology*, *73*(4), 459–471. http://doi.org/10.1002/ana.23894

Lesage, S., & Brice, A. (2009). Parkinson's disease: From monogenic forms to genetic susceptibility factors. *Human Molecular Genetics*, *18*(R1), 48–59. http://doi.org/10.1093/hmg/ddp012

Lesage, S., Dürr, A., Tazir, M., Lohmann, E., Leutenegger, A.-L., Janin, S., … French Parkinson's Disease Genetics Study Group. (2006). *LRRK2* G2019S as a Cause of Parkinson's Disease in North African Arabs. *New England Journal of Medicine*, *354*(4), 422–423. http://doi.org/10.1056/NEJMc055540

Li, Y., Liu, W., Oo, T. F., Wang, L., Tang, Y., Jackson-Lewis, V., … Li, C. (2009). Mutant LRRK2R1441G BAC transgenic mice recapitulate cardinal features of Parkinson's disease. *Nature Neuroscience*, *12*(7), 826–828. http://doi.org/10.1038/nn.2349

Lloyd, K. G., Davidson, L., & Hornykiewicz, O. (1975). The neurochemistry of Parkinson's disease: effect of L-dopa therapy. *Journal of Pharmacology and Experimental Therapeutics*, *195*(3).

Lohr, K. M., Bernstein, A. I., Stout, K. A., Dunn, A. R., Lazo, C. R., Alter, S. P., … Miller, G. W. (2014). Increased vesicular monoamine transporter enhances dopamine release and opposes Parkinson disease-related neurodegeneration in vivo. *Proceedings of the National Academy of Sciences of the United States of America*, *111*(27), 9977–82. http://doi.org/10.1073/pnas.1402134111

Lohr, K. M., Masoud, S. T., Salahpour, A., & Miller, G. W. (2017). Membrane transporters as mediators of synaptic dopamine dynamics: implications for disease. *The European Journal of Neuroscience*, *45*(1), 20–33. http://doi.org/10.1111/ejn.13357

Lohr, K. M., Stout, K. A., Dunn, A. R., Wang, M., Salahpour, A., Guillot, T. S., & Miller, G. W. (2015). Increased Vesicular Monoamine Transporter 2 (VMAT2; *Slc18a2*) Protects against Methamphetamine Toxicity. *ACS Chemical Neuroscience*, *6*(5), 790–799. http://doi.org/10.1021/acschemneuro.5b00010

Longo, F., Mercatelli, D., Novello, S., Arcuri, L., Brugnoli, A., Vincenzi, F., … Morari, M.

(2017). Age-dependent dopamine transporter dysfunction and Serine129 phospho-α-synuclein overload in G2019S LRRK2 mice. *Acta Neuropathologica Communications*, *5*(1), 22. http://doi.org/10.1186/s40478-017-0426-8

Longo, F., Russo, I., Shimshek, D. R., Greggio, E., & Morari, M. (2014). Genetic and pharmacological evidence that G2019S LRRK2 confers a hyperkinetic phenotype, resistant to motor decline associated with aging. *Neurobiology of Disease*, *71*, 62–73. http://doi.org/10.1016/j.nbd.2014.07.013

Lorefalt, B., Ganowiak, W., Palhagen, S., Toss, G., Unosson, M., & Granerus, A.-K. (2004). Factors of importance for weight loss in elderly patients with Parkinson's disease. *Acta Neurologica Scandinavica*, *110*(3), 180–187. http://doi.org/10.1111/j.1600-0404.2004.00307.x

Lotharius, J., Barg, S., Wiekop, P., Lundberg, C., Raymon, H. K., & Brundin, P. (2002). Effect of Mutant α-Synuclein on Dopamine Homeostasis in a New Human Mesencephalic Cell Line. *Journal of Biological Chemistry*, *277*(41), 38884–38894. http://doi.org/10.1074/jbc.M205518200

Lu, X.-H., Fleming, S. M., Meurers, B., Ackerson, L. C., Mortazavi, F., Lo, V., … Yang, X. W. (2009). Bacterial Artificial Chromosome Transgenic Mice Expressing a Truncated Mutant Parkin Exhibit Age-Dependent Hypokinetic Motor Deficits, Dopaminergic Neuron Degeneration, and Accumulation of Proteinase K-Resistant -Synuclein. *Journal of Neuroscience*, *29*(7), 1962–1976. http://doi.org/10.1523/JNEUROSCI.5351-08.2009

MacLeod, D. A., Rhinn, H., Kuwahara, T., Zolin, A., Di Paolo, G., McCabe, B. D., … Abeliovich, A. (2014). RAB7L1 interacts with LRRK2 to modify intraneuronal protein sorting and Parkinson's disease risk. *Neuron*, *77*(3), 425–439.

http://doi.org/10.1016/j.neuron.2012.11.033.RAB7L1

MacLeod, D., Dowman, J., Hammond, R., Leete, T., Inoue, K., & Abeliovich, A. (2006). The familial Parkinsonism gene LRRK2 regulates neurite process morphology. *Neuron*, *52*(4), 587–93. http://doi.org/10.1016/j.neuron.2006.10.008

Mahlknecht, P., Seppi, K., & Poewe, W. (2015). The Concept of Prodromal Parkinson's Disease. *Journal of Parkinson's Disease*, *5*(4), 681–97. http://doi.org/10.3233/JPD-150685

Masliah, E., Rockenstein, E., Veinbergs, I., Mallory, M., Hashimoto, M., Takeda, A., … Mucke, L. (2000). Dopaminergic loss and inclusion body formation in alpha-synuclein mice: implications for neurodegenerative disorders. *Science (New York, N.Y.)*, *287*(5456), 1265–9. Retrieved from http://www.ncbi.nlm.nih.gov/pubmed/10678833

Mata, I. F., Jang, Y., Kim, C.-H., Hanna, D. S., Dorschner, M. O., Samii, A., … Zabetian, C. P. (2015). The RAB39B p.G192R mutation causes X-linked dominant Parkinson's disease. *Molecular Neurodegeneration*, *10*(1), 50. http://doi.org/10.1186/s13024-015-0045-4

Mata, I. F., Lockhart, P. J., & Farrer, M. J. (2004). Parkin genetics: one model for Parkinson's disease. *Human Molecular Genetics*, *13*(90001), 127R–133. http://doi.org/10.1093/hmg/ddh089

Matta, S., Van Kolen, K., da Cunha, R., van den Bogaart, G., Mandemakers, W., Miskiewicz, K., … Verstreken, P. (2012). LRRK2 Controls an EndoA Phosphorylation Cycle in Synaptic Endocytosis. *Neuron*, *75*(6), 1008–1021. http://doi.org/10.1016/j.neuron.2012.08.022

Meiser, J., Weindl, D., & Hiller, K. (2013). Complexity of dopamine metabolism, 1–18.

Meissner, W. G., Frasier, M., Gasser, T., Goetz, C. G., Lozano, A., Piccini, P., … Bezard, E. (2011). Priorities in Parkinson's disease research. *Nature Reviews Drug Discovery*, *10*(5), 377–393. http://doi.org/10.1038/nrd3430

Melrose, H. L., Dächsel, J. C., Behrouz, B., Lincoln, S. J., Yue, M., Hinkle, K. M., … Farrer, M. J. (2010). Impaired dopaminergic neurotransmission and microtubule-associated protein tau alterations in human LRRK2 transgenic mice. *Neurobiology of Disease, 40*(3), 503–517. http://doi.org/10.1016/j.nbd.2010.07.010

Milienne-Petiot, M., Groenink, L., Minassian, A., & Young, J. W. (2017). Blockade of dopamine D $_1$ -family receptors attenuates the mania-like hyperactive, risk-preferring, and high motivation behavioral profile of mice with low dopamine transporter levels. *Journal of Psychopharmacology*, *31*(10), 1334–1346. http://doi.org/10.1177/0269881117731162

Min, S.-W., Chen, X., Tracy, T. E., Li, Y., Zhou, Y., Wang, C., … Gan, L. (2015). Critical role of acetylation in tau-mediated neurodegeneration and cognitive deficits. *Nature Medicine*, *21*(10), 1154–62. http://doi.org/10.1038/nm.3951

Min, S.-W., Cho, S.-H., Zhou, Y., Schroeder, S., Haroutunian, V., Seeley, W. W., … Gan, L. (2010). Acetylation of tau inhibits its degradation and contributes to tauopathy. *Neuron*, *67*(6), 953–66. http://doi.org/10.1016/j.neuron.2010.08.044

Miura, E., Hasegawa, T., Konno, M., Suzuki, M., Sugeno, N., Fujikake, N., … Aoki, M. (2014). VPS35 dysfunction impairs lysosomal degradation of α-synuclein and exacerbates neurotoxicity in a Drosophila model of Parkinson's disease. *Neurobiology of Disease, 71*, 1–13. http://doi.org/10.1016/j.nbd.2014.07.014

Mizushima, N., Levine, B., Cuervo, A. M., & Klionsky, D. J. (2008). Autophagy fights disease through cellular self-digestion. *Nature, 451*(7182), 1069–75. http://doi.org/10.1038/nature06639

Mohan, M., & Mellick, G. D. (2016). Role of the VPS35 D620N mutation in Parkinson's disease. *Parkinsonism & Related Disorders*. http://doi.org/10.1016/j.parkreldis.2016.12.001

Moore, D. J., Dawson, V. L., & Dawson, T. M. (2006). Lessons from Drosophila models of DJ-1 deficiency. *Science of Aging Knowledge Environment : SAGE KE, 2006*(2), pe2. http://doi.org/10.1126/sageke.2006.2.pe2

Moore, D. J., Zhang, L., Dawson, T. M., & Dawson, V. L. (2003). A missense mutation (L166P) in DJ-1, linked to familial Parkinson's disease, confers reduced protein stability and impairs homo-oligomerization. *Journal of Neurochemistry, 87*(6), 1558–1567. http://doi.org/10.1111/j.1471-4159.2003.02265.x

Munsie, L. N., Milnerwood, A. J., Seibler, P., Tatarnikov, I., Khinda, J., Volta, M., … Farrer, M. J. (2015). Retromer-dependent neurotransmitter receptor trafficking to synapses is altered by the Parkinson's disease VPS35 mutation p.D620N. *Human Molecular Genetics*, *24*(6), 1691–1703. http://doi.org/10.1093/hmg/ddu582

Muntané, G., Dalfó, E., Martinez, A., & Ferrer, I. (2008). Phosphorylation of tau and α-synuclein in synaptic-enriched fractions of the frontal cortex in Alzheimer's disease, and in Parkinson's disease and related α-synucleinopathies. *Neuroscience, 152*(4), 913–923. http://doi.org/10.1016/j.neuroscience.2008.01.030

Narendra, D. P., & Youle, R. J. (2011). Targeting mitochondrial dysfunction: role for PINK1 and Parkin in mitochondrial quality control. *Antioxidants & Redox Signaling*, *14*(10), 1929–38. http://doi.org/10.1089/ars.2010.3799

Nicklas, W. J., Vyas, I., & Heikkila, R. E. (1985). Inhibition of NADH-linked oxidation in brain mitochondria by 1-methyl-4-phenyl-pyridine, a metabolite of the neurotoxin, 1-methyl-4-phenyl-1,2,5,6-tetrahydropyridine. *Life Sciences, 36*(26), 2503–8. Retrieved from http://www.ncbi.nlm.nih.gov/pubmed/2861548

Nishijima, H., & Tomiyama, M. (2016). What Mechanisms Are Responsible for the Reuptake of

Levodopa-Derived Dopamine in Parkinsonian Striatum? *Frontiers in Neuroscience*, *10*, 575. http://doi.org/10.3389/fnins.2016.00575

Nutt, J. G., & Carter, J. H. (2000). Apomorphine can sustain the long-duration response to L-DOPA in fluctuating PD. *Neurology*, *54*(1), 247–50. http://doi.org/10.1212/wnl.54.10.1884

Oertel, W. H. (2017). Recent advances in treating Parkinson's disease. *F1000Research*, *6*, 260. http://doi.org/10.12688/f1000research.10100.1

Orenstein, S. J., Kuo, S.-H., Tasset, I., Arias, E., Koga, H., Fernandez-Carasa, I., … Cuervo, A. M. (2013). Interplay of LRRK2 with chaperone-mediated autophagy. *Nature Neuroscience*, *16*(4), 394–406. http://doi.org/10.1038/nn.3350

Orr, C. F., Rowe, D. B., & Halliday, G. M. (2002). An inflammatory review of Parkinson's disease. *Progress in Neurobiology*, *68*(5), 325–340. http://doi.org/10.1016/S0301-0082(02)00127-2

Ovallath, S., & Deepa, P. (2013). The history of parkinsonism: Descriptions in ancient Indian medical literature. *Movement Disorders*, *28*(5), 566–568. http://doi.org/10.1002/mds.25420

Paisàn-Ruìz, C., Sàenz, A., Lòpez de Munain, A., Martì, I., Martìnez Gil, A., Martì-Massò, J. F., & Pèrez-Tur, J. (2005). Familial Parkinson's disease: clinical and genetic analysis of four Basque families. *Annals of Neurology*, *57*(3), 365–72. http://doi.org/10.1002/ana.20391

Palmiter, R. D. (2007). Is dopamine a physiologically relevant mediator of feeding behavior? *Trends in Neurosciences*, *30*(8), 375–381. http://doi.org/10.1016/j.tins.2007.06.004

Parkinson, J. (n.d.). An Essay on the Shaking Palsy, by James Parkinson. Retrieved December 27, 2015, from http://www.gutenberg.org/files/23777/23777-h/23777-h.htm

Parkinson Canada | Parkinson Canada. (n.d.). Retrieved December 27, 2017, from http://www.parkinson.ca/

Parmar, M. (2018). Towards stem cell based therapies for Parkinson's disease. *Development (Cambridge, England), 145*(1), dev156117. http://doi.org/10.1242/dev.156117

Pereira, D. B., Schmitz, Y., Mészáros, J., Merchant, P., Hu, G., Li, S., … Sulzer, D. (2016). Fluorescent false neurotransmitter reveals functionally silent dopamine vesicle clusters in the striatum. *Nature Neuroscience*, *19*(4), 578–586. http://doi.org/10.1038/nn.4252

Phillips, P. E. M., Hancock, P. J., & Stamford, J. A. (2002). Time window of autoreceptor-mediated inhibition of limbic and striatal dopamine release. *Synapse*, *44*(1), 15–22. http://doi.org/10.1002/syn.10049

Piccoli, G., Condliffe, S. B., Bauer, M., Giesert, F., Boldt, K., De Astis, S., … Ueffing, M. (2011). LRRK2 Controls Synaptic Vesicle Storage and Mobilization within the Recycling Pool. *Journal of Neuroscience*, *31*(6), 2225–2237. http://doi.org/10.1523/JNEUROSCI.3730-10.2011

Piccoli, G., Condliffe, S. B., Bauer, M., Giesert, F., Boldt, K., De Astis, S., … Ueffing, M. (2011). LRRK2 controls synaptic vesicle storage and mobilization within the recycling pool. *The Journal of Neuroscience : The Official Journal of the Society for Neuroscience*, *31*(6), 2225–37. http://doi.org/10.1523/JNEUROSCI.3730-10.2011

Pierot, L., Desnos, C., Blin, J., Raisman, R., Scherman, D., Javoy-Agid, F., … Agid, Y. (1988). D1 and D2-type dopamine receptors in patients with Parkinson's disease and progressive supranuclear palsy. *Journal of the Neurological Sciences*, *86*(2–3), 291–306. Retrieved from http://www.ncbi.nlm.nih.gov/pubmed/2975699

Poewe, W., & Antonini, A. (2015). Novel formulations and modes of delivery of levodopa. *Movement Disorders*, *30*(1), 114–120. http://doi.org/10.1002/mds.26078

Pollack, A. E. (2001). Anatomy, physiology, and pharmacology of the basal ganglia. *Neurologic*

Clinics, *19*(3), 523–534. http://doi.org/10.1016/S0733-8619(05)70032-3

Polymeropoulos, M. H. (1997). Mutation in the alpha-synuclein gene identified in families with Parkinson's disease. Retrieved December 28, 2015, from http://go.galegroup.com.ezproxy.library.ubc.ca/ps/i.do?p=HRCA&u=ubcolumbia&id=GALE%7CA19605419&v=2.1&it=r&sid=summon&userGroup=ubcolumbia&authCount=1

Postuma, R. B., Berg, D., Stern, M., Poewe, W., Olanow, C. W., Oertel, W., … Deuschl, G. (2015). MDS clinical diagnostic criteria for Parkinson's disease. *Movement Disorders*, *30*(12), 1591–1601. http://doi.org/10.1002/mds.26424

Potashkin, J. A., Blume, S. R., & Runkle, N. K. (2011). Limitations of Animal Models of Parkinson's Disease. *Parkinson's Disease*, *2011*, 1–7. http://doi.org/10.4061/2011/658083

Pramstaller, P. P., Schlossmacher, M. G., Jacques, T. S., Scaravilli, F., Eskelson, C., Pepivani, I., … Klein, C. (2005). Lewy body Parkinson's disease in a large pedigree with 77Parkin mutation carriers. *Annals of Neurology*, *58*(3), 411–422. http://doi.org/10.1002/ana.20587

Proukakis, C., Dudzik, C. G., Brier, T., MacKay, D. S., Cooper, J. M., Millhauser, G. L., … Schapira, A. H. (2013). A novel -synuclein missense mutation in Parkinson disease. *Neurology*, *80*(11), 1062–1064. http://doi.org/10.1212/WNL.0b013e31828727ba

Przedborski, S., & Jackson-Lewis, V. (1998). Mechanisms of MPTP toxicity. *Movement Disorders : Official Journal of the Movement Disorder Society*, *13 Suppl 1*, 35–8. Retrieved from http://www.ncbi.nlm.nih.gov/pubmed/9613716

Rajput, A., Dickson, D. W., Robinson, C. A., Ross, O. A., Dachsel, J. C., Lincoln, S. J., … Farrer, M. J. (2006). Parkinsonism, Lrrk2 G2019S, and tau neuropathology. *Neurology*, *67*(8), 1506–1508. http://doi.org/10.1212/01.wnl.0000240220.33950.0c

Ramirez, S., Tonegawa, S., & Liu, X. (2013). Identification and optogenetic manipulation of

memory engrams in the hippocampus. *Frontiers in Behavioral Neuroscience*, *7*(January), 226. http://doi.org/10.3389/fnbeh.2013.00226

Ray Chaudhuri, K., Qamar, M. A., Rajah, T., Loehrer, P., Sauerbier, A., Odin, P., & Jenner, P. (2016). Non-oral dopaminergic therapies for Parkinson's disease: current treatments and the future. *Npj Parkinson's Disease*, *2*(1), 16023. http://doi.org/10.1038/npjparkd.2016.23

Rice, M. E., & Patel, J. C. (2015). Somatodendritic dopamine release: recent mechanistic insights. *Philosophical Transactions of the Royal Society of London. Series B, Biological Sciences*, *370*(1672), 20140185. http://doi.org/10.1098/rstb.2014.0185

Rinne, J. O., Portin, R., Ruottinen, H., Nurmi, E., Bergman, J., Haaparanta, M., & Solin, O. (2000). Cognitive impairment and the brain dopaminergic system in Parkinson disease: [18F]fluorodopa positron emission tomographic study. *Archives of Neurology*, *57*(4), 470–5. Retrieved from http://www.ncbi.nlm.nih.gov/pubmed/10768619

Rivero-Ríos, P., Fernández, B., Madero-Pérez, J., Lozano, M. R., & Hilfiker, S. (2016). Two-Pore Channels and Parkinson's Disease: Where's the Link? *Messenger (Los Angeles, Calif. : Print)*, *5*(1–2), 67–75. http://doi.org/10.1166/msr.2016.1051

Rockenstein, E., Mallory, M., Hashimoto, M., Song, D., Shults, C. W., Lang, I., & Masliah, E. (2002). Differential neuropathological alterations in transgenic mice expressing alpha-synuclein from the platelet-derived growth factor and Thy-1 promoters. *Journal of Neuroscience Research*, *68*(5), 568–78. http://doi.org/10.1002/jnr.10231

Rogerio, R., & Takahashi, R. N. (1992). Anxiogenic properties of cocaine in the rat evaluated with the elevated plus-maze. *Pharmacology, Biochemistry and Behavior*, *43*(2), 631–633. http://doi.org/10.1016/0091-3057(92)90203-R

Ross, O. A., Toft, M., Whittle, A. J., Johnson, J. L., Papapetropoulos, S., Mash, D. C., …

Dickson, D. W. (2006). Lrrk2 and Lewy body disease. *Annals of Neurology*, *59*(2), 388–393. http://doi.org/10.1002/ana.20731

Roy, B., & Jackson, G. R. (2014). Interactions between Tau and α-synuclein augment neurotoxicity in a Drosophila model of Parkinson's disease. *Human Molecular Genetics*, *23*(11), 3008–23. http://doi.org/10.1093/hmg/ddu011

Sann, S., Wang, Z., Brown, H., & Jin, Y. (2009). Roles of endosomal trafficking in neurite outgrowth and guidance. *Trends in Cell Biology*, *19*(7), 317–324. http://doi.org/10.1016/j.tcb.2009.05.001

Schapira, A. H. V. (2007). Treatment Options in the Modern Management of Parkinson Disease. *Archives of Neurology*, *64*(8), 1083. http://doi.org/10.1001/archneur.64.8.1083

Schreij, A. M. A., Chaineau, M., Ruan, W., Lin, S., Barker, P. A., Fon, E. A., & McPherson, P. S. (2015). LRRK2 localizes to endosomes and interacts with clathrin-light chains to limit Rac1 activation. *EMBO Reports*, *16*(1), 79–86. http://doi.org/10.15252/embr.201438714

Seaman, M. N., & Freeman, C. L. (2014). Analysis of the Retromer complex-WASH complex interaction illuminates new avenues to explore in Parkinson disease. *Communicative & Integrative Biology*, *7*(August 2015), e29483. http://doi.org/10.4161/cib.29483

Sgroi, S., Kaelin-Lang, A., & Capper-Loup, C. (2014). Spontaneous locomotor activity and L-DOPA-induced dyskinesia are not linked in 6-OHDA parkinsonian rats. *Frontiers in Behavioral Neuroscience*, *8*, 331. http://doi.org/10.3389/fnbeh.2014.00331

Sharma, J. C., & Lewis, A. (2017). Weight in Parkinson's Disease: Phenotypical Significance. In *International review of neurobiology* (Vol. 134, pp. 891–919). http://doi.org/10.1016/bs.irn.2017.04.011

Sharma, J. C., & Turton, J. (2012). Olfaction, dyskinesia and profile of weight change in

Parkinson's disease: Identifying neurodegenerative phenotypes. *Parkinsonism & Related Disorders*, *18*(8), 964–970. http://doi.org/10.1016/J.PARKRELDIS.2012.05.004

Sharma, J. C., & Vassallo, M. (2014). Prognostic significance of weight changes in Parkinson's disease: the Park–weight phenotype. *Neurodegenerative Disease Management*, *4*(4), 309–316. http://doi.org/10.2217/nmt.14.25

Sharma, M., Ioannidis, J. P. A., Aasly, J. O., Annesi, G., Brice, A., Bertram, L., … GEOPD consortium. (2012). A multi-centre clinico-genetic analysis of the VPS35 gene in Parkinson disease indicates reduced penetrance for disease-associated variants. *Journal of Medical Genetics*, *49*(11), 721–726. http://doi.org/10.1136/jmedgenet-2012-101155

Sheng, Z., Zhang, S., Bustos, D., Kleinheinz, T., Le Pichon, C. E., Dominguez, S. L., … Zhu, H. (2012). Ser1292 Autophosphorylation Is an Indicator of LRRK2 Kinase Activity and Contributes to the Cellular Effects of PD Mutations. *Science Translational Medicine*, *4*(164), 164ra161-164ra161. http://doi.org/10.1126/scitranslmed.3004485

Shin, N., Jeong, H., Kwon, J., Heo, H. Y., Kwon, J. J., Yun, H. J., … Seol, W. (2008). LRRK2 regulates synaptic vesicle endocytosis. *Experimental Cell Research*, *314*(10), 2055–2065. http://doi.org/10.1016/j.yexcr.2008.02.015

Sidhu, S. S., Li, B., Chen, Y., Fellouse, F. A., Eigenbrot, C., & Fuh, G. (2004). Phage-displayed Antibody Libraries of Synthetic Heavy Chain Complementarity Determining Regions. *Journal of Molecular Biology*, *338*(2), 299–310. http://doi.org/10.1016/j.jmb.2004.02.050

Singleton, A. B., Farrer, M., Johnson, J., Singleton, A., Hague, S., Kachergus, J., … Gwinn-Hardy, K. (2003). alpha-Synuclein locus triplication causes Parkinson's disease. *Science (New York, N.Y.)*, *302*(5646), 841. http://doi.org/10.1126/science.1090278

Smolinsky, A. N., Bergner, C. L., LaPorte, J. L., & Kalueff, A. V. (2009). Analysis of Grooming

Behavior and Its Utility in Studying Animal Stress, Anxiety, and Depression (pp. 21–36). Humana Press, Totowa, NJ. http://doi.org/10.1007/978-1-60761-303-9_2

Sossi, V., de la Fuente-Fernández, R., Nandhagopal, R., Schulzer, M., McKenzie, J., Ruth, T. J., … Stoessl, J. a. (2010). Dopamine turnover increases in asymptomatic LRRK2 mutations carriers. *Movement Disorders : Official Journal of the Movement Disorder Society*, *25*(16), 2717–23. http://doi.org/10.1002/mds.23356

Spang, A. (2011). Signalling gets sorted by retromer. *The EMBO Journal*, *30*(15), 2988–2989. http://doi.org/10.1038/emboj.2011.232

Spillantini, M. G., Schmidt, M. L., Lee, V. M., Trojanowski, J. Q., Jakes, R., & Goedert, M. (1997). Alpha-synuclein in Lewy bodies. *Nature*, *388*(6645), 839–840. http://doi.org/10.1038/42166

Stefanis, L. (2012). α-Synuclein in Parkinson's disease. *Cold Spring Harbor Perspectives in Medicine*, *2*(2), a009399. http://doi.org/10.1101/cshperspect.a009399

Steger, M., Tonelli, F., Ito, G., Davies, P., Trost, M., Vetter, M., … Mann, M. (2016). Phosphoproteomics reveals that Parkinson's disease kinase LRRK2 regulates a subset of Rab GTPases. *eLife*, *5*, e12813. http://doi.org/10.7554/eLife.12813

Stenmark, H. (2009). Rab GTPases as coordinators of vesicle traffic. *Nature Reviews Molecular Cell Biology*, *10*(8), 513–525. http://doi.org/10.1038/nrm2728

Struhal, W., Presslauer, S., Spielberger, S., Zimprich, A., Auff, E., Bruecke, T., … Ransmayr, G. (2014). VPS35 Parkinson's disease phenotype resembles the sporadic disease. *Journal of Neural Transmission (Vienna, Austria : 1996)*, *121*(7), 755–9. http://doi.org/10.1007/s00702-014-1179-1

Surmeier, D. J. (2007). Calcium, ageing, and neuronal vulnerability in Parkinson's disease.

Lancet Neurology, *6*(10), 933–938. http://doi.org/10.1016/S1474-4422(07)70246-6

Swartz, H. M., Sarna, T., & Zecca, L. (1992). Modulation by neuromelanin of the availability and reactivity of metal ions. *Annals of Neurology, 32 Suppl*, S69-75. Retrieved from http://www.ncbi.nlm.nih.gov/pubmed/1510383

Tass, P. A., Qin, L., Hauptmann, C., Dovero, S., Bezard, E., Boraud, T., & Meissner, W. G. (2011). The translational value of the MPTP non-human primate model of Parkinsonism for deep brain stimulation research. In *2011 Annual International Conference of the IEEE Engineering in Medicine and Biology Society* (Vol. 2011, pp. 663–666). IEEE. http://doi.org/10.1109/IEMBS.2011.6090148

Temkin, P., Lauffer, B., Jäger, S., Cimermancic, P., Krogan, N. J., & von Zastrow, M. (2011). SNX27 mediates retromer tubule entry and endosome-to-plasma membrane trafficking of signalling receptors. *Nature Cell Biology*, *13*(6), 715–21. http://doi.org/10.1038/ncb2252

Tian, Y., Tang, F.-L., Sun, X., Wen, L., Mei, L., Tang, B.-S., & Xiong, W.-C. (2015). VPS35-deficiency results in an impaired AMPA receptor trafficking and decreased dendritic spine maturation. *Molecular Brain*, *8*(1), 70. http://doi.org/10.1186/s13041-015-0156-4

Tieu, K. (2011). A guide to neurotoxic animal models of Parkinson's disease. *Cold Spring Harbor Perspectives in Medicine*, *1*(1), a009316. http://doi.org/10.1101/cshperspect.a009316

Titova, N., Padmakumar, C., Lewis, S. J. G., & Chaudhuri, K. R. (2017). Parkinson's: a syndrome rather than a disease? *Journal of Neural Transmission*, *124*(8), 907–914. http://doi.org/10.1007/s00702-016-1667-6

Todorova, A., Jenner, P., & Ray Chaudhuri, K. (2014). Non-motor Parkinson's: integral to motor Parkinson's, yet often neglected. *Practical Neurology*, *14*(5), 310–22.

http://doi.org/10.1136/practneurol-2013-000741

Torrent, R., De Angelis Rigotti, F., Dell'Era, P., Memo, M., Raya, A., & Consiglio, A. (2015). Using iPS Cells toward the Understanding of Parkinson's Disease. *Journal of Clinical Medicine*, *4*(4), 548–66. http://doi.org/10.3390/jcm4040548

Trinh, J., & Farrer, M. (2013). Advances in the genetics of Parkinson disease. *Nature Reviews Neurology*, *9*(8), 445–454. http://doi.org/10.1038/nrneurol.2013.132

Uhl, G. (1998). Hypothesis : T h e Role of Do paminergic Transporters in Selective V J n e r a b i l G. *Annual of Neurology*, *43*(5), 555–560.

Valente, E. M., Bentivoglio, A. R., Dixon, P. H., Ferraris, A., Ialongo, T., Frontali, M., … Wood, N. W. (2001). Localization of a novel locus for autosomal recessive early-onset parkinsonism, PARK6, on human chromosome 1p35-p36. *American Journal of Human Genetics*, *68*(4), 895–900. Retrieved from http://www.ncbi.nlm.nih.gov/pubmed/11254447

Venken, K. J. T., Simpson, J. H., & Bellen, H. J. (2011). Genetic Manipulation of Genes and Cells in the Nervous System of the Fruit Fly. *Neuron*, *72*(2), 202–230. http://doi.org/10.1016/j.neuron.2011.09.021

Vieira, S. I., Rebelo, S., Esselmann, H., Wiltfang, J., Lah, J., Lane, R., … da Cruz E Silva, O. A. (2010). Retrieval of the Alzheimer's amyloid precursor protein from the endosome to the TGN is S655 phosphorylation state-dependent and retromer-mediated. *Molecular Neurodegeneration*, *5*(1), 40. http://doi.org/10.1186/1750-1326-5-40

Vilariño-Güell, C., Rajput, A., Milnerwood, A. J., Shah, B., Szu-Tu, C., Trinh, J., … Farrer, M. J. (2014). DNAJC13 mutations in Parkinson disease. *Human Molecular Genetics*, *23*(7), 1794–801. http://doi.org/10.1093/hmg/ddt570

Vilariño-Güell, C., Wider, C., Ross, O. A., Dachsel, J. C., Kachergus, J. M., Lincoln, S. J., …

Farrer, M. J. (2011a). VPS35 Mutations in Parkinson Disease. *The American Journal of Human Genetics*, *89*(1), 162–167. http://doi.org/10.1016/j.ajhg.2011.06.001

Vilariño-Güell, C., Wider, C., Ross, O. A., Dachsel, J. C., Kachergus, J. M., Lincoln, S. J., … Farrer, M. J. (2011b). VPS35 mutations in Parkinson disease. *American Journal of Human Genetics*, *89*(1), 162–7. http://doi.org/10.1016/j.ajhg.2011.06.001

Vogt Weisenhorn, D. M., Giesert, F., & Wurst, W. (2016). Diversity matters - heterogeneity of dopaminergic neurons in the ventral mesencephalon and its relation to Parkinson's Disease. *Journal of Neurochemistry*, *139*(S1), 8–26. http://doi.org/10.1111/jnc.13670

Volta, M., Beccano-Kelly, D. A., Paschall, S. A., Cataldi, S., MacIsaac, S. E., Kuhlmann, N., … Milnerwood, A. J. (2017). Initial elevations in glutamate and dopamine neurotransmission decline with age, as does exploratory behavior, in LRRK2 G2019S knock-in mice. *eLife*, *6*, e28377. http://doi.org/10.7554/eLife.28377

Volta, M., Milnerwood, A. J., & Farrer, M. J. (2015). Insights from late-onset familial parkinsonism on the pathogenesis of idiopathic Parkinson's disease. *The Lancet Neurology*, *14*(10), 1054–1064. http://doi.org/10.1016/S1474-4422(15)00186-6

Walker, M. D., Volta, M., Cataldi, S., Dinelle, K., Beccano-Kelly, D., Munsie, L., … Sossi, V. (2014). Behavioral deficits and striatal DA signaling in LRRK2 p.G2019S transgenic rats: a multimodal investigation including PET neuroimaging. *Journal of Parkinson's Disease*, *4*(3), 483–98. http://doi.org/10.3233/JPD-140344

Wall, P. M., & Messier, C. (2001). Methodological and conceptual issues in the use of the elevated plus-maze as a psychological measurement instrument of animal anxiety-like behavior, *25*.

Wang, C., Niu, M., Zhou, Z., Zheng, X., Zhang, L., Tian, Y., … Zhang, Y. wu. (2016). VPS35

regulates cell surface recycling and signaling of dopamine receptor D1. *Neurobiology of Aging*, *46*, 22–31. http://doi.org/10.1016/j.neurobiolaging.2016.05.016

West, A. B. (2015). Ten years and counting: moving leucine-rich repeat kinase 2 inhibitors to the clinic. *Movement Disorders : Official Journal of the Movement Disorder Society*, *30*(2), 180–9. http://doi.org/10.1002/mds.26075

West, A. B., Moore, D. J., Biskup, S., Bugayenko, A., Smith, W. W., Ross, C. A., … Dawson, T. M. (2005). From The Cover: Parkinson's disease-associated mutations in leucine-rich repeat kinase 2 augment kinase activity. *Proceedings of the National Academy of Sciences*, *102*(46), 16842–16847. http://doi.org/10.1073/pnas.0507360102

Whitworth, A. J. (2011). Drosophila Models of Parkinson's Disease. *Advances in Genetics*, *73*, 1–50. http://doi.org/10.1016/B978-0-12-380860-8.00001-X

Wichmann, T., Bergman, H., & DeLong, M. R. (2018). Basal ganglia, movement disorders and deep brain stimulation: advances made through non-human primate research. *Journal of Neural Transmission*, *125*(3), 419–430. http://doi.org/10.1007/s00702-017-1736-5

Wider, C., Vilariño-Güell, C., Jasinska-Myga, B., Heckman, M. G., Soto-Ortolaza, A. I., Cobb, S. A., … Ross, O. A. (2010). Association of the MAPT locus with Parkinson's disease. *European Journal of Neurology*, *17*(3), 483–6. http://doi.org/10.1111/j.1468-1331.2009.02847.x

Wile, D. J., Dinelle, K., Vafai, N., Mckenzie, J., Tsui, J. K., Schaffer, P., … Stoessl, A. J. (2016). A scan without evidence is not evidence of absence: Scans without evidence of dopaminergic deficit in a symptomatic leucine-rich repeat kinase 2 mutation carrier. *Movement Disorders*, *31*(3), 405–409. http://doi.org/10.1002/mds.26450

Wilson, G. R., Sim, J. C. H., McLean, C., Giannandrea, M., Galea, C. A., Riseley, J. R., …

Lockhart, P. J. (2014). Mutations in RAB39B Cause X-Linked Intellectual Disability and Early-Onset Parkinson Disease with α-Synuclein Pathology. *The American Journal of Human Genetics*, *95*(6), 729–735. http://doi.org/10.1016/j.ajhg.2014.10.015

Winner, B., Melrose, H. L., Zhao, C., Hinkle, K. M., Yue, M., Kent, C., … Gage, F. H. (2011). Adult neurogenesis and neurite outgrowth are impaired in LRRK2 G2019S mice. *Neurobiology of Disease*, *41*(3), 706–716. http://doi.org/10.1016/j.nbd.2010.12.008

Wray, S., & Lewis, P. A. (2010). A Tangled Web – Tau and Sporadic Parkinson's Disease. *Frontiers in Psychiatry*, *1*, 150. http://doi.org/10.3389/fpsyt.2010.00150

Wu, S., Fagan, R. R., Uttamapinant, C., Lifshitz, L. M., Fogarty, K. E., Ting, A. Y., & Melikian, H. E. (2017). The Dopamine Transporter Recycles via a Retromer-Dependent Postendocytic Mechanism: Tracking Studies Using a Novel Fluorophore-Coupling Approach. *The Journal of Neuroscience : The Official Journal of the Society for Neuroscience*, *37*(39), 9438–9452. http://doi.org/10.1523/JNEUROSCI.3885-16.2017

Yue, M., Hinkle, K., Davies, P., Trushina, E., Fiesel, F., Christenson, T., … Melrose, H. (2015). Progressive dopaminergic alterations and mitochondrial abnormalities in LRRK2 G2019S knock in mice. *Neurobiology of Disease*, *78*, 172–195. http://doi.org/10.1016/j.nbd.2015.02.031

Zarranz, J. J., Alegre, J., Gómez-Esteban, J. C., Lezcano, E., Ros, R., Ampuero, I., … de Yebenes, J. G. (2004). The new mutation, E46K, of α-synuclein causes parkinson and Lewy body dementia. *Annals of Neurology*, *55*(2), 164–173. http://doi.org/10.1002/ana.10795

Zavodszky, E., Seaman, M. N., Moreau, K., Jimenez-Sanchez, M., Breusegem, S. Y., Harbour, M. E., & Rubinsztein, D. C. (2014). Mutation in VPS35 associated with Parkinson's disease impairs WASH complex association and inhibits autophagy. *Nat Commun*, *5*(May), 3828.

http://doi.org/10.1038/ncomms4828

Zecca, L., Tampellini, D., Gerlach, M., Riederer, P., Fariello, R. G., & Sulzer, D. (2001). Substantia nigra neuromelanin: structure, synthesis, and molecular behaviour. *Molecular Pathology : MP*, *54*(6), 414–8. Retrieved from http://www.ncbi.nlm.nih.gov/pubmed/11724917

Zhang, D., Isack, N. R., Glodowski, D. R., Liu, J., Chen, C. C.-H., Xu, X. Z. S., … Rongo, C. (2012). RAB-6.2 and the retromer regulate glutamate receptor recycling through a retrograde pathway. *The Journal of Cell Biology*, *196*(1), 85–101. http://doi.org/10.1083/jcb.201104141

Zhou, H., Huang, C., Tong, J., Hong, W. C., Liu, Y.-J., & Xia, X.-G. (2011). Temporal expression of mutant LRRK2 in adult rats impairs dopamine reuptake. *International Journal of Biological Sciences*, *7*(6), 753–61. Retrieved from http://www.ncbi.nlm.nih.gov/pubmed/21698001

Zimprich, A., Benet-Pagès, A., Struhal, W., Graf, E., Eck, S. H., Offman, M. N., … Strom, T. M. (2011). A Mutation in VPS35, Encoding a Subunit of the Retromer Complex, Causes Late-Onset Parkinson Disease. *The American Journal of Human Genetics*, *89*(1), 168–175. http://doi.org/10.1016/j.ajhg.2011.06.008

Zimprich, A., Biskup, S., Leitner, P., Lichtner, P., Farrer, M., Lincoln, S., … Gasser, T. (2004). Mutations in LRRK2 cause autosomal-dominant parkinsonism with pleomorphic pathology. *Neuron*, *44*(4), 601–7. http://doi.org/10.1016/j.neuron.2004.11.005

Appendices

Appendix A

A.1 Supplementary methods: mouse validation

Table A.1. Primers sequences of *VPS35, Actb, Gapdh* and *Rpl19*.

Primer	Sequence 5′ to 3′	Tm	Gene name
Vps35 forward	AAGATGGACCCGGAATTCC	60	Vacuolar protein sorting 35
Vps35 reverse	GTAGTCCACACGATCAGGG		
Actb forward	GATCTGGCACCACACCTTCT	60	Actin beta
Actb reverse	CCATCACAATGCCTGTGGTA		
Gapdh forward	CTTTGGCATTGTGGAAGGG	60	Glyceraldehyde-3-phosphate dehydrogenase
Gapdh reverse	TGCAGGGATGATGTTCTGG		
Rpl19 forward	AATCGCCAATGCCAACTC	60	Ribosomal protein L19
Rpl19 reverse	GGAATGGACAGTCACAGG		

A.2 Supplementary methods: protein analysis

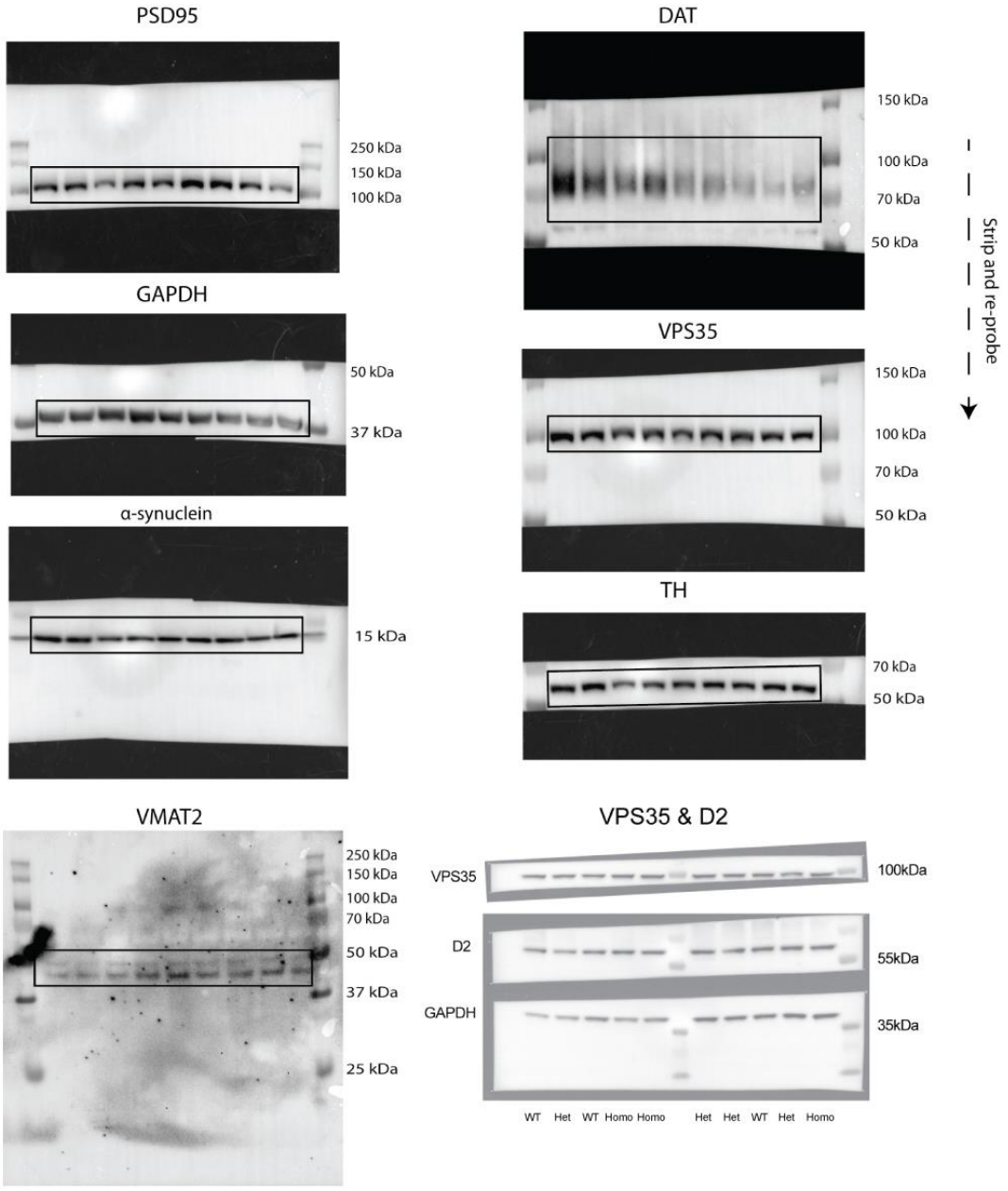

Figure A.1 Unprocessed Western blots

This figure contains example uncropped blots merged with corresponding ladder channel. Images were split into individual channels for presentation. Black boxes mark where western blots have been cropped for presentation in Figure 3.12, or else lane is labelled for comparison (VPS35 & D2 blot, bottom right). Molecular weights are indicated for each blot.

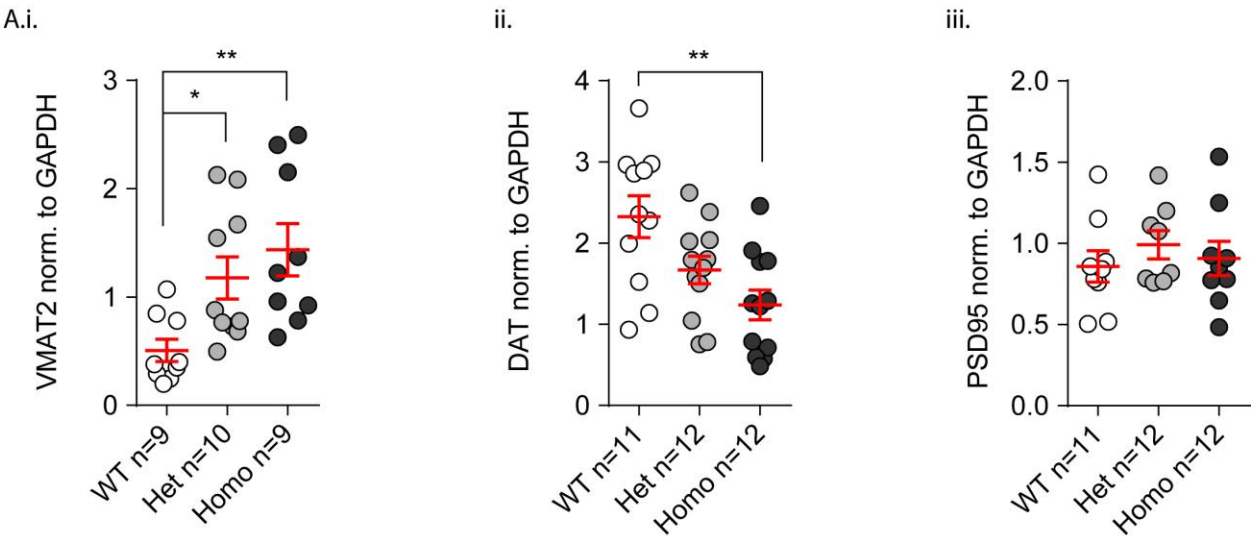

Figure A.2 VMAT2, DAT, and PSD95 normalized to GAPDH

A) Protein quantification for VMAT2, DAT and PSD95, showed in Figure 3.12 & Figure 3.14, here normalized to loading control GAPDH. VMAT2 is significantly increased in VKI mice (i, 1-way ANOVA $F_{2,25} = 6.19$, $p < 0.01$, *Bonferroni post-test* WT vs het $t_{(25)} = 2.25$, $p < 0.05$ & WT vs homo $t_{(25)} = 3.40$, $p < 0.01$, respectively), while there is a decrease in DAT levels in mutant animals (ii, 1-way ANOVA $F_{2,32} = 7.08$, $p < 0.01$, *Bonferroni post-test* WT vs het $t_{(25)} = 2.26$, $p = 0.06$ & WT vs homo $t_{(25)} = 3.74$, $p < 0.01$, respectively). There was no difference in total levels of PSD95 (iii, 1-way ANOVA $F_{2,23} = 0.46$, $p = 0.63$).

A.3 Supplementary methods: Voltammetry

Ai..

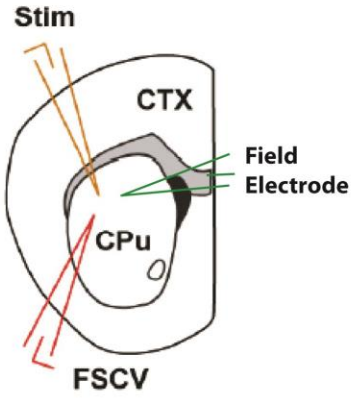

ii.

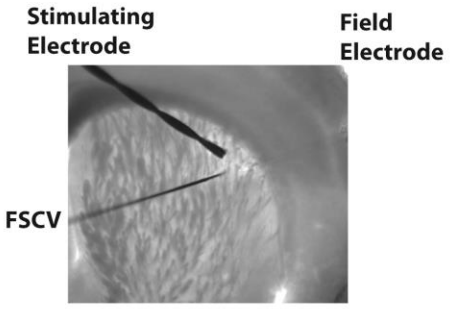

B.

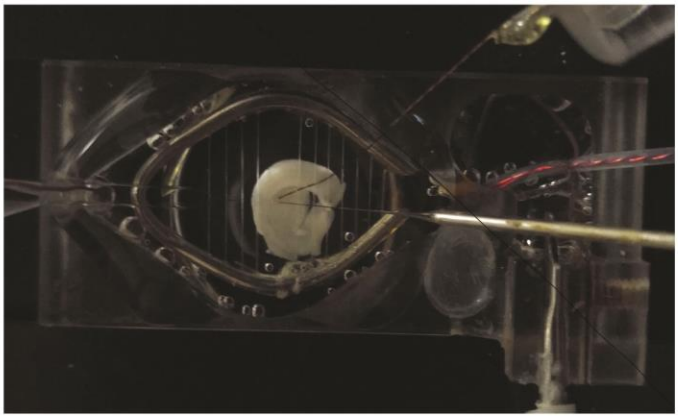

C.

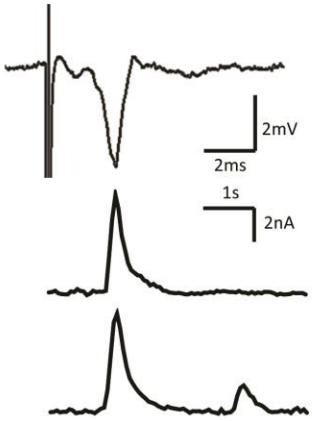

D.

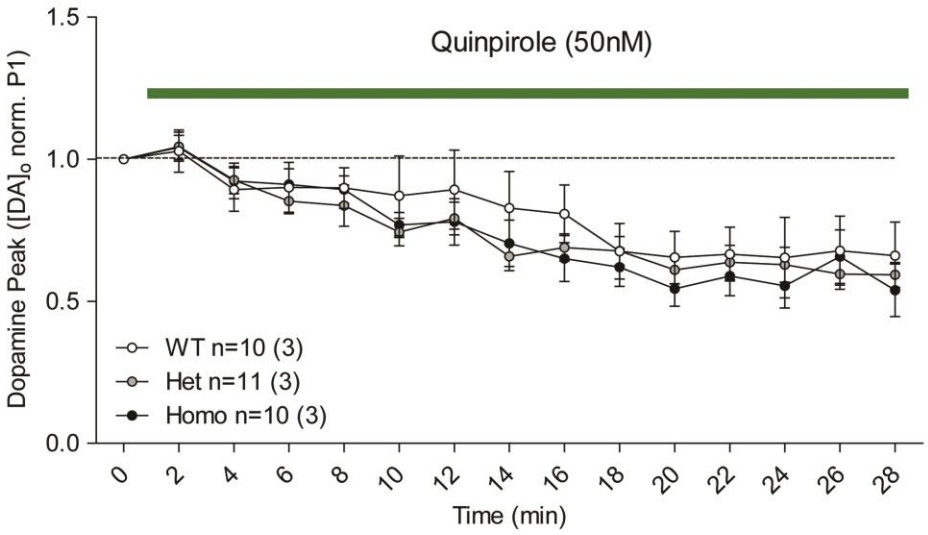

Figure A.3. Additional images and data for FSCV

A) A schematic and example picture of the placement of stimulating electrode (Stim, from top left), carbon-fiber microelectrode (FCSV, from bottom left), and field recording electrode (from right), in the dorsolateral striatum of a 300μm coronal slice from a mouse brain. The field recording electrode is made of glass, therefore hard to catch in a picture. B) A photo of the slice in the recording chamber. C) Example traces for field activity (top), dopamine response (middle) and paired pulse signal (bottom). D) In a separate cohort of 3-month-old VKI mice, the D2 agonist quinpirole (50nM) infused in the slice chamber gave a 20-50% reduction in dopamine release within ~ 5 minutes from reaching the slice. A series of stimuli was applied, with 2 minutes intervals, to evoke 50-70% maximum dopamine release. VKI slices showed a more rapid D2 inhibition compared to slices from wild-type littermates. 18-20 minutes from the start of treatment all slices from all genotype reach a 40-50% reduction (2-way ANOVA interaction $F_{28,392} = 0.66$, $p = 0.91$, time $F_{14,392} = 27.8$, $p < 0.0001$, genotype $F_{2,28} = 0.30$, $p = 0.057$, subjects $F_{28,392} = 23.94$, $p < 0.0001$, data did not reach significance by *Bonferroni post-test*).

Table A.2 Post-hoc statistical values input/output shown in Figure 3.10.A

Uncorrected Fisher's LSD	Mean Diff.	Significant?	Summary	Individual P Value	t
100					
Het n=25 (8) vs. WT n=23 (6)	0.003912	No	ns	0.9031	0.1219
Homo n=19 (7) vs. WT n=23 (6)	0.02407	No	ns	0.4914	0.6886
200					
Het n=25 (8) vs. WT n=23 (6)	0.03773	No	ns	0.2404	1.176
Homo n=19 (7) vs. WT n=23 (6)	0.06941	Yes	*	0.0477	1.985
300					
Het n=25 (8) vs. WT n=23 (6)	0.03581	No	ns	0.2652	1.116
Homo n=19 (7) vs. WT n=23 (6)	0.09487	Yes	**	0.0069	2.714
400					
Het n=25 (8) vs. WT n=23 (6)	0.05641	No	ns	0.0796	1.757
Homo n=19 (7) vs. WT n=23 (6)	0.1031	Yes	**	0.0034	2.948
500					
Het n=25 (8) vs. WT n=23 (6)	0.06375	Yes	#	0.0476	1.986
Homo n=19 (7) vs. WT n=23 (6)	0.08563	Yes	*	0.0147	2.449
600					
Het n=25 (8) vs. WT n=23 (6)	0.06562	Yes	#	0.0415	2.044
Homo n=19 (7) vs. WT n=23 (6)	0.1306	Yes	***	0.0002	3.735
700					

Het n=25 (8) vs. WT n=23 (6)	0.08286	Yes	#	0.0102	2.582
Homo n=19 (7) vs. WT n=23 (6)	0.1342	Yes	***	0.0001	3.838

Table A.3 Post-hoc values for quinpirole experiment shown in Figure 3.10.F

Bonferroni's multiple comparisons test	Mean Diff.	Significant?	Summary	Adjusted P Value	t
1					
WT n=22 (6) vs. Het n=20 (7)	0.0	No	ns	> 0.9999	0.0
WT n=22 (6) vs. Homo n=27 (7)	0.0	No	ns	> 0.9999	0.0
3					
WT n=22 (6) vs. Het n=20 (7)	0.01821	No	ns	> 0.9999	0.2860
WT n=22 (6) vs. Homo n=27 (7)	0.06542	No	ns	0.5548	1.087
5					
WT n=22 (6) vs. Het n=20 (7)	0.07579	No	ns	0.4688	1.190
WT n=22 (6) vs. Homo n=27 (7)	0.09147	No	ns	0.2580	1.520
7					
WT n=22 (6) vs. Het n=20 (7)	0.01530	No	ns	> 0.9999	0.2382
WT n=22 (6) vs. Homo n=27 (7)	0.1086	No	ns	0.1484	1.788
9					
WT n=22 (6) vs. Het n=20 (7)	0.1379	No	ns	0.0642	2.147
WT n=22 (6) vs. Homo n=27 (7)	0.1568	Yes	*	0.0200	2.582
11					
WT n=22 (6) vs. Het n=20 (7)	0.1768	Yes	*	0.0121	2.754
WT n=22 (6) vs. Homo n=27 (7)	0.1515	Yes	*	0.0257	2.494
13					
WT n=22 (6) vs. Het n=20 (7)	0.1424	Yes	*	0.0489	2.254
WT n=22 (6) vs. Homo n=27 (7)	0.2008	Yes	**	0.0018	3.336
15					
WT n=22 (6) vs. Het n=20 (7)	0.1563	Yes	*	0.0286	2.455
WT n=22 (6) vs. Homo n=27 (7)	0.1772	Yes	**	0.0073	2.918

Appendix B

B.1 Supplementary data on mouse behaviour

Table B.1. Additional information on mouse weight

		Genotype			
		WT	Het	Homo	
Age	2	14	21	12	
	3	21	27	18	
	9	9	13	6	
	12	8	11	8	
	15	8	9	6	
	18+	14	34	15	

WT vs Het							
Age	WT	Het	Difference	95% CI of diff.	t	P value	Summary
2	27.76	26.11	-1.643	-7.003 to 3.717	0.8862	P > 0.05	ns
3	30.18	30.73	0.5484	-3.757 to 4.854	0.3683	P > 0.05	ns
9	41.38	41.26	-0.1162	-6.852 to 6.620	0.04989	P > 0.05	ns
12	46.43	46.75	0.3205	-6.898 to 7.538	0.1284	P > 0.05	ns
15	52.81	43.94	-8.868	-16.42 to -1.320	3.397	P < 0.01	**
18+	55.28	47.80	-7.479	-11.72 to -3.235	5.095	P < 0.0001	****
WT vs Homo							
Age	WT	Homo	Difference	95% CI of diff.	t	P value	Summary
2	27.76	25.37	-2.390	-8.501 to 3.721	1.131	P > 0.05	ns
3	30.18	29.28	-0.8973	-5.586 to 3.791	0.5533	P > 0.05	ns
9	41.38	39.60	-1.778	-9.965 to 6.409	0.6278	P > 0.05	ns
12	46.43	42.76	-3.663	-11.43 to 4.104	1.363	P > 0.05	ns
15	52.81	43.78	-9.029	-17.42 to -0.6399	3.112	P < 0.05	*
18+	55.28	48.21	-7.065	-12.05 to -2.075	4.094	P < 0.001	***

Mice numbers for the mouse weight graphed in Figure 3.2, organized by age and genotype, with corresponding statistics.

Table B.2. Mice survival rate and overall breeding ratios

Died of natural causes	Used for experiments (or surplus euthanized)	Litter Average Size	Gestation Duration (days)	Wean Duration (days)	Male Percent	Female Percent
1-2%	98-99%	5.9	21	19	50.25	49.75

B.2 Supplementary methods and data: behaviour

Table B.3 List and order of behavioural experiments for each cohort of animals.

Cohort number	Elevated Plus Maze	Open Field	Rotarod	Cylinder Test	Radial Arm Maze	Objects familiarization
1		1st	2nd	3rd		
2	1st	2nd	3rd	4th		
3	1st	2nd	3rd	4th		
4	1st	2nd	3rd	4th		
5	1st	2nd	3rd	4th		
6	1st	2nd	3rd	4th		
7					1st	
8					1st	
9					1st	
10					1st	
11		1st				2nd

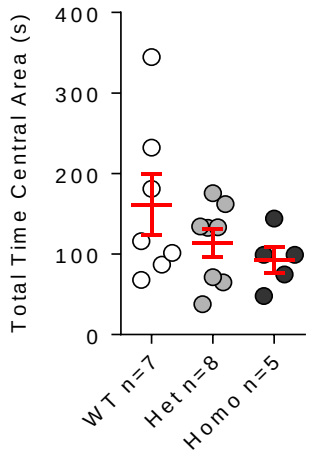

Figure B.4. Open field in the first cohort of young VKI mice
In figure is shown the time spent exploring the center of the arena for the first cohort of 3-month-old VKI. Mice were completely naive to behavioural testing, left exploring a 48x48cm open field arena for 15 minutes. There is a strong trend towards lower time spent exploring the center of the arena (1-way ANOVA $F_{2,19} = 1.61$, $p = 0.23$), suggesting increased anxiety-like phenotype.

Figure B.5. Example image of the bottle holder for experiments using sucrose-water
Bottle holder used for the radial arm maze experiment, providing the choice of two different type of water (regular or 30% sucrose-water) offered in the mouse home-cage, during the habituation period, for 3 days prior to radial arm maze testing.

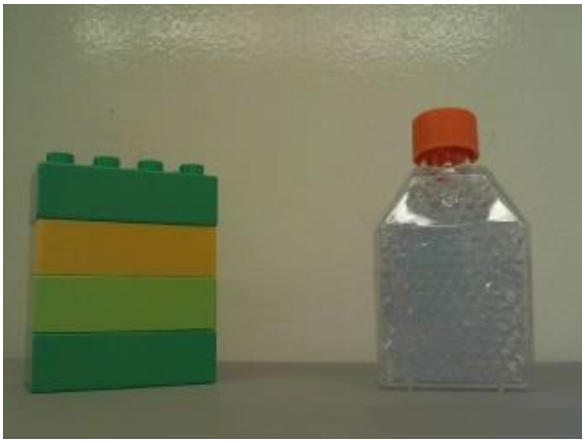

Figure B.6. Objects used for familiarization paradigms and related.
Objects used in the familiarization paradigm. Most mice showed a strong preference towards the object on the right, despite similar sizes and texture between the two objects.